LUT
Lappeenranta
University of Technology

Feiping Zhao

CROSS-LINKED CHITOSAN AND β-CYCLODEXTRIN AS FUNCTIONAL ADSORBENTS IN WATER TREATMENT

Thesis for the degree of Doctor of Science (Technology) to be presented with due permission for public examination and criticism in the MUC, Mikkeli University Consortium, Mikkeli, Finland on the 13th of December, 2017, at noon.

Acta Universitatis
Lappeenrantaensis 778

Supervisor	Professor Mika Sillanpää LUT School of Engineering Science Lappeenranta University of Technology Finland
Reviewers	Associate Professor Athanasios K. Karamalidis Civil & Environmental Engineering Carnegie Mellon University USA
	Associate Professor Amit Bhatnagar Department of Environmental and Biological Sciences University of Eastern Finland Finland
Opponent	Professor Shaobin Wang Department of Chemical Engineering Curtin University Australia

ISBN 978-952-335-178-3

ISBN 978-952-335-179-0 (PDF)

ISSN-L 1456-4491

ISSN 1456-4491

Lappeenrannan teknillinen yliopisto

Yliopistopaino 2017

Abstract

Feiping Zhao

Cross-linked chitosan and β-cyclodextrin as functional adsorbents in water treatment

Lappeenranta, 2017

138 pages

Acta Universitatis Lappeenrantaensis 778

Diss. Lappeenranta University of Technology

ISBN 978-952-335-178-3, ISBN 978-952-335-179-0 (PDF), ISSN-L 1456-4491, ISSN 1456-4491

In recent decades, the worldwide occurrence in water resources of various pollutants, such as toxic heavy metals, dyes, and pharmaceuticals, has raised increasing public attention about the inverse effects on human health and environment. Polysaccharides, such as chitosan and β-cyclodextrin, have the potential to remove these pollutants from water. The present thesis consists of the preparation of five poly(carboxylic acid)s (PACs) or their dianhydrides cross-linked chitosan and/or β-cyclodextrin adsorbents, their characterizations, their applications in water treatment, their kinetic and isotherm studies, their probable adsorption mechanisms, and their regeneration abilities.

In these settings, chitosan is considered as the backbone of the adsorbents; PACs, such as EDTA and DTPA, act as not only linkages but also chelating groups, which are effective in adsorption of metal ions, and thus enhance the metal uptake abilities of the polysaccharide materials significantly; the immobilized β-cyclodextrin cavities are expected to capture organic molecules through host-guest inclusion interaction. These settings combined the advantages of each component while at the same time diminishing their disadvantages.

Based on this design, the selective adsorption of targeted metals from multi-metal system was realized by magnetic EDTA-/DTPA-chitosan, due to the fact that the chelating groups possess different binding affinities toward different metals; the simultaneous and efficient removal of metal and dyes were achieved by EDTA-cross-linked β-cyclodextrin (EDTA-CDP). The adsorption kinetics were very fast for all the prepared adsorbents. The isotherms revealed the adsorption mechanisms of chelation for metals as well as host-guest inclusion for organic pollutants. These also indicated the regeneration methods for the spent adsorbents, such as diluted nitrate acid for metal-loaded adsorbents and ethanol solvent for organic pollutant-loaded adsorbents. The stability and regenerability guaranteed their applications in practical wastewater such as a real industrial effluent from a nonferrous metal smelter. Lastly, prior to analysis, EDTA-CDP was successfully applied to preconcentrate rare earth elements from seawaters. Overall, both the experimental results and theoretical studies suggest that the studied cross-linked chitosan and/or cyclodextrin polymers are the promising adsorbents in wastewater treatment.

Keywords: water treatment, chitosan, beta-cyclodextrin, EDTA, cross-linking, heavy metals, dyes, rare earth elements, organic micropollutant, adsorption isotherm, adsorption mechanism, simultaneous adsorption, selective adsorption, preconcentration.

Acknowledgements

The research work of this thesis was carried out at the Laboratory of Green Chemistry, Lappeenranta University of Technology, Mikkeli, during June 2013 - October 2016. Studies were financially supported by the European Regional Development Fund, Development of cleantech expertise of green chemistry –project.

Dear Prof. Mika Sillanpää, thank you for being my supervisor, for providing me the opportunity and your support to carry out this study and for showing me the beauty of Green Chemistry, and thank you for being a friend. Your supervising was paramount in providing a well-rounded experience consistent my long-term career goals. I leaned and benefited so much from you, and I will always admire your enthusiasm in science, and worship your exceptional research and management abilities. Dr. Eveliina Repo, thank you very much for introducing me to the adsorption field and for your invaluable guidance in experimental work and selfless help.

I express my sincerely gratitude to Associate Professor Athanasios K. Karamalidis and Associate Professor Amit Bhatnagar for reviewing my thesis, and Professor Shaobin Wang for acting as an opponent.

Dear Prof. Dulin Yin, thank you for precise discussion and comments on whole my studies, for sharing your wisdom, and for helping me and my family. Without you, I would not have been able to work on research this far. Prof. Michael Tam, thank you for guiding me into the world of cross-linking hydrogel. I would never forget the valuable discussion with you at Quantum-Nano Centre, at Grand Bend, and at Owen Sound in Canada. Dr. Li Chen, Dr. Reynard Tang, and Nate Grishkewich, thank you for collaboration, for your help and for friendship.

I would like to thank all the members of the LGC for all the support and help. Special gratitude to Dr. Jean-Marie Fontmorin, Dr. Yunfan Zhang, and Simo Kalliola for humor, entertainment, and friendship during my PhD study. I am also grateful to my office-mates Dr. Shila Jafari and Dr. Samia Ben Hammouda during my PhD study. I also thank Dr. Marina

Shestakova and Evgenia Lakovleva for helping my wife in Finland. I would like to thank Mikko Rantalankila and Sanna Tomperi for administration help. Thank Prof. Walter Tang, and Xueting Wang for contribution as co-authors. I also would like to thank all my friends and all my colleagues from LGC, who have helped me with this project. Moreover, I would like to thank the two basketball teams in Mikkeli: Mikkelin Minmky and Mikkelin FUN. I want to thank all my teammates for believing in me, for pushing me to be my best, for forming friendships and brotherhoods that will last a lifetime.

And lastly, I would like to thank my family for everything, especially my parents, for their support, unending encouragement and love. Finally, and most importantly, I would like to thank you, Xiaowei, my beautiful wife. You deserved a wonderful career, but you interrupted it to follow me to Finland without hesitation. Thank you for unwavering love, for selfless sacrifice, and for standing beside me throughout my PhD study. I do love you my darling. My son, Fengqi Zhao, your birth has brightened up my world. I am so blessed of having both of you.

Mikkeli, October 2017

Feiping Zhao

LIST OF PUBLICATIONS

I **Zhao, F.**, Repo, E., Yin, D., Sillanpää, M., Adsorption of Cd (II) and Pb (II) by a novel EGTA-modified chitosan material: Kinetics and isotherms, *Journal of colloid and interface science* 409 (2013) 174–182.

II **Zhao, F.**, Repo, E., Sillanpää, M., Meng, Y., Yin, D., Tang W., Green synthesis of magnetic EDTA-and/or DTPA-cross-linked chitosan adsorbents for highly efficient removal of metals, *Industrial & Engineering Chemistry Research* 54 (2015) 1271-1281.

III **Zhao, F.**, Repo, E., Yin, D., Meng, Y., Jafari, S., Sillanpää, M., EDTA-Cross-Linked β-Cyclodextrin: An Environmentally Friendly Bifunctional Adsorbent for Simultaneous Adsorption of Metals and Cationic Dyes, *Environmental science & technology* 49 (2015) 10570-10580.

IV **Zhao, F.**, Repo, E., Meng, Y., Wang, X., Yin, D., Sillanpää, M., An EDTA-β-cyclodextrin material for the adsorption of rare earth elements and its application in preconcentration of rare earth elements in seawater, *Journal of Colloid and Interface Science* 465 (2016) 215–224.

V. **Zhao, F.**, Repo, E., Yin, D., Chen, L., Kalliola, S., Tang, J., Iakovleva, E., Tam, M., Sillanpää, M., One-pot synthesis of trifunctional chitosan-EDTA-β-cyclodextrin polymer for simultaneous removal of metals and organic micropollutants, *Scientific Reports* 7 (2017) 15811. DOI: 10.1038/s41598-017-16222-7.

The author's contribution in the publications

I The author carried out all experiments, analyzed the data, and had the main responsibility for writing the manuscript.

II The author carried out all experiments, analyzed the data, and had the main responsibility for writing the manuscript.

III The author carried out most of experiments, analyzed the data, and had the main responsibility for writing the manuscript. Shila Jafari helped ζ-potential measurement.

IV The author planned and supervised most of the experiments, analyzed data and had the main responsibility for writing the manuscript. Xueting Wang carried out adsorption tests.

V The author carried out most of the experiments, analyzed data, and had the main responsibility for writing the manuscript. Dr. Reynard Tang prepared amino-cyclodextrin, Dr. Li Chen, Simo Kalliola, and Evgenia Iakovleva conducted conductometric-potentiometric titration, elemental analysis, and HPLC, respectively.

OTHER PUBLICATIONS BY THE SAME AUTHOR

I **Zhao, F.**, Repo, E., Song Y., Yin D., Ben Hammouda S., Chen L., Kalliola S., Tang J., Tam C. K., Sillanpää M., Polyethylenimine-cross-linked cellulose nanocrystals for highly efficient recovery of rare earth elements from water and a mechanism study, *Green Chemistry* 19 (2017) 4816-4828.

II **Zhao, F.**, Repo, E., Sillanpää, M., Meng, Y., Yin, D., Tang W., Adsorption kinetics, isotherms and mechanisms of Cd(II), Pb(II), Co(II)and Ni(II) by a modified magnetic polyacrylamide microcomposite adsorbent, *Journal of Water Process Engineering* 4 (2014) 47-57.

Contents

Abstract

Acknowledgements

List of publications

Nomenclature

1. INTRODUCTION 19

2. CHITOSAN, CYCLODEXTRIN, AND THEIR PROPERTIES 21

2.1 Chitosan and its physicochemical characteristics 21

2.2 Cyclodextrins and inclusion properties 23

3. FUNCTIONALIZED CHITOSAN AND CYCLODEXTRIN ADSORBENTS..... 26

3.1 Covalently cross-linked chitosan and CD adsorbents..... 26

3.1.1 Epichlorohydrin cross-linker..... 27

3.1.2 Glutaraldehyde cross-linker 33

3.1.3 Ethyleneglycol diglycidylether cross-linker 37

3.1.4 Diisocyanates cross-linker 39

3.1.5 Poly(carboxylic acid)s cross-linker..... 43

3.1.6 Dianhydrides cross-linker 46

3.1.7 Other cross-linkers 58

3.2 Surface modification of cross-linked chitosan and CD adsorbents..... 63

3.2.1 Functionalized with amino groups 63

3.2.2 Functionalized with carboxyl groups 68

3.2.3 Functionalized with sulfur groups 73

3.2.4 Modified by other functional groups 78

4. APPLICATIONS OF CROSS-LINKED ADSORBENTS IN WATER TREATMENT 82

4.1 Simultaneous removal of multi pollutants from wastewater 82

4.2 Selective adsorption and separation of target pollutants 83

4.3 Preconcentration of trace adsorbates 85

5. OBJECTIVES AND STRUCTURE OF THE WORK 87

6. Experimental section 89

6.1 Synthesis of the adsorbents 89

6.2 Characterization of the adsorbents 89

6.3 Adsorption and desorption experiments 90

6.4 Analysis of solutions 91

6.5 Simultaneous removal experiments 91

6.6 Preconcentration experiments 92

6.7 Practical industrial effluent experiments 92

6.8 Environmentally (μg L^{-1}) relevant concentration adsorption experiments 92

6.9 Modeling of adsorption isotherms and kinetics 93

6.9.1 Adsorption isotherms 93

6.9.2 Kinetic modeling 96

7. RESULTS AND DISCUSSION 98

7.1 Characterization 98

7.2 Adsorption studies 102

7.2.1 Effect of solution pH 102

7.2.2 Adsorption kinetics 103

7.2.3 Isotherm studies 106

6.2.3.1 Adsorption in single component solutions 106

6.2.3.2 Adsorption in binary and multi component solutions 111

7.3 Application testing of the cross-linked polysaccharide adsorbents 112

7.3.1 Simultaneous removal of heavy metal and dyes from wastewater 112

7.3.2 Selective adsorption test 112

7.3.3 Practical industrial effluent experiments 113

7.3.4 Environmentally (µg L^{-1}) relevant concentration adsorption experiments 113

7.3.5 Preconcentration of trace adsorbates 114

7.4 Adsorption mechanism 114

7.5 Regeneration study 115

7.6 Cost estimation of synthesized adsorbents 117

8. CONCLUSIONS AND FURTHER RESEARCH 119

REFERENCES 121

NOMENCLATURE

List of symbols

α	Initial adsorption rate constant of Elovich model	mmol g^{-1} min^{-1}
β	Surface coverage constant of Elovich model	g $mmol^{-1}$
C_e	Equilibrium concentration	mmol L^{-1}
C_i	Initial concentration	mmol L^{-1}
C_{id}	Intraparticle diffusion	mmol g^{-1}
G	Standard Gibbs free energy	J or J mol^{-1}
k_1	Pseudo-first-order rate constant	1 min^{-1}
k_2	Pseudo-second-order rate constant	g $mmol^{-1}$ min^{-1}
k_{id}	Rate constant of intraparticle diffusion	mmol g^{-1} $min^{-0.5}$
K_F	Freundlich affinity constant	L $mmol^{-1}$
K_L	Langmuir affinity constant	L $mmol^{-1}$
K_S	Sips affinity constant	L $mmol^{-1}$
Log K	stability constant	-
M	Molecular mass	g $mmol^{-1}$

m	Weight of the adsorbent	g
n	Mole amount of material	mol
n_F	Freundlich heterogeneity factor	-
n_S	Sips heterogeneity factor	-
q_e	Equilibrium adsorption capacity	mmol g^{-1}
q_m	Maximum adsorption capacity	mmol g^{-1}
$q_{m,exp}$	Experimental maximum adsorption capacity	mmol g^{-1}
q_t	Adsorption capacity at time t	mmol g^{-1}
R^2	Coefficient of determination/correlation coefficient	-
pH_{PZC}	Isoelectric point of ζ-potential	-
RE	Regeneration efficiency	%
S_{BET}	Brunauer-Emmett-Teller surface area	m^2 g^{-1}
T	Temperature	K or ^oC
V	Volume of the solution	mL
v	Wavelength	cm^{-1}
wt.	Weight percent	%

Abbreviations

AA	Acrylic acid

AM	Acrylamide
BADGE	Bisphenol A diglycidyl ether
BPA	Bisphenol-A
BPMAMFP	2[-bis-(pyridylmethyl) aminomethyl]4-methyl-6-formyl-phenol
BPS	Bisphenol-S
BSA	Bovine serum albumin
BTCA	1,2,3,4-butane tetra carboxylic acid
BTCAD	BTCA dianhydride
BTCA	Benzophenone-3,3’,4,4’-tetracarboxylic dianhydride
CD	Cyclodextrin
COD	Chemical oxygen demand
CS	Chitosan
CS-ED-CD	EDTAD-cross-linked chitosan and β-CD via one-pot synthesis
CMC	Carboxymethylcellulose
DA	Degree of acetylation
DFT	Density functional theory
DD	Degree of deacetylation
DEGDE	Diethylene glycol diglycidyl ether
DL	Determination limit

DMA	Dynamic mechanical analysis
DMF	Dimethylformamide
DMSO	Dimethyl sulfoxide
DTCS	DTPAD cross-linked chitosan
DTPA	Diethylenetriaminepentaacetic acid
DTPAD	DTPA dianhydride
EDA	Ethylenediamine
EDCS	EDTAD cross-linked chitosan
EDTA	Ethylenediaminetetraacetic acid
EDPA-CDP	EDTA-cross-linked β-CD polymer
EDTAD	EDTA dianhydride
EGDE	Ethylene glycol diglycidyl ether
EGDMA	Ethyl glycol dimethacrylate
EGTA	Ethylene glycol-bis(2-aminoethylether)-N,N,N’,N’-tetraacetic acid
EGTA-chitosan	EGTA-modified chitosan
EGTAD	EGTA dianhydride
EODD	7-ethyl octadecane diacid diglycidyl
EPI	Epichlorohydrin
EPI-CS	Epichlorohydrin cross-linked chitosan

EPI-CDP	Epichlorohydrin cross-linked CD polymer
HFPD	4,4’-(hexafluoroisopropylidene) diphthalic dianhydride
FDA	Formaldehyde dimethyl acetal
GLA	Glutaraldehyde
GLA-CDP	Glutaraldehyde cross-linked β-CD polymer
GLA-CS	Glutaraldehyde cross-linked chitosan
GLA-CSL	GLA cross-linked chitosan with low-molecular weight
GLA-CSH	GLA cross-linked chitosan with high-molecular weight
HFPD	4,4’-(hexafluoroisopropylidene) diphthalic dianhydride
HMDI	1,6-hexamethylene diisocyanate
HM-CDP	HMDI cross-linked β-CD polymer
HP-CD	Hydroxyproplyl-β-CD
IDA	Iminodiacetic acid
MIP	Molecularly imprinted polymer
MDI	4,4’-methylene-bis-phenyldiisocyanate
MNP	Magnetic nanoparticles
MEDCS	Magnetic EDTAD-cross-linked chitosan
MDTCS	Magnetic DTPAD-cross-linked chitosan
NMP	N-methyl-2-pyrrolidinone

ODPA	4,4’-oxydiphthalic anhydride
PAA	Polyacrylic acid
PAC	Poly(carboxylic acid)
PAMAM	Polyamidoamine
PEGDE	Polyethylene glycol diglycidyl ether
PEI	Polyethylenimine
PMDA	Pyromellitic dianhydride
PMAA	Poly(methacrylic acid)
REE	Rare earth element
RM-CD	Randomly methylated β-cyclodextrin
Suc-	Succinate anhydride modified-
TEOS	Tetraethylorthosilicate
TEPA	Tetraethylenepentamine
THF	Tetrahydrofuran
TDI	Tolylene-2,4-diisocyanate
TGA	Thermogravimetry analysis
TsCl	Toluenesulfonyl chloride
TSSA	Trisulfonated sodium amine

1. INTRODUCTION

The increasing worldwide contamination of water resources with thousands of inorganic and organic pollutants, such as toxic metals, dyes, pharmaceuticals, pesticides, and endocrine disrupting chemicals, has raised more and more serious environmental problems facing humanity in almost all part of the world [1, 2]. Nowadays, these compounds are the common contaminants in water systems, and most of them are hazardous or carcinogenic. For instance, cadmium, lead, cobalt, nickel, and copper are known to cause health disorders such as allergy or organ damages if ingested beyond the permitted level [3]. Dyes are extensively used in various industries such as textile, paper, plastics, and cosmetics [4]. Dyes have become one of the major sources of the serious aquatic pollutions as the result of the rapid industrialization. The discharge of the colorant effluent has caused severe and specific pollutions characterized by high chemical oxygen demand (COD), toxicity, and color, which has a negative effect on photosynthesis in aquatic ecosystems [5]. Pharmaceuticals have been considered as a class of emerging pollutants in water systems, since their environmental persistence and ecological impact are uncertain [6]. The most frequently founded pharmaceutical pollutants in effluents are antibiotics, anti-inflammatories, steroids, anesthetics, and antidepressants. Though pharmaceutical pollutants are presented in the environment at low concentrations, they still represent a long-term risk for the aquatic and terrestrial ecosystems, due to the continuous intake and their bio-accumulation [7]. Thus the removal of those harmful substances from the contaminated water is urgent prior to discharge.

A large number of treatment technologies have been reported and are currently used to remove metals and organic pollutants from wastewater, primarily including membrane separation [8, 9], adsorption [10-12], electrochemical technologies [13-15], advanced oxidation processes [16, 17], and biodegradation [18, 19]. Among them, adsorption by using adsorbents has been considered as one of the best methods for water treatment due to its ease of operation, low cost, and high efficiency without secondary pollution [1, 11, 20].

Activated carbon has undoubtedly been the most widespread adsorbent used to remove pollutants from aqueous solutions because of its high surface area and porous structure but it has several deficiencies, including its high cost and its poor removal of heavy metals and hydrophilic organic pollutants [1]. Moreover, the thermal regeneration of spent active carbon is energy consuming and could not fully restore sorption performance [21]. All these restrict its industrial scale application in water treatment and the same limitation applies to some other commercial adsorbents such as activated alumina, zeolites, and synthetic polymer resins [22-24].

Therefore, it is important to develop novel efficient, economic, eco-friendly, and widely available adsorbents [25, 26]. From this perspective, the use of natural polysaccharide materials such as chitosan and cyclodextrin (CD) as adsorbents in water treatment has attracted increasing attentions in recent years [27-29] by several important advantages: firstly, the resources of these polysaccharides are very abundant in nature and are available to be produced commercially from the natural resources at low price now; secondly, the presence of functional groups such as hydroxyl and amino groups as well as their well-defined structures endows these biopolymers high reactivity and excellent selectivity towards metals or aromatic compounds; thirdly, their chemical stability ensures these biosorbents possible to be regenerated and reused after adsorption saturation; fourthly, the polysaccharides are renewable and biodegradable, thus they would not bring further pollutions. Because of their solubility in water or diluted acid solutions, the raw chitosan and CDs cannot be directly used for adsorption purposes. Prior to application, therefore, the polysaccharides have to be immobilized on an insoluble support by grafting, or to be cross-linked with various cross-linkers, resulting in insoluble polymer materials. In the present literature review, an overview of several recent approaches used to synthesize and prepare chitosan and CD based adsorbents, in particular cross-linking methods, were given. Furthermore, the application of chitosan and CD based adsorbents for the removal of various pollutants (e.g., toxic metals, dyes, and pharmaceuticals, etc.) from water and wastewater were also reviewed. The adsorption mechanisms and the influence of the modifications were also discussed in this literature review.

2. CHITOSAN, CYCLODEXTRIN, AND THEIR PROPERTIES

2.1 Chitosan and its physicochemical characteristics

Chitosan, a type of natural aminopolysaccharide, is produced from the deacetylation of chitin, which is the second abundant biopolymer in nature, only after cellulose. Chitin can be commercially extracted from marine crustacean shells, as a by-product of seafood processing industries. Chitin, the second most abundant polysaccharide in the world, is a linear polymer composed of β-(1→4)-2-acetoamido-2-deoxy-D-glucose (**Figure 1**) [30, 31]. During the alkaline deacetylation of chitin, the acetyl groups are hydrolyzed and transformed into free amine groups, resulting in chitosan, which has a similar structure as cellulose but has amine groups on the C-2 positions replacing the hydroxyl groups. When the degree of deacetylation (DD) is larger than 40%, chitosan is soluble in acidic media because of the protonation of the amino groups on the chitosan chains at low pH. The amine groups make the biopolymer a natural cationic polyelectrolyte with a pK_a of 6.5. However, the extensive intramolecular and intermolecular hydrogen bonding between the chitosan chains results in its crystalline structure, making chitosan insoluble in neutral and alkaline aqueous, and most common organic solvents (e.g. ethanol, pyridine, DMF, DMSO) [32].

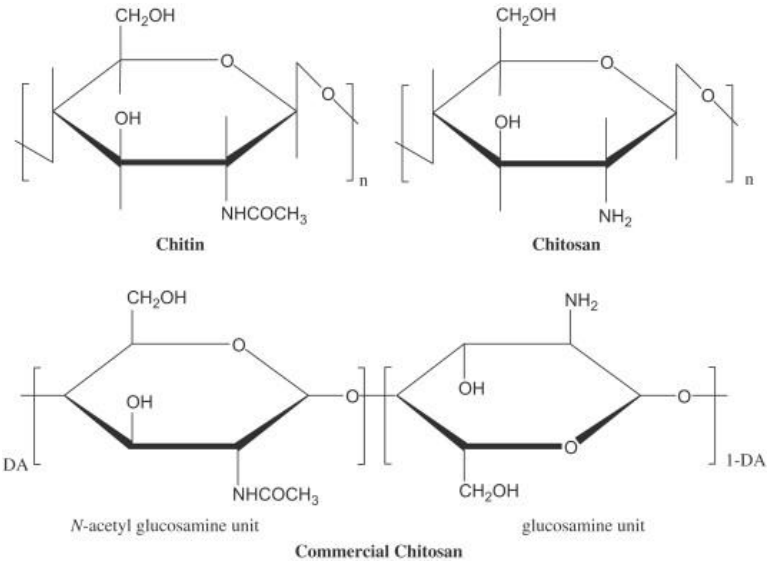

Figure 1. Chemical structure of chitin, chitosan, and commercial chitosan partly deacetylated. DA represents degree of acetylation (Reproduced from ref.[30], with permission from Elsevier).

Importantly, three types of reactive functional groups, i.e., amino group, primary and second hydroxyl groups, co-exist at the C-2, C-3, and C-6 positions of chitosan glucosamine units, respectively. The presence of these groups especially amino groups results in several drawbacks such as solubility in acidic aqueous, low acid stability, swelling, and insufficient mechanical properties but also brings exceptional advantages: on one hand, the abundant amine groups on chitosan chains are able to act as coordination sites for metals and dyes, which effectively enhances the uptake ability of pollutants, especially transition metals [33]; on the other hand, these groups are very active, providing opportunity to conduct easily both physical and chemical modifications, such as impregnation, cross-linking, and grafting. These modifications might prevent swelling, reinforce mechanical resistance, enhance the acid stability, as well as refrain the solubility in acidic environments [27]. More significantly, some of these modifications are available to improve the adsorption performance of the adsorbents by introduction of extra functional groups such as hydroxyquinoline [34], sulfonate [35], succinic acid [36], and aminopolycarboxylic acid [37]. Additionally, several

substances, such as silica [38], montmorillonite [39], graphene [40], and magnet [41], have been employed to form composite with chitosan, resulting in chitosan composite adsorbents or hybrid adsorbents.

2.2 Cyclodextrins and inclusion properties

Cyclodextrins (CDs), a family of torus-shaped macrocyclic oligosaccharides, have attracted significant attentions in a wide range of medicinal and environmental processes since they were firstly discovered by Villiers in 1891 [1, 42, 43]. The CDs are usually produced from the enzymatic degradation of starch by bacteria (e.g., *Bacillus macerans* and *Klebsiella pneumonia*). These oligosaccharides contain six to twelve glucose units, where each glucose units are linked by α-1,4 glycosidic bonds to constitute a cyclic structure. Among them, the three smallest CDs, α-, β-, and γ-CDs, are the most known and commercial available, which consist of six, seven, and eight glucose units, respectively. By far, β-CD has been commercially the most attractive due to its facile synthesis, abundant availability and excellent properties. The torus-shaped CDs own hollow, tapered cavities of 0.79 nm in depth, while their diameters grow in number of glucose units (**Figure 2**) [42]. All glucose units in the torus-shaped CDs possess the thermodynamically favored chair conformation since all substituents are in the equatorial position. As a result, all secondary hydroxyl groups are situated on one side of the cavity, while all primary hydroxyl groups are on the other side. The secondary hydroxyl groups on the C-2 and C-3 positions of the glucose unit form a larger opening than the one of primary hydroxyl groups on the C-6 position, resulting in the truncated cone shape of CDs. The abundant hydroxyl groups on the exterior of the cavities endow the CDs high water solubility. The hydroxyl group on C-2 of one glucose unit can form a hydrogen bond with the one on C-3 of the adjacent glucose unit, endowing the CDs rigid structure. The hydrophilic exterior and hydrophobic interior of the CD cavities enable them to form inclusion complexes with a variety of small organic molecules in solution or in the solid state through host-guest inclusion interactions [44, 45].

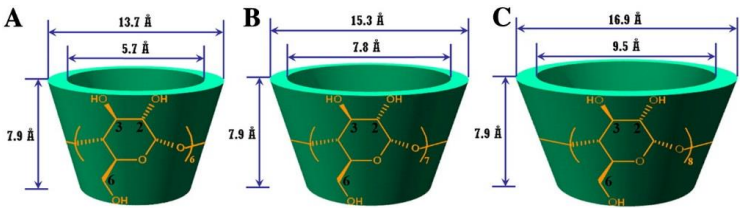

Figure 2. Molecular structures and dimensions of α-CD (A), β-CD (B), and γ-CD (C) (Reproduced from ref.[42], with permission from Elsevier).

The term of host-guest inclusion, as the name suggested, one or more guest molecules are admitted into the cavity of the host, forming stable inclusion complexes, without break and formation of any covalent bonds. Zeolites is the most typical inorganic host molecules and crown ethers, calixarene, and CDs are the typical organic host molecules. The formation of inclusion complex is a dimensional fit and also a specific spatial interaction between host cavity and guest molecule. According to some authors [46], hydrophobic interactions, which induce the none-polar moiety of the guest molecule to preferentially access the cavity, are the principal driving forces for CD-based host-guest compounds. Moreover, other factors such as Van der Waals interaction, hydrogen bonding between the guest molecule and the secondary hydroxyl groups of the cavity, steric effect, as well as the sizes match between guest molecule and host cavities, also play significant roles in the formation of CD inclusion complex. Generally, one guest molecule is enveloped into one CD cavity to form a 1:1 complex. However, in the case of some small guest molecules, more than one guest molecules can be included into one CD cavity (e.g., 1:2); on the contrary, in the case of some large molecules, more than one cavities are involved to form an inclusion complex with one guest molecule (e.g., 2:1). Among them, 1:1 complex is the simplest and most common case, enabling for the application of stoichiometric analysis [47].

The complex formation of guest molecules within the host CD cavities is not permanent but rather is a dynamic equilibrium, which is represented by the following equations[48]:

$$\mathrm{CD} + \mathrm{G} \rightleftarrows \mathrm{CD} \cdot \mathrm{G} \qquad (1)$$

$$K_f = \frac{[\mathrm{CD} \cdot \mathrm{G}]}{[\mathrm{CD}][\mathrm{G}]} \qquad (2)$$

where G is the guest molecule, K_f is the equilibrium constant, [CD·G], [CD], and [G] present the concentration of the host-gest complex, uncomplexed CD, and free guest molecule, respectively. The greater the K_f value, the more stable the inclusion complex would be [46]. The equilibrium kinetics of the CD complex formation is usually very fast at initial (often with minutes), while the final equilibrium might take more time to reach. The dissociation of CD inclusion complex is usually forced by a substantial increase of water molecules in the surrounding of CD cavities. Moreover, the polarity of the CD cavity has been found to be similar to that of ethanol [48]. Thus ethanol solutions were usually used to dissociate guest molecules from CD cavities as eluent.

The exceptional inclusion character as well as their other specific properties such as water-solubility, non-toxicity, non-allergy, and selectivity have led to the extensive application of CDs in biomedical, pharmaceutical, cosmetic, and food processing industries [49-51]. In addition, the high density of hydroxyl groups on the exterior of CDs (e.g., β-CD contains 21 hydroxyl groups) are possible to be modified by various functional groups, such as aminations, esterifications, alkylations and carboxymethylations, endowing the cavities with more properties [52]. For instance, the most commercial available CD derivatives, hydroxyproplyl-β-CD (HPCD) and carboxymethyle-β-CD (CMCD), are much more soluble in aqueous than the native CDs and even soluble in some organic solvents, which enhance the application of CDs in drug release [53] and in decontamination of wastewater, air, and soil [44, 54]. On the other side, CDs have often been reacted with cross-linking agent or be grafted on support to obtain water-insoluble materials for separation application [55, 56].

3. FUNCTIONALIZED CHITOSAN AND CYCLODEXTRIN ADSORBENTS

The polymerization of chitosan and CDs also brings more functionalities and opportunities. There have been a large number of studies in literature on the preparation of water insoluble adsorbents containing chitosan or CDs. Most of their synthesis methods could be generally classified into two ways: first, cross-linking, chitosan and CDs could be cross-linked by a reaction between the amino or hydroxyl groups of the polysaccharides with a cross-linking agent to form insoluble polymer networks in the form of gel or bead [57, 58]. These networks are often divided into two classifications (covalently cross-linked networks and networks formed by physical interactions); the second relies on the covalent immobilization of chitosan or CDs on insoluble supports by grafting, resulting in hybrid or composite materials.

3.1 Covalently cross-linked chitosan and CD adsorbents

Physical networks are formed by various reversible links while chemical networks are formed by irreversible covalent links. Chitosan is an amphoteric polyelectrolyte and an unsaturated macromonomer, enabling the facile preparation of both physical and chemical chitosan-based gels and beads [59]. For example, tripolyphosphate (TPP) is commonly used to irritate the ionotropic gelation of chitosan. However, the amphoteric polyelectrolyte is not available to CDs and there have been rarely reports on the CD networks formed by physical interactions. Thus the discussion in this review will be limited in covalent cross-linked polymers. The chemical reactivity of the abundant hydroxyl groups at C-3, C-6, and amino groups at C-2 positions in the glucose unit of chitosan as well as the hydroxyl groups at C-2, C-3, and C-6 of CDs, allows the polysaccharides to form insoluble networks by chemical cross-linking reactions. In the cross-linking reaction, the cross-linking agents (as known as cross-linker), which have at least two reactive functional groups, could react with the functional groups on the same or different polysaccharide molecules, introducing the intra-/inter-molecular bridges (linkages) between polysaccharide macromolecules. In the case of chitosan, this cross-linking occurs between chitosan chains, while in the case of CDs, two and more covalently cross-linked CD cavities are named CD dimers and polymers, respectively. If the degree of cross-linking is sufficiently high, the CD matrix becomes insoluble (**Figure 3**)

[43]. Cross-linking could significantly reduce the mobility of each segment in the polymer matrix, as well as interconnected chains by linkages, resulting in the formation of a three dimensional network with swollen ability in aqueous without dissolution [28]. The aim of cross-linking is to reinforce mechanical resistance and to prevent CDs from dissolving in water while to prevent chitosan from dissolving in acidic media, enabling the use of CD and chitosan based materials as adsorbents in drastic pH. To date, the most common cross-linkers used with chitosan and CDs for environmental application are epoxides such as epichlorohydrin (EPI) [60, 61] and ethylene glycol diglycidyl ether (EGDE) [62, 63], dialdehydes such as formaldehyde and in particular glutaraldehyde (GLA) [64, 65], diisocyanates [66], and other cross-linkers (carboxylic acids, dianhydrides, etc.).

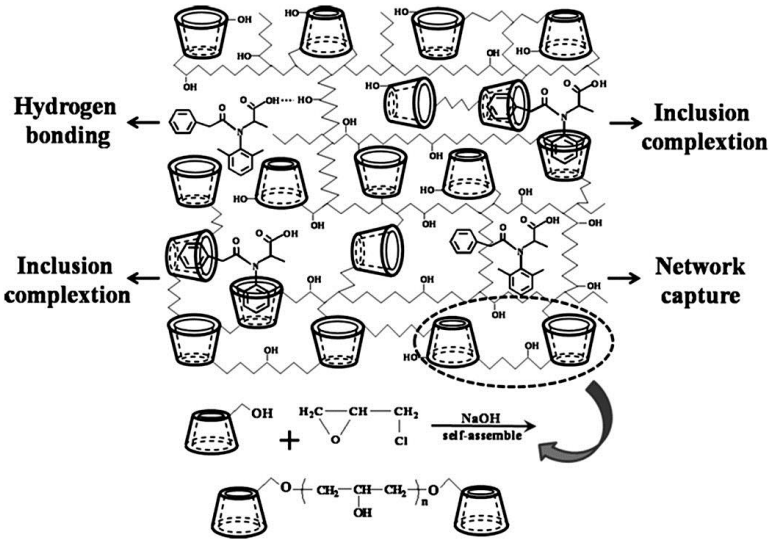

Figure 3. Schematic of cross-linked structure of cyclodextrin polymer and adsorption mechanisms (Reproduced from ref.[43], with permission from Elsevier).

3.1.1 Epichlorohydrin cross-linker

Among the cross-linkers, the most commonly used is epichlorohydrin (chloromethyl oxirane, C_3H_5ClO, abbreviated EPI), which is an important chemical intermediate in many fields – from epoxy resins to anion and cation exchange resins, although it is considered to be hazardous to environment and human beings. **Table 1** presents the EPI-cross-linked chitosan

and/or β-CD adsorbent materials for water treatment. This cross-linker has been developed for more than 90 years and is known to be relatively easy to use. It is a bi-functional cross-linker, containing a highly reactive epoxide group and a chloroalkyl moiety [67], which can bind with hydroxyl groups under alkaline conditions. Therefore, EPI can react with CD cavities obtaining cross-linked networks (cross-linking step) and/or react with itself obtaining polymerized epichlorohydrin chains (polymerization step). The resulting EPI cross-linked CD polymers (in the term of EPI-CDP) are usually 3D networks of CD units covalently jointed by repeating glyceryl linkers (**Figure 4**) [29]. These cross-linking and polymerization convert CD from water-soluble monomer into hydrophilic, insoluble network-shaped polymer with high swelling capacity in aqueous solutions (in the form of gels or hydrogels) as well as plenty of adsorption sites [68]. EPI-CDP keeps the cavity structure of CDs, endowing the polymer capability of forming inclusion complexes with a variety of guest molecules [55, 69]. Chen Q. et al. prepared spherical particles of α-, β-, and γ-CD polymers by reverse suspension polymerization with EPI as cross-linker. These CD spherical polymer particles were found to be ideal candidates for the selective removal of phenol from waste water owing to the selective inclusion associations between CD cavities and phenol molecule. Among them, β-CD polymer showed the best adsorption ability (29.6 mg g^{-1}), corresponding to its lowest free energy (spontaneous adsorption nature) [70]. Grini G. et Al. produced β-CD polymers using EPI as cross-linker in the presence of carboxymethylcellulose for the removal of Basic Blue 9 with a maximum sorption capacity of 56.5 mg g^{-1} [71]. Seven spherical porous EPI-CDPs were prepared for adsorption and separation of pesticides from water and the adsorption mechanism were investigated by Liu H. et al. [43]. Although it was evident that the inclusion of CD cavity is the primary adsorption mechanism, the hydrogen bonding, target molecule loading into swelling water, and physical sorption also play some roles. Pratt D. Y. et al. synthesized EPI-CDPs by reacting varying mole ratios (1:15, 1:25 and 1:35) of β-CD/EPI and applied them for the adsorption of *p*-nitrophenol from aqueous solutions [61]. The sorption of *p*-nitrophenol could occur at intracavity (CD cavity) or extracavity (interstitial domain) sites of the polymer framework. Generally, adsorption potential of the CD polymers is related mainly to CD content. In this work, however, it was observed that the sorption capacity tends to correlate with the increasing EPI content of the polymer. Authors

explained the reason could be the increasingly microporous polymer framework structures along with the increasing EPI contents. EPI-CDPs have been shown to be an effective adsorbent for adsorption of organic pollutants, but there are few literature reports on its removal of heavy metals. Tajuddin S. M. et al. applied EPI-CDP for the adsorption of copper and the maximum sorption capacity was estimated to be 111.11 mg g^{-1} by Langmuir model. It is reported that Cu(II) ions could be complexed by CD via the hydroxyl groups [72].

EPI is also popular to be used as cross-linker to reinforce the mechanical resistance and improve the stability of chitosan in acidic solutions. Compared to other cross-linkers, EPI possesses advantage that it does not eliminate the amount of the major adsorption sites (amine groups) on chitosan since EPI mostly reacts with hydroxyl groups (**Figure 5**), while most of other cross-linkers bind with amine groups. Thus the cross-linking by EPI would not significantly reduce the adsorption ability of chitosan, even somehow it might improve the adsorption capacity of chitosan. An EPI cross-linked chitosan adsorbent (in the term of EPI-CS) was prepared by Li C. et al. for the removal of Congo red from water solutions. The results showed that the maximum sorption capacity of the cross-linked chitosan was higher than that of pristine chitosan [73]. The extra adsorption ability could be due to the introduction of hydroxyl groups (glyceryl linkers) during the EPI cross-linking (the ring-open of epoxy). However, another work also reported that EPI cross-linking reduced slightly the sorption capacity of chitosan toward Reactive Black 5 from 0.72 mmol g^{-1} to 0.68 mmol g^{-1} [74]. Chen A. et al. investigated the adsorption of Cu(II), Zn(II), and Pb(II) ions from aqueous solutions by EPI-CS in batch experiments. The obtained maximum sorption capacities were 35.46 mg g^{-1}, 34.13 mg g^{-1}, and 10.21 mg g^{-1} for Cu(II), Zn(II), and Pb(II), respectively at pH 7.0 and 0.5 molar ratio of EPI/chitosan [60]. R. Laus et al. evaluated the adsorption of Cu(II) and Cd(II) from aqueous solutions by EPI-CS in single and binary metal systems. In single adsorption, the maximum sorption capacities were obtained to be 130.72 and 83.75 mg g^{-1} for Cu(II) and Cd(II), respectively, while the binary adsorption showed a significant competition effect and the selective sorption towards Cu(II) rather than Cd(II) [75]. The EPI-CS was also applied in the removal of toxic radioactivity elements such as Uranium (VI) from aqueous solution and the maximum sorption capacity was 72.46 mg g^{-1} at 25 ^{o}C with a pH of 3.0 [76].

To improve the adsorption ability of chitosan for organic pollutants as well as to eliminate the water-solubility of CDs, a few researchers have grafted CDs on chitosan by using EPI as cross-linker in two steps, obtaining multi-functional CD and chitosan adsorbents [77, 78]. With the protecting of amine groups by benzaldehyde, Zhang X. et al. firstly employed EPI to react with C-6 hydroxyl groups of chitosan, and then the epoxy-activated chitosan was further reacted with β-CD under alkaline condition, resulting in yellow, solid β-CD-chitosan (in the term of CS-CD). The amount of β-CD grafting was determined as 25.8 μmol g^{-1}. The highest saturated sorption capacity of *p*-dihydroxybenzene of this novel adsorbent (51.68 mg g^{-1}) was found to be significantly higher than that of pristine chitosan (31.64 mg g^{-1}). The authors elaborated the presence of β-CD allowed the inclusion of the target molecules into their hydrophobic cavities [77]. Later, this EPI cross-linked β-CD-chitosan adsorbent was studied by Li J. et al. to remove *p*-Chlorophenol from waste water. The adsorption capacity of CS-CD (179.73 mg g^{-1}) was comparatively higher than those of pristine chitosan (2.58 mg g^{-1}), salicylaldehyde modified chitosan (20.49 mg g^{-1}) and EPI-CDP (74.25 mg g^{-1}), indicating that all the functional groups of β-CD (inclusion), chitosan (amine group, hydrogen bonding), and glyceryl linkers (hydroxyl group, hydrogen bonding) play important roles in the sorption of phenols [78].

Table 1. EPI cross-linked chitosan and β-CD adsorbents.

Polysaccharide	Cross-linked form	Target adsorbate	Contact time (h)	pH	q_m (mmol g^{-1})	Ref
Chitosan	Microgel	Cu(II)	5	7.0	0.558	[60]
		Zn(II)			0.156	
		Pb(II)			0.165	
Chitosan	Membrane	Hg(II)	24	6.0	0.151	[79]
Chitosan	Cross-linked network	Uranium (VI)	2	3.0	0.30	[76]
Chitosan	Membrane	Cr(VI)	24	2.0	0.358	[80]
				6.0	1.888	
Chitosan	Bead	Reactive Black 5	2	3.0	2.06	[74]

Chitosan	Gel	Uranium (VI)	5	4.0	1.45	[81]
Chitosan	Bead	Cu(II)	6	4.0	0.183	[82]
Chitosan	Powder	Pb(II)	4	5.0	0.155	[83]
		Cu(II)			0.710	
		Cd(II)			0.332	
		Ni(II)			0.595	
		Co(II)			0.172	
β-CD 1:15[a]	Co-polymer	*p*-nitrophenol	24	4.6	0.119	[61]
β-CD 1:25[a]					0.784	
β-CD 1:35[a]					0.810	
β-CD	Bead	Cu(II)	12	6.0	1.750	[72]
β-CD, RM-CD and HP-CD 40:30:30[b]	Polymer network	Fomesafen	2	7.2	0.056	[43]
β-CD	Gel	Phenol	1.5	-	0.034	[84]
		Naphthol	2.5	-	0.140	
β-CD	Gel	Phenol	-	7.0	1.397	[78]
		p-Chlorophenol			0.577	
		p-nitrophenol			0.296	
Chitosan, β-CD	Yellow solid powder	*p*-dihydroxybenzene	8	-	0.469	[77]
Chitosan, β-CD	Yellow solid powder	Phenol	3	5.0	0.283	[85]
		2-chlorophenol			0.250	
		4-chlorophenol			0.288	
		2,4-dichlorophenol			0.401	
		2,4,6-trichlorophenol			0.406	

[a] different mole ratios (1 : 15, 1 : 25 and 1 : 35) of β-CD with EPI.

[b] Mass ratio; RM-CD, randomly methylated β-cyclodextrin; HP-CD, (2-Hydroxypropyl)-β-cyclodextrin.

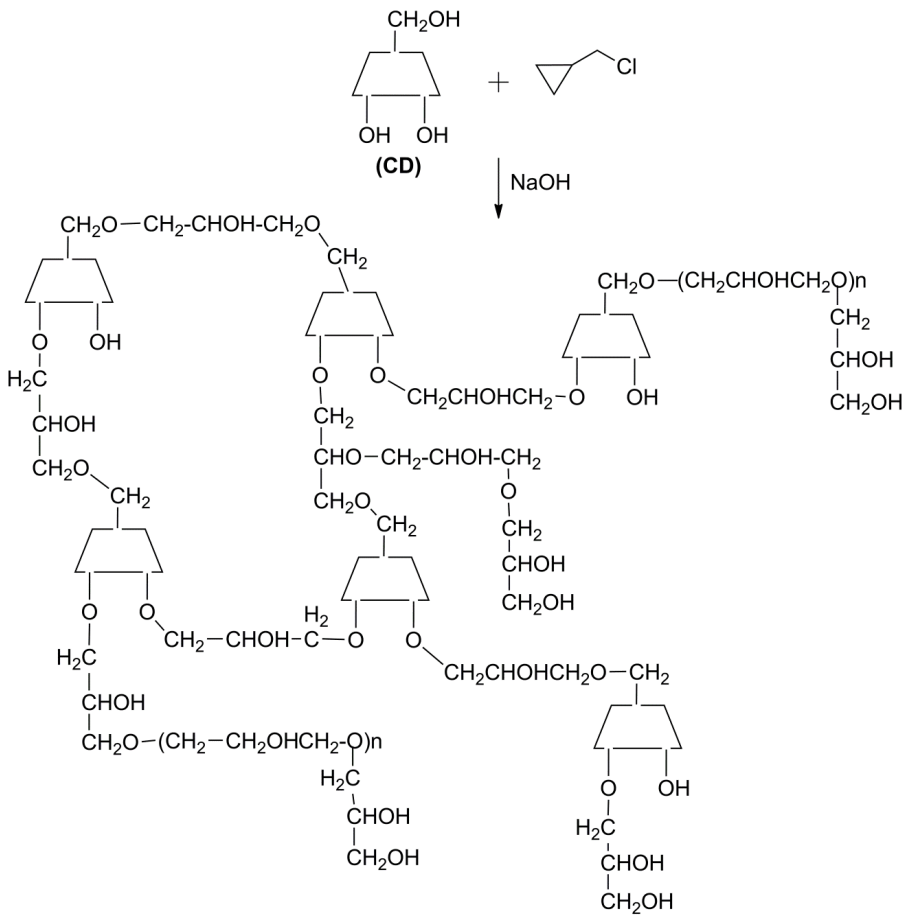

Figure 4. Synthesis schematic diagram of water-insoluble EPI-cross-linked β-CD (modified from [29])

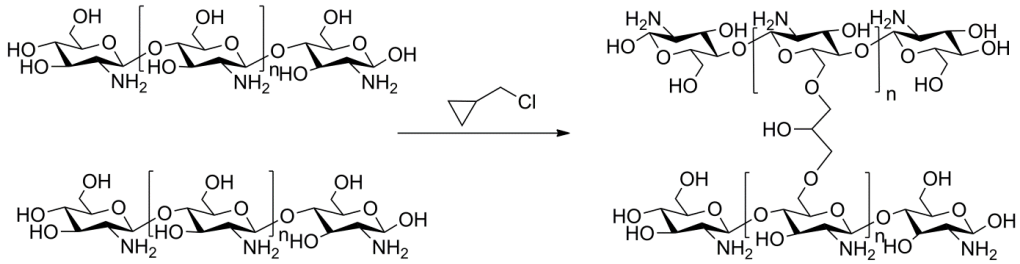

Figure 5. Synthesis schematic diagram of water-insoluble EPI-cross-linked chitosan polymer.

3.1.2 Glutaraldehyde cross-linker

Glutaraldehyde (HCO-$(CH_2)_3$-CHO, abbreviated GLA), which contains two aldehyde groups and a three-methylene chain, has also been widely used to cross-link polysaccharides, in particular chitosan (**Table 2**) [28], even though it has been reported to have high level of cytotoxicity and carcinogenicity to human beings and animals [86]. The reaction mechanism of GLA cross-linking was generally considered as a Schiff's base reaction between the primary amine groups of chitosan and the aldehyde groups of GLA, where the aldehyde bond is replaced by an imine bond, which is stabilized by resonance with the adjacent ethylenic double bond (**Figure 6**) [87, 88]. However, the GLA cross-linking with hydroxyl groups of chitosan could not be excluded [28, 89]. Dumitriu S. et al. proposed a possible mechanism that two aldehyde groups of a GLA molecule react with four hydroxyl groups from two glucosamine units of chitosan, resulting in formation of two stable six-membered oxygen heterocycles [89]. However, this view has not received much support and most researchers still believe that the Schiff's base reaction with amine groups is the main mechanism. This also could reflect that seldom researchers have cross-linked β-CD by using GLA as a cross-linker. The only one case, Singh K. et al. prepared GLA cross-linked β-CD polymer (in the term of GLA-CDP) membrane for the enantiomeric separation of amino acids [65]. Its proposed cross-linking reaction scheme is shown in **Figure 7**. Thus the precise reaction mechanism and the exact structure of the formed chemical compounds are still questioned.

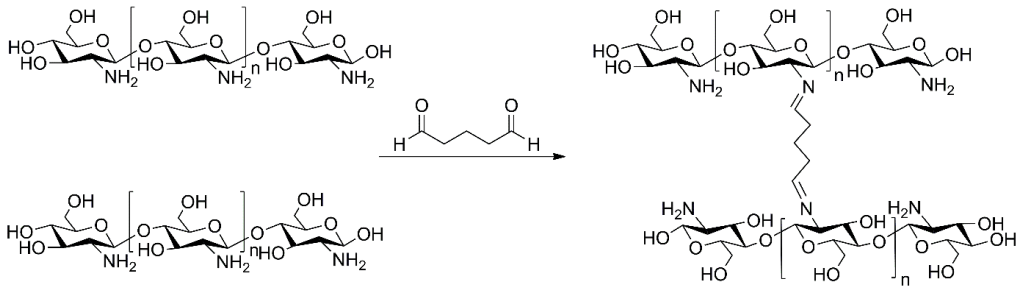

Figure 6. Synthesis schematic diagram of water-insoluble GLA-cross-linked chitosan polymer.

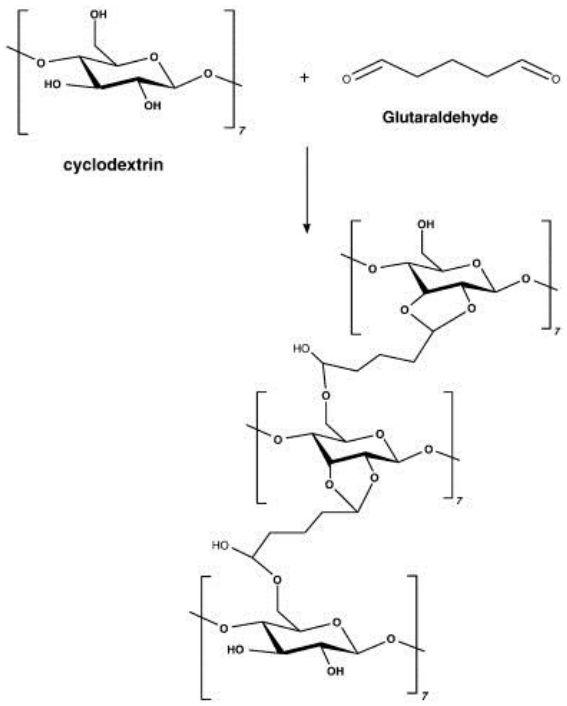

Figure 7. Possible reaction scheme of β-CD with GLA-cross-linker (Reproduced from ref.[65], with permission from Elsevier).

Poon L. et al. investigated the synthesis of GLA cross-linked chitosan (in the term of GLA-CS) polymers at variable reaction conditions, such as reaction pH, gelation temperatures, and GLA/NH_2 (glucosamine unit of chitosan) ratios [88]. The authors also assessed the relationship between the reaction conditions and their sorption properties toward *p*-nitrophenol. It is observed that the pH and cross-linking ratio have greater effect on the adsorption capacity of GLA-CS, in comparison with the gelation temperature. The optimal adsorption occurred at the 4:1 GLA/NH_2 ratio under acidic pH conditions. GLA-CS beads with enhanced stability in acidic conditions were prepared by Park S. et al. and used for the adsorption of Au(III) and Pd(II) from binary-metal solutions [90]. These GLA-CS beads showed

selective sorption of Au(III) from the Au(III)-Pd(II) mixture. Interestingly, X-ray diffraction (XRD) analyses indicated that Au(III) selectivity could be attributed to reduction-couple adsorption of Au(III) via GLA groups, unlike Pd(II) that remained unreduced after adsorption. A full factorial design (2^3, sorbent mass, sorption temperature, and initial dye concentration) was employed to evaluate the adsorption of indigo carmine dye from aqueous solutions on GLA-CS [91]. The thermodynamic results revealed an endothermic adsorption whereas a significant antagonistic interaction effect between the sorbent mass and temperature were observed via the factorial design. A series of GLA-CS sorbents were prepared by Pratt D. Y. et al. at variable chitosan/GLA (w/w) ratios using chitosan with low- and high-molecular weights (denoted as GLA-CSL and GLA-CSH), respectively, for the sorption of *p*-nitorphenolate and $HAsO_4^{2-}$ [92]. The adsorption capacities decreased with the increased GLA contents in the polymer for GLA-CSL; however, the Q_m values for GLA-CSH increased with the GLA contents. Notably, authors employed Sips isotherm model to obtain sorbent surface areas, which were well in agreement with their adsorption capacities. Baroni P. et al. have comparatively studied the batch adsorption of chromium ions on pristine chitosan, EPI-CS and GLA-CS membranes, respectively [80]. At pH 6.0, it is observed that GLA-CS possessed lower sorption capacity (29.5 mg g^{-1}) than those of pristine chitosan (65.7 mg g^{-1}) and EPI-CS (98.2 mg g^{-1}), while GLA-CS exhibited the best sorption at pH 2.0. These results verified that the Cr(VI) sorption occurred preferably with amine groups of chitosan, once they became unavailable after GLA cross-linking reaction.

To date, GLA is the most common cross-linker used with chitosan [93], due to its advantages compared with other common cross-linkers such as EPI: the good water solubility of GLA allows direct cross-linking reaction in aqueous media with a wide range of cross-linking degrees, while the water solubility of EPI is limited; GLA could be used under mild conditions, including alkaline, neutral, and in particular acidic solutions, where chitosan must be dissolved in diluted acetic acid prior to cross-linking [87], but EPI cross-linking only occurs under alkaline condition; moreover, GLA cross-linking does not need to add any auxiliary agents such as initiators, catalysts, and reducers. The main drawbacks of GLA cross-linking are its toxic potential in applications as well as the decline in the account of major sorption sites (amine groups) on chitosan. Vieira R. S. et al. have evaluated the capacities of Hg(II)

adsorption as 25.3, 30.3 and 75.5 mg g^{-1} for pristine chitosan, EPI-CS, and GLA-CS membranes, respectively at pH 6.0 [79]. GLA linked with amine group, but it showed the best adsorption ability. Authors interpreted that amino groups were unavailable in this situation, and other groups, such as imino bonds, unreacted aldehyde groups as well as unreacted hydroxyl groups from chitosan, play more important roles.

Table 2. GLA cross-linked chitosan and β-CD adsorbents.

Polysaccharide	Cross-linked form	Target adsorbate	Contact time (h)	pH	q_m (mmol g^{-1})	Ref
Chitosan	Co-polymer	*p*-nitrophenol	24	8.5	0.822	[92]
		As(V)			3.044	
Chitosan	Gel	Indigo carmine dye	4	4.0	0.237	[91]
Chitosan	Membrane	Hg(II)	24	6.0	0.376	[79]
Chitosan	Gel	U(VI)	5	4.0	0.618	[81]
Chitosan	Bead	Cu(II)	6	4.0	0.066	[82]
Chitosan 1%[a]	Bead	Pd(II)	48	-	1.175	[90]
		Au(III)			0.761	
Chitosan 3%[a]		Pd(II)			1.128	
		Au(III)			1.142	
Chitosan 5%[a]		Pd(II)			1.269	
		Au(III)			1.422	
Chitosan	Membrane	Cr(VI)	24	2.0	1.560	[80]
				6.0	0.567	
Chitosan, Fe_3O_4	Bead	Cu(II)	12	5.0	0.495	[94]
		Cd(II)			0.040	
		Pb(II)			0.045	
Chitosan, β-CD	Co-polymer	*p*-Nitrophenolate	24	8.5	1.83	[95]
		As(V)			0.602	

[a] different concentrations of GLA.

3.1.3 Ethyleneglycol diglycidylether cross-linker

Ethyleneglycol diglycidylether (EGDE), a non-toxic, and environmentally friendly cross-linker, possesses two epoxy groups, both of which have the same reactivity and are able to react simultaneously with the amino and hydroxyl groups of polysaccharides in aqueous solution under mild conditions (at about 50 ^{o}C) (**Table 3**) [49, 96]. To enhance their chemical resistance and mechanical strength, chitosan beads were cross-linked by EGDE at a cross-link ratio of 1:1 (EGDE:NH_2, mol:mol) and applied for the adsorption of dyes Acid Red 37 and Acid Blue 25 from aqueous solution (**Figure 8**) [62]. However, it was observed that the adsorption capacities of the chitosan beads for both acid dyes declined significantly after cross-linking (see **Table 3**). Authors explained that this is mainly because the EGDE cross-linking decreased the amount of NH_2 groups on chitosan, which were considered as the major sorption sites. To dissolve this problem, in another literature, the amino-groups of chitosan were shielded by formaldehyde before cross-linking, while the amino-groups were released by HCl treatment after EGDE cross-linking [97]. The amine-shielded EGDE cross-linked chitosan beads performed much better adsorption of Cu(II) in comparison with the beads cross-linked directly with EGDE. Moreover, EGDE has also been used as a cross-linker for CDs to prepare water-insoluble CDPs [63]. The EGDE cross-linked β-CDP displayed high adsorption abilities toward bisphenol A. Kono H. et al. reported the synthesis of β-CD incorporated carboxymethylcellulose (CMC) hydrogel beads (CDCMC) from β-CD and CMC by using EGDE as a cross-linker under alkaline conditions [98]. Authors indicated that the linkage positions of β-CD and CMC preferred at C6 and C6', respectively. Increase the molar feed ratio of β-CD to CMC lead to the increase of the degree of cross-linking as well as the increase of the adsorption abilities toward Bisphenol A.

Table 3. EGDE cross-linked chitosan and β-CD adsorbents.

Polysaccharide	Cross-linkers	Degree of cross-linking	Target adsorbate	Contact time (h)	pH	q_m (mmol g^{-1})	Ref
Chitosan	EGDE	-	Acid Red 37	1.67	6.0	0.116	[62]
			Acid Blue 25	2.33	4.0	0.343	
	Control	-	Acid Red 37	1.67	6.0	0.249	
			Acid Blue 25	2.33	4.0	0.632	
Chitosan	EGDE	-	Cu(II)	6	4.0	0.166	[82]
Chitosan	EGDE (Amine-Shielded)	-	Cu(II)	24	4.0	2.579	[97]
	EGDE	-	Cu(II)	24	4.0	1.896	
Chitosan	EGDE		Au(III)	4	2.0	0.863	[99]
			Pt(IV)			0.628	
			Pd(II)			1.131	
Chitosan	EGDE	-	U(VI)	5	4.0	0.284	[81]
β-CD	EGDE	6.21	Bisphenol A	24	-	0.344	[63]
	PEGDE[a]	4.22				0.313	
		5.11				0.260	
		5.76				0.216	
β-CD and CMC	EGDE	0.31	Bisphenol A	24	-	0.062	[98]
		0.88				0.096	
		1.6				0.146	
		1.9				0.167	

[a] Polyethylene glycol diglycidyl ether.

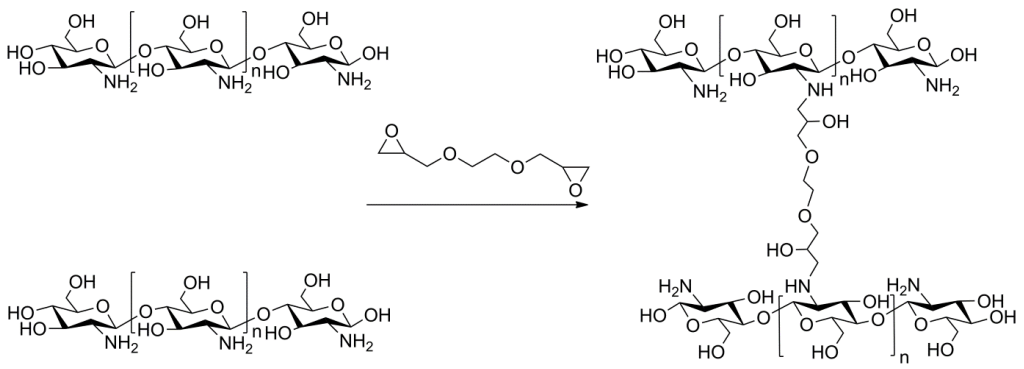

Figure 8. Synthesis schematic diagram of water-insoluble EGDE-cross-linked chitosan polymer.

3.1.4 Diisocyanates cross-linker

Diisocyanates, in particular 1,6-hexamethylene diisocyanate (HMDI) and tolylene-2,4-diisocyanate (TDI), have been also widely utilized as cross-linkers for chitosan and/or CDs since they possess two isocyanate groups (-N=C=O), which could react with amino or hydroxyl groups [100]. The less polar networks, obtained through cross-linking CDs with diisocyanates, have been shown helpful for the selective sorption of organic molecules, especially aromatic compounds. The diisocyanates cross-linked chitosan and β-CD adsorbent materials for water treatment are presented in **Table 4**. To ascertain the roles of the CD cavities and the cross-linking networks in the adsorption, the sorption of phenol and 1-naphthol from water by several β-CD polymers cross-linked by different cross-linking reagents (EPI, succinyl chloride, HMDI, and TDI) has been analyzed using isosteric heat approach, since these two studied sorbates possessed significant differences of affinity towards CD cavities and cross-linking networks [84]. Later, Romo A. et al. have compared the adsorption capacities of those CD polymers for the removal of phenol, *o*-cresol, *m*-cresol and *p*-cresol [101]. Both these studies concluded that for more polar networks, as in EPI-CDP, the CD units control the sorption; while in less polar networks, such as those of HMDI cross-linked β-CD polymer (HM-CDP), more sorbate molecules can be trapped by the crosslinking structures. Besides phenolic molecules, diisocyanates cross-linked CDPs are very effective toward dyes. A series of HM-CDPs with varying mole ratios of CD/HMDI (1:1, 1:3.7, and 1:10)

were synthesized in one step in *N,N'*-dimethylformamide (DMF) at 70 ^{o}C for 4 h [102]. The mole ratio of 1:3.7 HM-CDP displayed the best sorption efficiency toward azo dyes, especially Direct Violent 51. The possible sorption mechanism was attributed to the hydrogen bonding and other physical surfaces adsorption in the polymeric network, as well as the inclusion interaction due to β-CD cavity. These polymers were easily regenerated by using ethanol as washing solvent. CDs cross-linked with diisocyanates, have been reported to produce dimers and trimers of CDs in the network, which are adequately oriented to cooperatively bind large molecules such as steroids [49, 103].

Zha F. et al. have prepared chitosan beads bearing β-CD by two steps for the adsorption of hydroquinone [104]. Chitosan was firstly cross-linked with GLA by an inverse emulsion polymerization method to form microspheres, then the obtained GLA-CS microspheres were further cross-linked with β-CD by using HMDI as cross-linker in DMF (**Figure 9**). The substitution degree of β-CD in this product was determined as 4.3%. The adsorption capacity increased with increasing temperature and pH value, while the thermodynamic study revealed this adsorption is a spontaneous, endothermic and a random process. HMDI has also been used for the one-step immobilization of β-CD on chitosan, as a cross-linker [105, 106]. The hypothetical illustration of one-step cross-linking of chitosan with β-CD using HMDI as a cross-linker was shown in **Figure 10**. Under acidic conditions, an isocyanate (-N=C=O) reacted with hydroxyl group of chitosan, forming a urethane (-NH-CO-O-), via the proton transfer from hydroxyl of chitosan to nitrogen atom of isocyanate. Moreover, the other isocyanate could also react with hydroxyl group of β-CD to form a same urethane bond. In this hypothesis, HMDI could not bind to amino groups of chitosan but only hydroxyl groups due to the lower affinity for amino groups in comparison with hydroxyl groups at low pH conditions [107]. Based on these facts, Chiu S. et al. reported an adsorbent prepared by coupling β-CD to chitosan using HMDI. The produced β-CD-chitosan beads exhibited excellent sorption capacity (330 mg g^{-1}) for cholesterol. Moreover, 96% of adsorbed cholesterol could be dissociated by using 95% ethanol and the regenerated β-CD-chitosan beads retained 84% adsorption capacity after 12 uses [106]. More recently, a diisocyanate-modified chitosan was synthesized in aqueous acetic acid. A diphenyl methane diisocyanate

was employed as cross-linker. However, this report proposed that diisocyanate reacted with amino groups of chitosan to form urea bonds (-NH-CO-NH-) [108].

Diisocyanates cross-linking chitosan and/or CDs brings two main advantages: the versatile cross-linking networks for target molecule trapping and scaffolds, as a supplementary for adsorption; selective hosting of macromolecules via simultaneously inclusion with two or more adjacent CDs. However, this kind of cross-linkers also have drawbacks, as most of the cross-linkings are reacted in organic solvents such as DMF, as well as the nonspecific sorption with the cross-linkers through hydrogen bonding or hydrophobic interaction, although it could improve the uptake for some applications.

Table 4. Diisocyanates cross-linked chitosan and β-CD adsorbents.

Polysaccharide	Cross-linkers	Target adsorbate	Contact time (h)	pH	q_m (mmol g^{-1})	Ref
β-CD	4,4'-methylene-bis-phenyldiisocyanate (MDI)	Congo Red	3	5.8	0.052	[66]
β-CD	HMDI	Phenol	2.5	-	0.020	[84]
		Naphthol	1.5	-	0.104	
	TDI	Phenol	2.5	-	0.025	
		Naphthol	1.5	-	0.091	
β-CD	TDI	Remazol Red 3BS	4	2.0	0.042	[109]
Chitosan, β-CD	1) GLA; 2) HMDI	Hydroquinone	10	11	0.212	[104]
Chitosan, β-CD	HMDI	Cholesterol	1	-	0.853	[106]

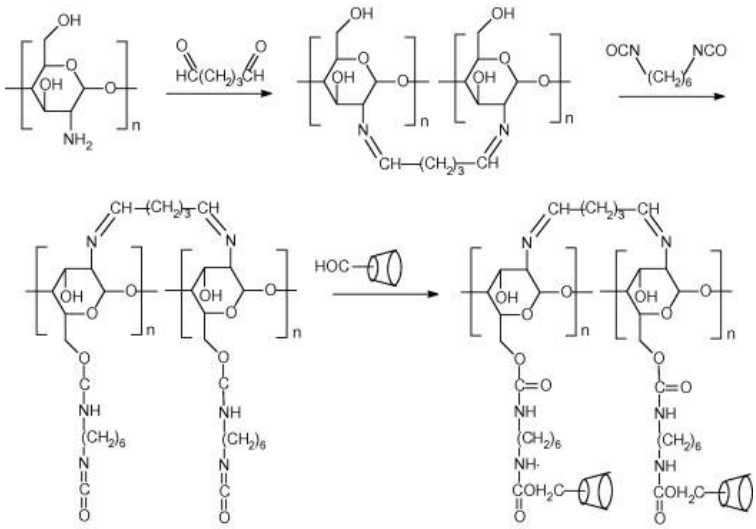

Figure 9. Preparation of chitosan beads bearing β-CD cross-linked by HMDI (Reproduced from ref.[104], with permission from Elsevier).

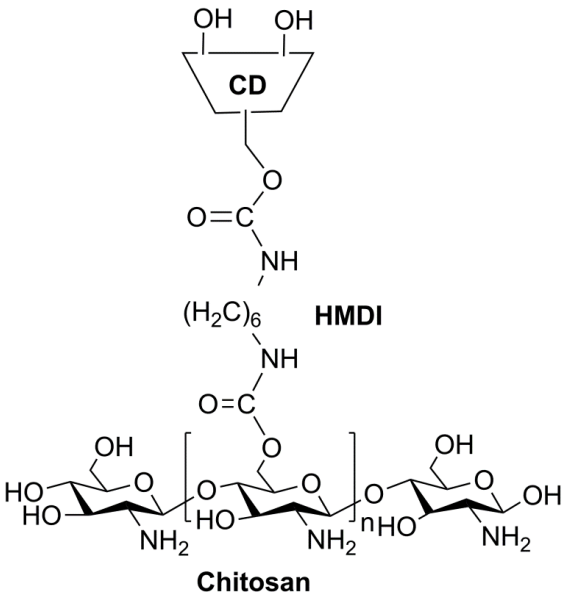

Figure 10. Hypothetical illustration of β-CD immobilized onto chitosan using HMDI as a cross-linker (modified from [106]).

3.1.5 Poly(carboxylic acid)s cross-linker

The cross-linkers discussed above either are toxic, expensive or could not provide sufficient reinforcement to the performance properties. Therefore, recently, some other cheaper, more environmentally friendly cross-linkers and new synthetic routes, have been proposed. Poly(carboxylic acid)s (in the term of PACs), a category of compounds containing two or more carboxyl groups, appeared to be promising inexpensive and sustainable cross-linkers which have been widely applied to enhance the performance abilities of cellulose and proteins in textile industries [110-112]. Malonic acid has been employed as a 'Green' cross-linker to cross-link films of native starches to enhance their mechanical properties and decrease the hydrophilicity [113]. Other PACs, such as succinic acid, malic acid, citric acid, 1,2,3,4-butane tetra carboxylic acid (BTCA), glutaric acid, and adipic acid, have all been used as relatively new cross-linkers for cross-linking of various polysaccharides such as cellulose [114], starch [115], CDs [116, 117], and chitosan [118, 119] via esterification reaction (**Table 5**). Reddy N. and Yang Y. proposed the mechanism of this esterification through an anhydride intermediate mechanism [115]. As seen from **Figure 11**, a cyclic anhydride of adjacent carboxylic acids was formed via intramolecular dehydration in the presence of acid catalysts, such as phosphates. The cyclic anhydride is a reactive intermediate and readily esterifies when reaction sites such as hydroxyl group of polysaccharides are available [120].

Among all these PACs, citric acid might be the most widely used in industries for cross-linking due to its natural source, low cost, biocompatibility and potent cross-linking ability [121]. Zhao D. et al. has reported the synthesis and applications of water-insoluble β-CD polymer (β-CDP) by using citric acid as cross-linker, sodium dihydrogen phosphate as catalyst and PEG-400 as modifier at 140 ^{o}C for 4 h. The as-produced β-CDP showed a much greater sorption capacity toward aniline than that of EPI-CDP, indicating the important role of carboxylate groups in the sorption toward aniline [122]. More later, three different polymers

P1, P2, and P3 (P1 containing both β-CD and carboxylate, P2 containing only β-CD and P3 containing only carboxylate), were comparatively studied by the same authors to adsorb aniline, 1-naphthylamine and methylene blue from waste water [123]. It was found that P1 containing both β-CD and carboxylate were overwhelmingly better than P2 and P3 in the romoval of the target pollutants. Its nontoxic raw materials and environmental friendly fabrication procedures, endow the citric acid cross-linked β-CD material potential to be an efficient and green sorbent for water purification. Ducoroy et al. applied citric acid cross-linked β-CD for the decontamination of water solutions containing Pb(II), Ni(II), and Cd(II) with adsorption capacity of 0.3 mmol g^{-1} for each cation [124]. An ion exchange mechanism was proposed and the metal uptake was not attributed to CDs, but to the unreacted carboxylic groups in the CD polymer.

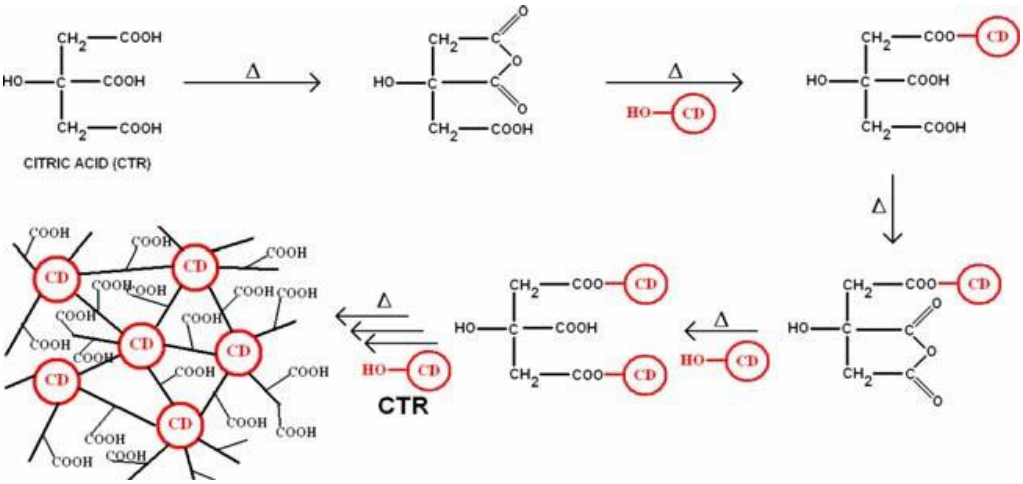

Figure 11. Reaction mechanism of polyesterification between citric acid and CDs (Reproduced from ref.[124], with permission from Springer).

Citric acid has also been employed to cross-link chitosan with alginic acid at varying conditions, which were optimized as curing at 180 °C for 9 min in presence of citric acid/sodium hypophosphite ratio of 1 and citric acid/polysaccharide ratio of 0.6 [119]. Hsieh S. H. et al. cross-linked chitosan to cotton fabrics by using BTCA and citric acid as cross-

linking reagents [125]. The cross-linking step was achieved via esterification and amidation at different curing temperatures and time. The presence of chitosan lead to a much better adsorption capacity of Cu(II) and Zn(II) than that without chitosan. The adsorption increased along with the raised curing temperature and time, and the best adsorption was observed at curing temperature of 150 ^{o}C and time of 8 min. The cross-linked material adsorb Cu(II) faster than Zn(II).

Generally, PCAs cross-linking of starch, CDs, and chitosan are more common in comparison with cellulose, due to their more easily accessible hydroxyl groups [115]. Moreover, PCAs with more carboxyl groups have better cross-linking effects such as cross-linking degree, and more effective properties such as tensile and adsorption. However, as an effective non-formaldehyde cross-linker, BTCA did not have industrial use as wide as citric acid, due to its high cost [121]. As a relatively new cross-linker, PACs take into account several good points: 1) relatively inexpensive and non-toxic reagents; 2) green, facile, water based reaction process; 3) tunable cross-linking degrees by adjusting PACs/polysaccharide ratio, and tunable linkage lengths by selecting different PACs; 4) functional groups (e.g. unreacted carboxylates) on the linkages for extra adsorption sites, while most of common cross-linkers reduce the adsorption sites; 5) the unreacted carboxylates are reactive and potential for further modification. The drawbacks of the PCAs cross-linking method are the high reaction temperature (> 140 ^{o}C), the use of sodium phosphate catalysts, and relatively low yields.

Table 5. PAC cross-linked chitosan and β-CD adsorbents.

Polysaccharide	Cross-linkers	Loaded COOH amount (mmol g^{-1})	Target adsorbate	Contact time (h)	pH	q_m (mmol g^{-1})	Ref
β-CD	Citric acid	0.55	Pb(II)	2	5	0.28	[126]
			Cd(II)			0.19	
			Zn(II)			0.29	
			Ni(II)			0.28	

	BTCA	0.90	Pb(II)			0.43	
			Cd(II)			0.31	
			Zn(II)			0.43	
			Ni(II)			0.40	
	PAA[a]	0.78	Pb(II)			0.19	
			Cd(II)			0.17	
			Zn(II)			0.19	
			Ni(II)			0.11	
β-CD	Citric acid	0.55	Pb(II)	1	2	0.28	[124]
			Cd(II)			0.19	
			Ni(II)			0.28	
β-CD	Citric acid	4.5	Aniline	1	-	0.104	[123]
			1-naphthylamine			0.184	
			Methylene Blue			0.200	
β-CD	Citric acid	-	Phenol	12	-	0.147	[127]
			Methylene Blue			0.329	

[a]PAA, Polyacrylic acid.

3.1.6 Dianhydrides cross-linker

As discussed in the case of PCAs cross-linkers, anhydrides are extremely active to react with amino and hydroxyl groups of polysaccharides. Various monoanhydrides, such as succinic anhydride [128, 129], maleic anhydride [130], phthalic anhydride, and trimellitic anhydride [131], have been immobilized on chitosan and CDs based materials to enhance their adsorption properties. In the most of these cases, however, the monoanhydrides, which contains only one anhydride group in their molecules, could not act as cross-linkers. To do so, the dianhydrides contains double carboxylic anhydrides within their structures, each of

which reacts readily with the specific functional groups, including amino and hydroxyl groups, to undergo cross-linking. Aliphatic dianhydride, such as 1,2,3,4-butanetetracarboxylic dianhydride (BTCAD), ethylenediaminetetraacetic acid dianhydride (EDTAD), diethylenetriaminepentaacetic acid dianhydride (DTPAD), and ethylene glycol-bis(2-aminoethylether)-N,N,N',N'-tetraacetic acid dianhydride (EGTAD), as well as aromatic dianhydrides, such as pyromellitic dianhydride (PMDA), benzophenone-3,3',4,4'-tetracarboxylic dianhydride (BTDA), 4,4'-(hexafluoroisopropylidene) diphthalic dianhydride (HFPD), and 4,4'-oxydiphthalic anhydride (ODPA), are the most frequently used dianhydrides for the cross-linking of chitosan and CDs. The structures of various dianhydride cross-linkers are represented in **Figure 12**. The dianhydrides are usually synthesized by the reaction of their PCAs with acetic anhydride in anhydrous pyridine or DMF at 65 ^{o}C (**Figure 13**) [132, 133]. The adsorption properties of dianhydride cross-linked chitosan and CD materials are presented in **Table 6**. In general, the dianhydrides play roles of not only as cross-linkers but also as functional groups.

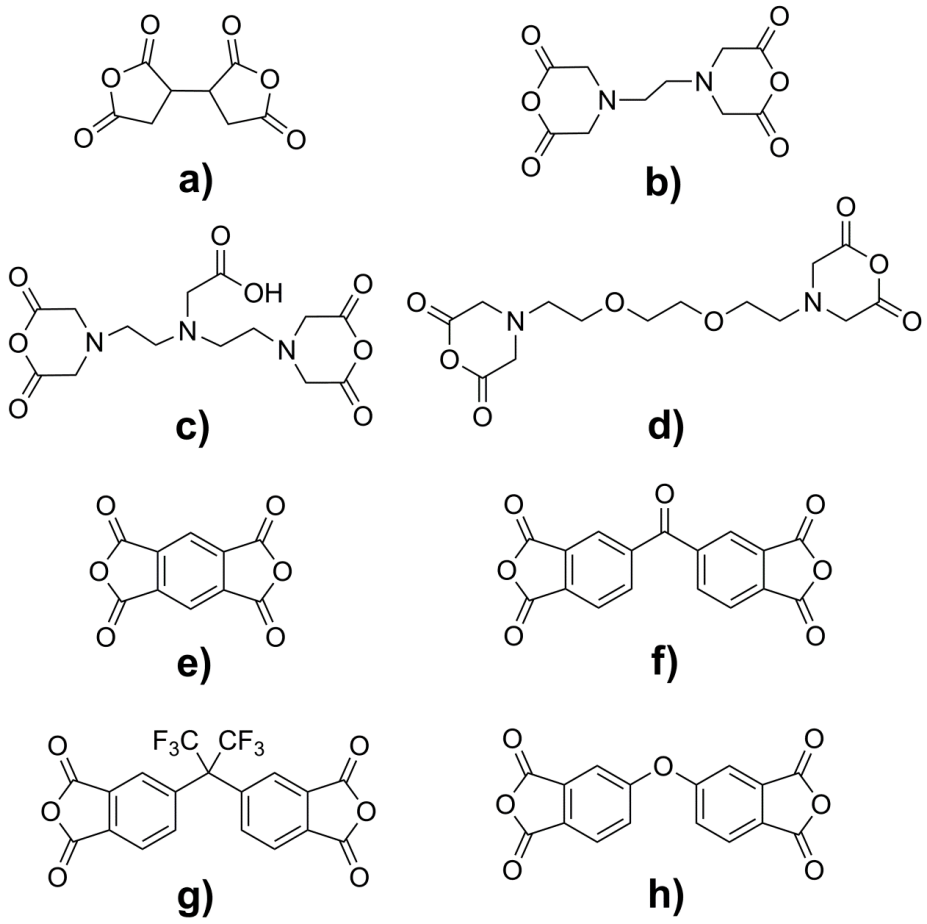

Figure 12. Structures of the most common dianhydrides for cross-linking. BTCAD (a), EDTAD (b), DTPAD (c), EGTAD (d), and aromatic dianhydrides: PMDA (e), BTDA (f), HFPD (g), and ODPA (h).

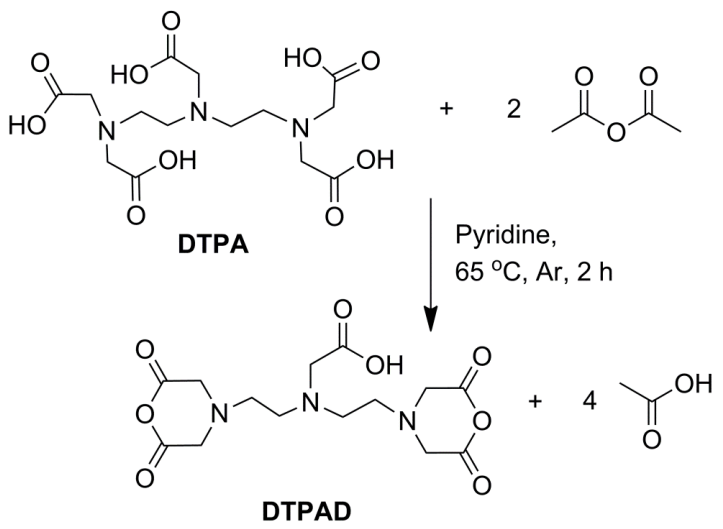

Figure 13. The synthesis of dianhydride (illustrated by the case of DTPAD).

BTCAD is the simplest dianhydride cross-linker containing two five-member cyclic anhydrides (**Figure 12** a). Several superabsorbent hydrogels were prepared from chitosan and cellulose dissolved in lithium chloride and N-methyl-2-pyrrolidinone (NMP) by using BTCAD as cross-linker under mild conditions [134]. The hydrogels performed the maximum water absorbency of 345 g water/ g polymer and excellent biodegradability by chitinase. Another chitosan hydrogel were synthesized in 10% aqueous acetic acid/NMP via one-step cross-linking of chitosan with BTCAD [135]. The molecular structure of the obtained hydrogel as showed in **Figure 14**a was determined by FT-IR and solid-state ^{13}C NMR spectroscopic analyses in detail. The hydrogel exhibited the maximum adsorption capacity (2.2 mg/mg) of bovine serum albumin (BSA) at pH 4.5 and a high desorption efficiency of 89% at pH 2.0. Later, the same authors synthesized a series of β-CDPs from β-CD by using BTCAD as a cross-linker and using pyridine as both the solvent and the catalyst (**Figure 14**b) [136]. The water solubility of the produced β-CDPs were found to be dependent on the BTCAD feed ratio as well as reaction temperature. Water insoluble β-CDPs were generated at high BTCAD feed ratios and high reaction temperatures. The BTCAD cross-linked β-CDPs were successfully used in the adsorption of bisphenol A (BPA) from aqueous solution. Interestingly, the lower

BTCA content thus higher β-CD content in the polymer obtained higher BPA sorption capacities.

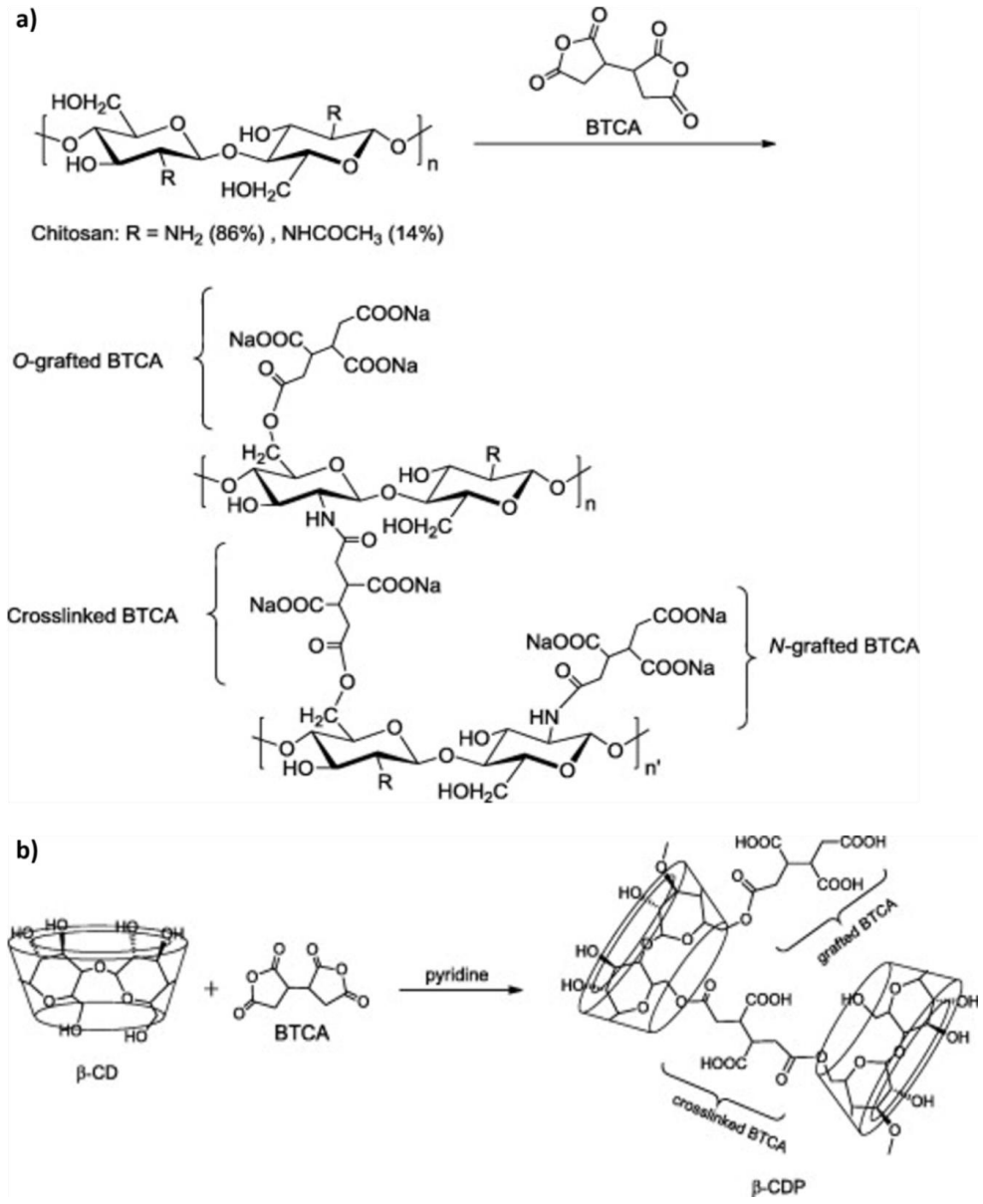

Figure 14. Depiction of the synthesis of chitosan polymer [135] (a) and β-CDP [136] (b) (Reproduced with permission from Elsevier) by using BTCAD as cross-linker.

EDTAD and DTPAD, biodegradable and powerful complexing agents which contain two anhydride groups in its molecule (**Figure 12**b and c), are frequently used to cross-link chitosan as well as introduce chelating abilities to the products through esterification reaction (**Figure 15**a) [137]. The esterification reaction mechanism involves the nucleophilic attack of the amino groups of chitosan on the carbonyl carbon of the anhydride groups (**Figure 16**). The popularity of EDTAD and DTPAD arise from their local availability, low price, as well as the strong metal chelating ability and stability of EDTA and DTPA [37]. Repo et al. have reported the synthesis of EDTAD and DTPAD cross-linked chitosan (in the term of EDCS and DTCS, respectively) in acetic acid/MeOH solution and applied for the adsorption of Co(II) and Ni(II) [132]. These modified chitosan materials displayed much better adsorption of the studied metals than pristine chitosan, indicating that the cross-linkers also played roles in metal binding. The adsorbents were found very stable in extreme pHs and reached a maximum adsorption at pH about 2.1 for Co(II) and at 1.1 for Ni(II), due to the speciation of EDTA and DTPA at those pHs. Authors also studied the competitive adsorption of Co(II) and Ni(II). Both EDCS and DTCS showed higher affinity for Ni(II) than for Co(II) in two-component systems. The adsorbents could be effectively regenerated by 2 M HNO_3. Later, EDCS and DTCS have been employed for the adsorption of rare earth elements (REEs) from acidic nitrate solutions [138]. DTCS had a slightly higher maximum loading capacity of Nd(III) as well as significantly larger equilibrium constant *K* values (obtained from Langmuir modeling) than those of EDCS, in agreement with the larger stability constant of Nd(III) with DTPA (log K = 21.6) than that of EDTA (log K = 16.6). In binary solutions, selectivity could be achieved by adjusting the pH of the feed solutions.

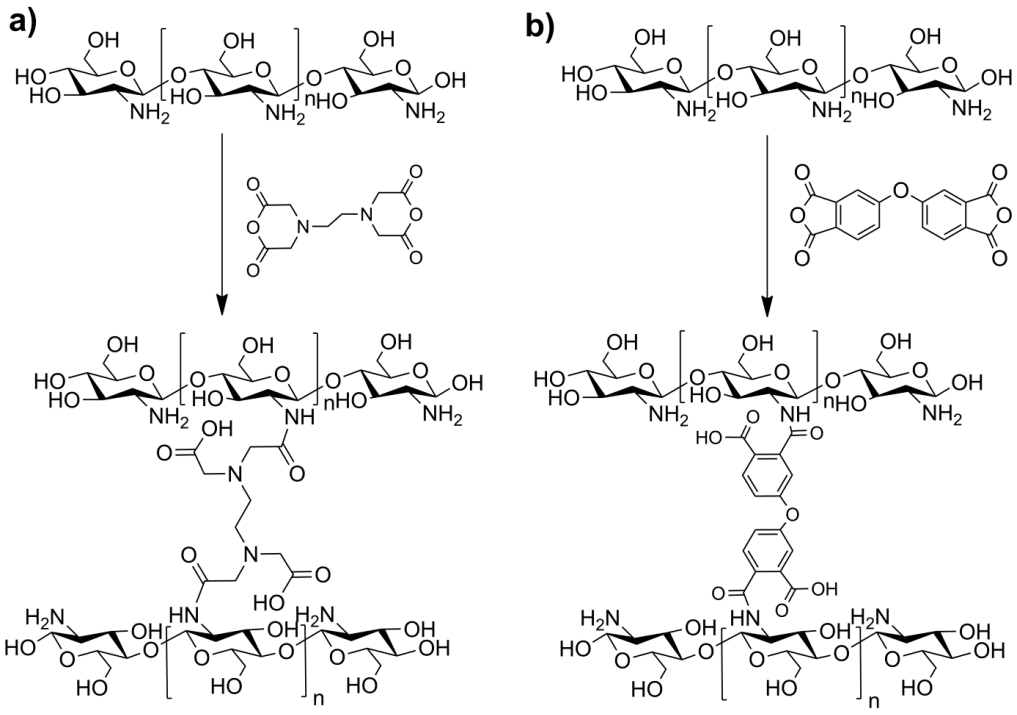

Figure 15. Synthesis of EDTAD (a) and ODPA (b) cross-linked chitosan.

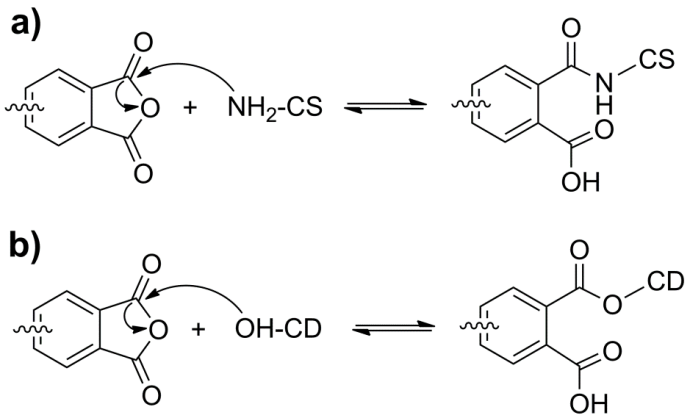

Figure 16. General nucleophilic substitution reaction mechanisms of chitosan (a) and CDs (b) with anhydride group.

EDTAD was also used for the cross-linking of chitosan-silica hybrid materials [38], which were synthesized by reacting 2 g of chitosan with 15, 30, 60 mL of tetraethylorthosilicate (TEOS). Amino groups of chitosan part made available for EDTAD cross-linking, while Silica part endowed the materials porous and rigid enhancing their mechanical properties, which is important in the column and chromatographic separation application. The material with highest chitosan content showed the best adsorption efficiency toward Co(II), Ni(II), Cd(II), and Pb(II) due to the highest amino amount available for EDTAD reaction. The kinetics study suggested the important of pore diffusion in the adsorption. Recently, in a similar synthesis way, DTPAD cross-linked chitosan-silica (DTPA-chitosan-silica) was synthesized and used for the recovery of Sc(III) from leachates of Greek bauxite residue [139]. In the separation of REEs from other elements, the chemical similarities between REEs and Fe(III) arise the most challenge. However, it was found difficult to achieve selectivity of Sc(III) and Fe(III) by DTPA-chitosan-silica due to the close stability constants of DTPA with Sc(III) (log K = 27.43) and with Fe(III) (log K = 28.60). Thus another chelating agent dianhydride cross-linker, EGTAD, which has a greater selective preference for REEs, was chosen to functionalize the chitosan-silica (EGTA-chitosan-silica) [139]. An exceptionally high selectivity for Sc(III) was verified in equimolar, binary solutions of Sc(III) and Fe(III), due to the much higher stability constants of EGTA with Sc(III) (log K = 25.40) than that with Fe(III) (log K = 20.50). Moreover, EGTA-chitosan-silica was exploited for the chromatographic separation of Sc(III) from other elements by a decreasing pH gradient with HNO_3.

Magnetic core-chitosan hybrid has raised attentions in water treatment due to the combination of the advantages of both magnetic cores (magnetic separation techniques) and chitosan (surface functionalization) [94]. An EDTA-chitosan magnetic adsorbent was facilely synthesized by cross-linking chitosan with EDTAD in presence of polyethylene imine (PEI) coated magnetic microspheres in an aqueous solution of acetic acid/MeOH. In this method, not only chitosan was cross-linked and functionalized by EDTA ligands, but also the magnetic cores were embedded in cross-linked chitosan at the same time. Furthermore, the amino groups of PEI coated magnetic microspheres provided availability to react with EDTAD, resulting in cross-linking between the magnetic cores and chitosan through covalent

bonds, which could inhibit the magnetic core leaking at acidic conditions. This adsorbent displayed excellent sorption properties for the removal of Pb(II) from aqueous solution at low pHs, and could also be effectively regenerated by 0.1 M Na_2EDTA solution [94].

Another similar synthetic route as depicted above was introduced by Almeida F. et al. for the preparation of a bifunctionalized chitosan material with zewitterionic properties [140]. However, they did not react dianhydride with amino groups, but the hydroxyl groups of chitosan. Prior to cross-linking by EDTAD, the amino groups of chitosan were quaternized by CH_3I at alkaline solution. Then the hydroxyl groups of the quaternized chitosan were esterified with EDTAD in anhydrous DMF. These combined reactions endowed the adsorbent both cationic (quaternary ammonium group) and anionic (carboxylic group) characteristics. The bifunctional groups were identified by FTIR and solid-state ^{13}C NMR spectroscopy. The carboxylic groups coordinated with divalent metals while quaternary ammonium groups with oxyanions of Cr(VI), where $HCrO_4^-$ and $Cr_2O_7^{2-}$ are the main species at the studied pHs. This bifunctional adsorbent possessed lower sorption capacities of Co(II) and Ni(II) compared to EDCS prepared by Repo [132] even though they had close EDTA content. This might be attributed to the antagonism effect between the cationic quaternary ammonium and anionic carboxylic groups.

Aromatic dianhydrides, including PMDA, BTDA, HFPD, and ODPA, are well-known as the monomers for the synthesis of polyimides [141] and famous for their excellent mechanical and thermal features and low water sorption [142]. To introduce the rigidity of chitosan polymer, chitosan dissolved in 0.1 M AcOH was cross-linked by using ODPA as cross-linker in N-methyl pyrrolidone (NMP) at 150 ^oC for 6 h (**Figure 15**b) [143]. The reinforcement effect of ODPA cross-linking toward chitosan was confirmed by thermogravimetry analysis (TGA) and dynamic mechanical analysis (DMA). The same year, some other authors used four symmetrical aromatic dianhydride cross-linkers, PMDA, BTDA, HFPD, and ODPA to cross-link chitosan in DMF, resulting in four hydrogels, which were further applied for the adsorption of seven kinds of metal ions [142]. The adsorption results showed that these aromatic dianhydrides cross-linkers significantly improved the metal uptake capacity of chitosan from

1.8 to 7.8 times. Authors explained that the cross-linkers were taking part in the metal uptake. More significantly, the rigid aromatic linkers were able to strengthen the mechanical abilities of chitosan, important for chromatographic application. PMDA has also been employed to graft with β-CD microspheres in DMF [144]. The adsorption capacities of Pb(II) and Cd(II) were significantly increased due to the presence of large number of carboxyl groups. The metal loaded β-CDP adsorbent could be successfully regenerated by 0.2 M HCl.

In the reaction of the polysaccharides with these dianhydrides, generally, two free carboxyl groups were formed while the chitosan chains or CD cavities were cross-linked. The advantage of this cross-linking method is the simultaneous introduction of functionalities and cross-links into the polysaccharides. Another advantage of this method is the mild reaction condition and high ligand loading without the need for derivatization procedures. Normally, the five-member cyclic dianhydrides (e.g. BTCAD and PMDA) are more effective in cross-linking polysaccharides in comparison with six-member cyclic anhydrides (e.g. EDTAD and DTPAD) [120]. In the case of chitosan cross-linking, due to the stronger nucleophilic ability, dianhydride cross-linkers tend to form the covalently bonds with NH_2 rather than OH. The dianhydride cross-linkers are interesting since they differ in the kind of the linkers to satisfy different applications. For instance, the most challenge of the CDs cross-linking is to obtain water-insoluble CDPs, thus high BTCAD feed ratios and high reaction temperatures were commonly used [136]. As an alternative, aromatic dianhydrides with rigid structure and hydrophobic group, especially the two inexpensive PMDA and BTDA, might be easier to generate water-insoluble CDPs. The defect of this cross-linking method is the uses of organic solvents in some of the cases.

Table 6. Dianhydride cross-linked chitosan and β-CD adsorbents.

Polysaccharide	Cross-linkers	Cross-linker amount (mmol g^{-1})	Target adsorbate	Contact time (h)	pH	q_m (mmol g^{-1})	Ref
Chitosan	EDTAD	1.43[a]	Cu(II) Co(II)	6	4.5	1.125 0.698	[140]

			Ni(II)		7.5	0.725	
			Cr(VI)	12	2	1.910	
Chitosan	EDTAD	1.4	Co(II)	24	2.1	1.069	[132]
			Ni(II)			1.210	
	DTPAD	0.96	Co(II)			0.833	
			Ni(II)			0.905	
Chitosan	EDTAD	99%[b]	Nd(III)	-	-	0.513	[138]
	DTPAD	94%[b]	Nd(III)	-	-	0.534	
Chitosan-silica	EDTAD	-	Co(II)	24	3.0	0.25	[38]
2:60			Ni(II)			0.30	
			Cd(II)			0.26	
			Pb(II)			0.24	
Chitosan-silica	EDTAD		Co(II)			0.42	
2:30			Ni(II)			0.44	
			Cd(II)			0.43	
			Pb(II)			0.43	
Chitosan-silica	EDTAD		Co(II)			0.63	
2:15			Ni(II)			0.61	
			Cd(II)			0.60	
			Pb(II)			0.62	
Chitosan-silica	DTPAD	-	Sc(III)	4	2.02	≈ 0.20	[139]
			Fe(III)			≈ 0.18	
	EGTAD	-	Sc(III)			≈ 0.16	
			Fe(III)			≈ 0.04	
Chitosan-Fe_3O_4	EDTAD	-	Pb(II)	24	4	1.014	[145]
Chitosan	PMDA	60%[b]	Cr(III)	14	6.0	0.697	[142]
			Mn(II)			1.222	
			Fe(II)			0.681	
			Co(II)			0.943	
			Ni(II)			0.800	

			Cu(II)	24		0.768	
			Zn(II)			1.177	
Chitosan	BTDA	65%[b]	Cr(III)	14		0.920	
			Mn(II)			0.892	
			Fe(II)			0.589	
			Co(II)			0.898	
			Ni(II)			0.865	
			Cu(II)	24		0.667	
			Zn(II)			0.840	
Chitosan	ODPA	41%[b]	Cr(III)	14		0.899	
			Mn(II)			0.582	
			Fe(II)			0.702	
			Co(II)			1.022	
			Ni(II)			0.883	
			Cu(II)	24		0.807	
			Zn(II)			1.108	
Chitosan	HFPD	41%[b]	Cr(III)	14		0.707	
			Mn(II)			0.423	
			Fe(II)			0.475	
			Co(II)			0.633	
			Ni(II)			0.713	
			Cu(II)	24		0.650	
			Zn(II)			0.318	
β-CD	BTCAD	1.496[c]	Bisphenol A (BPA)	12	-	0.178	[136]
		2.143[c]	Bisphenol A (BPA)			0.132	
β-CD microsphere	PMDA	-	Pb(II)	1	5.0	0.655	[144]
		-	Cd(II)		6.2	0.826	

[a] converted from the percent weight gain (*pwg*) presented in the literature.

[b] degree of substitution (DS) of the dianhydride.

[c] calculated from the molar ratio (n_{BTCA}) of BTCA to β-CD in β-CDP: $n_{BTCA}/(n_{BTCA} \times M_{BTCA} + 1 \times M_{CD})$.

3.1.7 Other cross-linkers

Besides the cross-linkers discussed above, other cross-linkers with bi/multifunctional groups, have also been studied, such as crown ether, glyoxal, divinyl sulfone, and succinyl chloride (**Table 7**).

Crown ethers, which are considered as the first generation of supramolecular macrocylic hosts, have excellent complex ability and selectivity towards many metals [146]. Several crown ether cross-linked chitosan adsorbents have been prepared by few researchers [146-149]. All of the syntheses were based on the reaction between the $–NH_2$ of chitosan and di-functional groups of the crown ethers, such as dialdehyde and diallyl. The crown ether cross-linking retained much higher metal uptake of chitosan and, at the same time, enhanced the acidic resistance of chitosan. More importantly, the cross-linked chitosan adsorbents possessed exceptional selectivity towards Pd(II), Hg(II) over Pb(II) and Ni(II). Some of the crown ether cross-linked chitosan adsorbents could be effectively regenerated by treatment with 0.1 M HCl and 0.1 M NaOH, successively. Glyoxal, the simplest dialdhyde, can cross-link polysaccharides via two ways: 1) through acetal formation between the aldehyde groups of glyoxal and the hydroxyl groups of CDs or chitosan; 2) through Schiff's base formation between the aldehyde groups of glyoxal and the amino groups of chitosan [150]. The glyoxal cross-linking might reduce the sorption efficiency especially in the case involving amino groups. To remedy the adsorption capacity, therefore, the efforts have been directed towards modification with chelating functionalities before glyoxal cross-linking [151, 152] or using dialdehyde containing metal complexing groups as cross-linkers [153]. Currently, the potential of divinyl sulfone (DVS) to act as a non-zero length cross-linker has been exploited for the preparation of novel water-insoluble CDPs by cross-linking pristine α-CD and β-CD [57]. The obtained CDPs are efficient for the removal of a variety of phenolic pollutants.

More recently, porous CDPs have raised concerns due to their high surface area and permanent porosity. Dichtel W.R. group prepared a porous β-CDP for rapid removal of organic micropollutants from water by cross-linking β-CD with rigid aromatic group, tetrafluoroterephthalonitrile (TFP) (**Figure 17**a) [1]. As shown in **Figure 17**b and c, the obtained porous TFP-CDP owned a Brunauer-Emmett-Teller surface area (S_{BET}) of 263 m^2 g^{-1}, while non-porous EPI-CD possessed the S_{BET} value of 23 m^2 g^{-1} as a control. The high surface and permanent porosity of the porous CDP allowed the rapid removal of organic pollutants from water. Later, the same authors grafted TFP-CDP onto cotton fabric by reacting β-CD, TFP, and cotton fabric in a 9:1 tetrahydrofuran (THF):H_2O solvent at 80 ^oC [54]. The obtained CD-TFP@cotton sequestered bisphenol A from water with a capacity 10-fold higher than that of pristine cotton fabric. A hyper-cross-linked porous β-CDP was synthesized by cross-link benzylated-β-CD with formaldehyde dimethyl acetal (FDA) as a cross-linker and $FeCl_3$ as a Lewis acid catalyst *via* a simple Friedel-Crafts alkylation route [154]. Notably, the obtained CDP owned a superior S_{BET} value of 1225 m^2 g^{-1} and a total pore volume of 1.71 cm^3 g^{-1}, resulting from not only the inherent CD cavities but also the rigid and contorted benzene rings. The hyper-cross-linked CDP adsorbent displayed super high sorption capacity of 4-chlorophenol, which exceeded the amount of CD cavities in the adsorbent (up to 330 % in molar ratio). This revealed that the sorption occurred not only in the CD moieties via 1:1 inclusion complexation, but also in the nanopores of the hyper-cross-linked polymer.

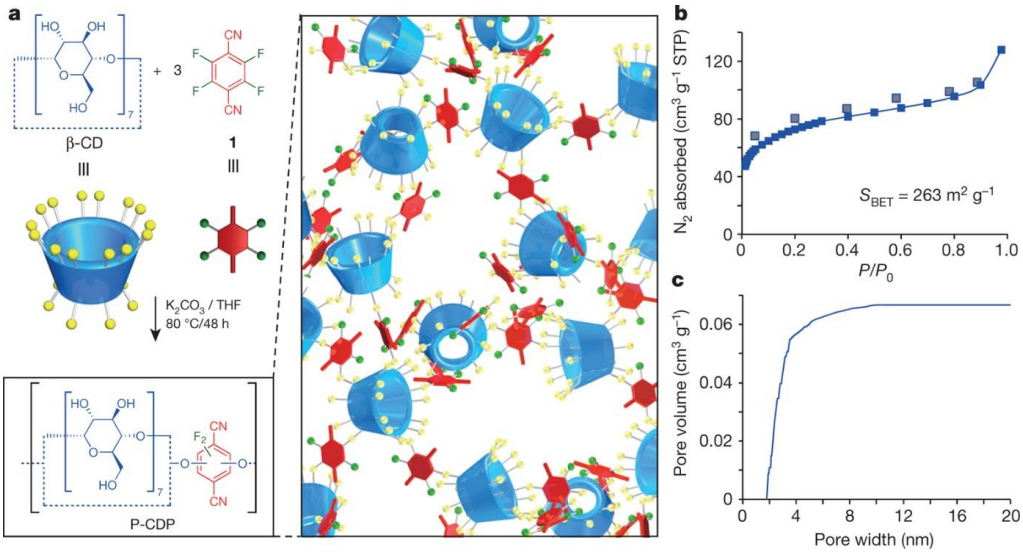

Figure 17. The synthesis schematic of the porous tetrafluoroterephthalonitrile-cross-linked β-CDP (a) and the results of its BET surface area (b) and cumulative pore volume (c). (Reproduced from ref. [1], with permission from Nature Publishing Group).

Table 7. Other cross-linked chitosan and β-CD adsorbents.

Polysaccharide	Cross-linkers	Target adsorbate	Contact time (h)	pH	q_m (mmol g^{-1})	Ref
Chitosan	N,N'-diallyl dibenzo 18-crown-6 crown ether	Pd(II)	8	4.0	2.331	[147]
		Ag(I)			1.463	
		Cu(II)			0.538	
		Pb(II)			0.084	
		Cd(II)			0.068	
		Ni(II)			0.139	
		Co(II)			0.112	
Chitosan	4,4'-diformyldibenzo-	Pb(II)	24	6.0	1.18	[149]
		Hg (II)			1.58	

	18-crown-6 crown ether					
Chitosan	N-allyl benzo 15-crown-5 crown ether.	Pd(II) Ag(I)	8	4	0.900 0.836	[148]
Chitosan	6,6'-piperazine-1,4-diyldimethylenebis (4-methyl-2-formyl) phenol	Cu(II) Ni(II) Co(II) Mn(II)	4	6.5	1.21 0.65 0.46 0.43	[153]
Chitosan-Fe_3O_4	Glyoxal	Cu(II) Co(II) Ni(II)	8	5.0	1.496 1.017 0.801	[150]
Chitosan-Fe_3O_4	2-aminopyridine-glyoxal	Cu(II) Cd(II) Ni(II)	8	5.0	1.953 0.747 1.142	[155]
Chitosan	N-N'-[bis(2-hydroxy-3-formyl-5-methylbenzyl-dimethyl)]-ethylenediamine	Cu(II)	2	6.1	1.79	[156]
α-CD 1:1[a]	Divinyl sulfone	Phenol 4-nitrophenol Bisphenol A β-naphthol	3	-	0.655 1.068 0.523 0.521	[57]
α-CD 2:1[a]		Phenol 4-nitrophenol			1.035 1.069	
β-CD 1:1[a]		Phenol			0.720	

		4-nitrophenol			1.440	
		Bisphenol A			0.303	
		β-naphthol			0.506	
β-CD	Succinyl chloride	Phenol	2.5	-	0.041	[84]
		Naphthol	1.5		0.110	
β-CD	FDA	4-nitrophenol	24	-	0.47	[154]
		Phenol			0.65	
		4-chlorophenol			1.10	
β-CD	Tetrafluoro-terephthalonitrile	Bisphenol A	0.17	-	0.385	[1]

[a] The stoichiometric molar ratios of divinyl sulfone/glucose unit.

In general, the cross-linking reinforces the mechanical resistance, reduces the water solubility, and enhances the chemical stability of chitosan and CDs in acidic and alkaline aqueous solutions as well as organic solvents. In addition, most of the cross-linked polysaccharides could be easily regenerated by washing with acid solutions or organic solvents. However, the cross-linking also decreases the amounts of free and available hydroxyl groups or amino groups on the surface of the polysaccharides. Moreover, the cross-linking forming polymer network could reduce the flexibility, the mobility and the crystallinity of the pristine polysaccharides, and hence the accessibility to adsorption sites. Therefore, the cross-linking might result in a considerable reduction of adsorption ability of the polysaccharides, especially in the case that amino groups involved. To minimize these negative effects and also improve the adsorption capacities, efforts have been made to keep the degree of cross-linking as low as possible, followed by further surface modification on the cross-linked chitosan and CDs.

3.2 Surface modification of cross-linked chitosan and CD adsorbents

Chemical surface modification to improve the adsorption and selectivity characteristics of polysaccharides has received a particular attention. Despite the amino groups or hydroxyl groups were attacked by cross-linkers during cross-linking, a part of free amino or hydroxyl groups could still remain on the surface of chitosan and CDs, providing feasibility for further chemical modification. The modification are able to increase the density of the sorption sites as well as introduce various new functional groups on the cross-linked polymers. The new functional groups might change the surface polarity and hydrophilicity, leading to affinity for polar sorbates and hence adsorption selectivity toward the target pollutants. Even though the modification decorates the properties of chitosan and CDs, importantly, most of the surface modification does not change the inherent characteristics of the polysaccharides, such as muco-adhesivity, host-gust inclusion ability, biocompatibility, and biodegradability [27]. The amino groups, carboxyl groups, and sulfur groups, have been regarded as the most studied functional groups for the surface modification of cross-linked chitosan and CDs for the purpose of water treatment.

3.2.1 Functionalized with amino groups

The method of amination can introduce extra amino groups to the polymer, improving the adsorption ability for anionic dyes or metal ions (**Table 8**). It is known that modification by NH_4OH is a facile, convenient and inexpensive way of introduction amino groups into polysaccharides [157]. Several water-insoluble cross-linked polysaccharides containing tertiary amino groups have been synthesized by cross-linking starch-enriched flour with EPI in the presence of NH_4OH. These weakly basic adsorbents have been successfully applied for the removal of various anionic [157] and non-ionic [158] dyes and phenolic derivatives [159] from aqueous solutions. The results showed that the presence of the tertiary amine groups could enhance the adsorption performance of the polymers. Moreover, the adsorption kinetics and adsorption capacities were dependent on the amount of the presence of tertiary amine groups in the polymer networks. Anirudhan T. S. and Rijith S. have immobilized ethylenediamine (EDA) on the GLA cross-linked chitosan beads, obtaining an

efficient adsorbent for the removal of Cu(II) from aqueous solution [64]. The as-prepared chitosan adsorbent was also successfully applied for the treatment of practical electroplating industry wastewater with an initial Cu(II) concentration of 0.32 mmol L^{-1}. The regeneration of the used EDA-chitosan adsorbent was achieved by washing with 0.1 M HCl. EDA-modified chitosan was also employed for the removal of anionic dye Eosin Y from aqueous solution [160]. The preparation of EDA-chitosan in this work was carried out in three steps, including the preparation of chitosan gel beads, the cross-linking with EPI, and then followed by the modification with EDA. The EDA-modified chitosan possessed a much higher adsorption capacity of eosin Y in comparison with unmodified chitosan bead. Moreover, the modified chitosan displayed satisfactory chemical stability in acid medium. Thus the EDA-chitosan could be used as a low-cost and efficient adsorbent for the removal of anionic dye from wastewater. Later, the same authors modified EPI cross-linked chitosan with tetraethylenepentamine (TEPA), which owns more imino groups in longer chain than EDA [161]. The authors predicted the TEPA-modification would result in better adsorption capacity toward anionic dye than EDA-modification. Finally, however, the TEPA-CS exhibited a close maximum adsorption capacity (0.451 mmol g^{-1}) of eosin Y to that of EDA-CS (0.453 mmol g^{-1}). This might be attributed to the different amounts of the functional groups immobilized on the surface of the cross-linked chitosan. EDA has also been widely used to functionalize GLA or EPI cross-linked magnetic chitosan and the modified magnetic chitosan adsorbents have been successfully applied for the adsorption of Cr(VI), Hg(II), Pt(IV), and Pd(II) from aqueous solution (**Figure 18**) [162-164]. The amino groups have been popularly introduced to β-CDs through a route of tosylation of β-CD by toluenesulfonyl chloride (TsCl) and followed amination with EDA [50, 165, 166]. The active amino groups of these aminated CDs endowed CDs availability of further cross-link reactions [167].

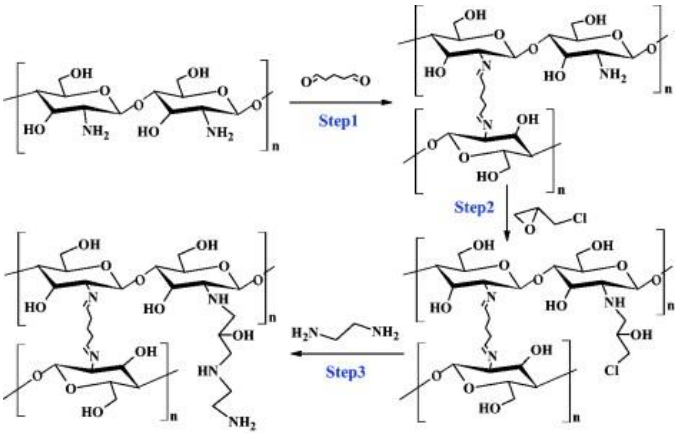

Figure 18. Scheme for the synthesis of EDA-modified cross-linked magnetic chitosan resin (Reproduced from ref.[162], with permission from Elsevier).

Polyethylenimine (PEI), which is composed of abundant amine groups on the line or dendrimeric type macromolecules, exhibits strong ability to complex metal ions [168]. The adsorption capacities of EPI cross-linked chitosan (EPI-CS) beads before and after PEI grafting have been investigated by Chatterjee S. et al [169]. It was found that the adsorption performance of EPI-CS was significantly enhanced through PEI modification, i.e. the maximum adsorption capacity of PEI functionalized EPI-CS was 3.51 times higher than that of unmodified EPI-CS. This could be attributed to the introduction of plenty of binding sites (polyaminated groups) on the surface of the chitosan beads during the modification. Kyzas G. et al. have grafted amido and imino groups on the cross-linked chitosan by reactions with acrylamide (AM) and PEI, respectively [170]. The obtained chitosan adsorbents were applied for the treatment of real industrial dyeing effluents which composed three reactive dyes: Remazol Red 3BS, Remazol Blue RN, and Remazol Yellow Gelb 3RS. The adsorption capacity followed the order PEI-modified chitosan > AM-modified chitosan > unmodified chitosan (only cross-linked). Only PEI-modified chitosan could approvingly reduce the dye concentration of the practical effluent below the legislation limit of 300 ADMI units (American Dyestuff Manufacturer Institute). The results suggested that PEI-modified chitosan was an effective adsorbent for the wastewater treatment.

Polyamidoamine (PAMAM), constructed based on an EDA core, repetitively amides, and terminated with amino groups, is a class of highly branched, well defined, and commercialized dendrimer. Li N. and co-workers have reported the synthesis of an insoluble cross-linked β-CD polymer functionalized with PAMAM (generation 2) (in the term of PAMAM-CD) [171]. The produced PAMAM-CD polymer exhibited high adsorption capacities and excellent removal efficiencies toward both the metal ions and organic pollutants. Notably, the maximum adsorption capacities of all the organic compounds (0.495 - 1.035 mmol g^{-1}) were found to be higher than the β-CD amount in the polymer (0.360 mmol g^{-1}) obtained from elemental analysis. So it seemed that the plenty of amino groups on PAMAM-CD accounted for a part of the sorption capacity when assuming a 1:1 organic adsorbate:β-CD complex stoichiometry. The PAMAM-CD polymer was further applied for the removal of chlorophenols from aqueous solutions [172]. The adsorption capacities for the studied three chlorophenols followed the order 2,4,6-trichlorophenol > 2,4-dichlorophenol > 4-chlorophenol. The authors explained this was mainly attributed to: i) inclusion effect. The guest molecules with more hydrophobicity would have greater inclusion interaction with the hydrophobic CD cavities. The hydrophobic coefficient of chlorophenols increased with the degree of chlorination; ii) hydrogen bonding between the $–NH_2$, -NH or –OH groups of PAMAM-CD and the –OH groups of chlorophenols. The more chlorine atoms the stronger hydrogen bonds, due to the electron-withdrawing effect of chlorine on phenyl rings. The used PAMAM-CD could be regenerated by washing with ethanol for five times.

Table 8. Amino-modified cross-linked chitosan and β-CD adsorbents.

Polysaccharide	Cross-linkers	Modifier	Target pollutants	Time (h)	pH	q_m (mmol g^{-1})	Ref
Chitosan	GLA	EDA	Cu(II)	3	6.0	3.24	[64]
Chitosan	EPI	EDA	Ecosin Y	24	5	0.453	[160]
Chitosan	GLA	EDA	Hg(II)	3	5.1	2.3	[172]
			UO_2(II)		3.9	1.9	
Chitosan	EPI	TEPA	Eosin Y	24	5	0.451	[161]
Chitosan-	GLA	EDA	Cr(VI)	1	2.0	0.938	[162]

Fe_3O_4							
Chitosan-Fe_3O_4	EPI	EDA	Hg(II)	4	5	2.69	[163]
Chitosan-Fe_3O_4	EPI	EDA	Pt(IV)	1	2.0	0.877	[164]
			Pd(II)			1.300	
Chitosan	EPI	DETA	Pd(II)	8	4.0	1.29	[173]
			Ag(I)			1.15	
			Ni(II)			0.52	
			Cu(II)			0.57	
			Co(II)			0.14	
			Cd(II)			0.33	
Chitosan	EPI	PEI	Reactive Black 5	24	6	0.715	[169]
Chitosan	GLA	PEI	Remazol Red 3BS	24	10	1.243	[170]
			Remazol Yellow Gelb 3RS			1.358	
			Remazol Blue RN			2.123	
		AM	Remazol Red 3BS			1.025	
Starch	EPI	NH_4OH	Beta-naphthol	1	6	0.132	[159]
			Para-naphthol			0.176	
			Para-chlorophenol			0.062	
			Pentachlorophenol			0.069	
β-CD-MGO	TsCl	EDA	Cr(VI)	24	3	1.172	[167]
β-CD	TsCl	PAMAM	Pb(II)	28	4.8	0.482	[171]
			Cu(II)	18	4.8	1.705	

			2,4-Dichlorophenol	2	6	0.620	
			2,4,6-Trichlorophenol	3	4	1.035	
			Ponceau 4R	9	5.6	0.495	
β-CD	TsCl	PAMAM	4-Chlorophenol	1.5	4.8-9.2	0.132	[172]
			2,4-Dichlorophenol	1.5	4.8-9.2	0.609	
			2,4,6-Trichlorophenol	2.2	3.8-5.4	0.887	

3.2.2 Functionalized with carboxyl groups

Carboxyl groups, which act as acid by donating a proton and coordinating with metal ions and cationic organic compounds, do not exist in the pristine chitosan and CDs. They typical carboxylic-modified cross-linked chitosan and β-CD adsorbents are presented in **Table 9**. To improve the adsorption capacity of Pb(II) ion, succinate anhydride was grafted onto chitosan that had been cross-linked by EGDE, diethylene glycol diglycidyl ether (DEGDE), and bisphenol A diglycidyl ether (BADGE), resulting in Suc-EGDE-CS, Suc-DEGDE-CS, and Suc-BADGE-CS, respectively [174]. The maximum Pb(II) uptake of the produced three adsorbents occurred at pH 5, which was in good agreement with the pKa value (4.6) of carboxylate group. The adsorption capacities of Pb(II) followed the order: Suc-EGDE-CS < Suc-DEGDE-CS << Suc-BADGE-CS. Authors explained that the cross-linker BADGE with benzene ring, which was rich with an electron, could bind Pb(II) through π electrons on its ring, resulting in the best adsorption of Pb(II). Özkahraman B. et al. have grafted itaconic acid and crotonic acid onto the cross-linked chitosan beads by using ammonium persulfate as initiator [175]. The adsorption kinetics and isotherms of a cationic dye (Brilliant Green) onto the modified chitosan beads were investigated. The itaconic acid modified chitosan displayed higher

adsorption capacity of Brilliant Green in comparison with crotonic acid modified chitosan, might due to the higher amount of carboxyl groups on itaconic acid modified chitosan. Poly(methacrylic acid) (PMAA) modified GLA-CS microspheres have been prepared and applied for the removal of cationic dyes from aqueous solution, such as Methylene Blue and Malachite Green [176]. The adsorption capacities of the PMAA-GLA-CS microspheres were enhanced 10 times for Methylene Blue and 15 times for Malachite Green, respectively, in comparison before the modification. The aromatic dianhydride, PMDA, has been grafted on GLA-CS beads, significantly improving the adsorption of cationic dyes from printing and dyeing effluents [177].

Shimizu synthesized novel chitosan-based materials by using 7-ethyl octadecane diacid diglycidyl (EODD) as a cross-linker, and the EODD-CS materials were further modified by EDTAD in DMSO solvent at 60 ^{o}C for 24 [178]. The adsorption results showed that the addition of EDTA residues on the cross-linked chitosan significantly enhanced the adsorption properties toward metal ions, and the metal uptake abilities of the obtained adsorbents were depended on the amount of free EDTA groups. Ge H. and Huang S. proposed another EDTA modification route that EDTAD reacted with EPI O-cross-linked chitosan under microwave irradiation (**Figure 19**) [83]. The amino groups of chitosan were protected by benzaldehyde during O-cross-link, leading to higher EDTA functionality and thus higher metal uptake. More recently, several EDTA-functionalized magnetic chitosan were fabricated and applied for the removal of cationic dyes [179, 180] and metal ions from aqueous solution [94]. As seen in **Figure 20**, the adsorbent was prepared by surface modification of magnetic cross-linked chitosan with EDTA using water-soluble carbodiimide as the coupling agent.

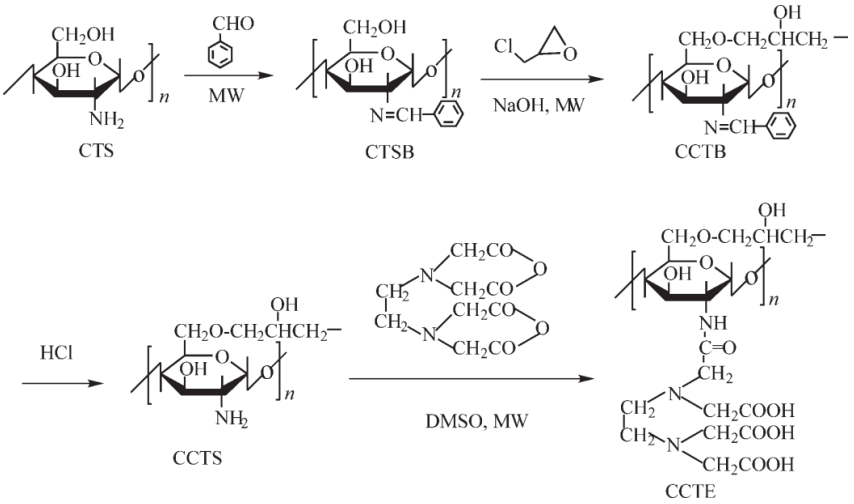

Figure 19. The synthetic route of EDTA-functionalized EPI O-cross-linked chitosan (Reproduced from ref.[83], with permission from Wiley).

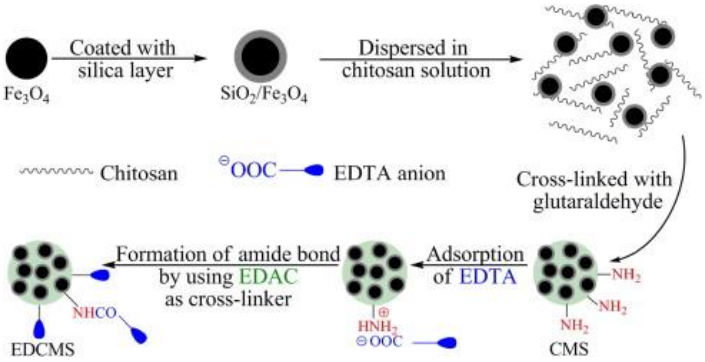

Figure 20. The procedure for preparation of GLA cross-linked chitosan/SiO_2/Fe_3O_4 gel and magnetic EDTA-modified chitosan/SiO_2/Fe_3O_4 adsorbent (Reproduced from ref.[94], with permission from Elsevier).

Grini G. and Peindy H. grafted carboxymethylcellulose (CMC) onto EPI cross-linked β-CD to confer the ability to adsorb basic dyes on the polymer beads [71]. It was observed that the presence of carboxyl groups in the polymer improved significantly the sorption properties, due to the adsorption mechanism through electrostatic interactions between COO^- groups and the cationic groups of Basic Blue 9. Moreover, the carboxyl groups immobilized onto CD

might serve as electron donors in an alkaline media to endow the CD cavities ability to adsorb basic dyes. Iminodiacetic acid (IDA), as a carboxyl ligand, has been bond with the EPI cross-linked β-CD to increase the binding affinity toward metal ions and α-amylase [181]. Li F. and co-workers have grafted PMDA onto the surface of TDI cross-linked β-CD microspheres introducing a large number of carboxyl groups for the removal of Pb(II) and Cd(II) from aqueous solution [144]. The adsorption capacities of the PMDA modified β-CD microspheres for the studied metals were 7.7-10.7 times higher than those of unmodified ones. The metal loaded CD microspheres could be regenerated with 0.2 M HCl.

Table 9. Carboxylic-modified cross-linked chitosan and β-CD adsorbents.

Polysaccharide	Cross-linkers	Modifier	Target pollutants	Time (h)	pH	q_m (mmol g^{-1})	Ref
Chitosan	EGDE	Succinate anhydride	Pb(II)	2	5	0.333	[174]
	DEGDE					0.355	
	BADGE					0.898	
Chitosan	EPI	Itaconic acid	Brilliant Green	-	-	0.280	[175]
		Crotonic acid				0.224	
Chitosan	GLA	N-(2-carboxybenzyl)	Pramipexole dihydrochloride	24	10	1.080	[35]
Chitosan	GLA	PMAA	Methylene Blue	12	7.1	3.126	[176]
			Malachite Green		4.2	1.435	
Chitosan	GLA	PMDA	Methylene Blue	-	5	2.923	[177]
			Neutral Red			3.148	
Chitosan	EODD	EDTAD 1[a]	Ni(II)	72	6	≈ 0.75	[178]
		EDTAD 2[b]	Ni(II)			≈ 1.3	
			Cu(II)			≈ 1.5	

			Cd(II)			≈ 1.25	
			Pb(II)			≈ 1.25	
			Ca(II)			≈ 0.72	
Chitosan	EPI	EDTAD	Pb(II)	4	5	1.28	[83]
			Cu(II)			2.13	
			Cd(II)			1.29	
			Ni(II)			1.34	
			Co(II)			1.28	
Chitosan-Fe_3O_4	GLA	EDTAD	Methylene Blue	0.5	7	0.35	[179]
Chitosan-Fe_3O_4	GLA	EDTAD	Methylene Blue	0.5	6.0	0.354	[180]
Chitosan-SiO_2-Fe_3O_4	GLA	EDTA	Cu(II)	12	5.0	0.699	[94]
			Pb(II)			0.596	
			Cd(II)			0.563	
β-CD	EPI	CMC	Basic Blue 9	2	8	0.177	[71]
β-CD	EPI	CMC	Basic Green 4	2	8	0.252	[182]
β-CD	EPI	CMC	Basic Blue 3	2	8	0.133	[183]
			Basic Violet 3			0.104	
			Basic Violet 10			0.075	
β-CD	TDI	PMDA	Pb(II)	1	5.0	0.656	[144]
			Cd(II)		6.2	0.829	

[a] The amount of free EDTA groups on the modified adsorbent 1.44 mmol g^{-1}.

[b] The amount of free EDTA groups on the modified adsorbent 1.64 mmol g^{-1}.

3.2.3 Functionalized with sulfur groups

Sulfur-containing functional groups, such as thiol, thiourea, sulfonate and xanthate, are known to bind strongly with most trace metals [184] and cationic compounds [35]. Moreover, sulfur-containing groups trend to form strong coordination bonds with metal ions and could enhance metal adsorption selectively [184]. A large number of studies have been carried out on the sulfur modification of cross-linked chitosan and CDs (**Table 10**).

Similar to carboxyl groups, sulfo/sulfonate groups ($-SO_3H/-SO_3^-$) were supposed to enhance the adsorption properties of polysaccharides as well. A sulfonate group modified β-CD polymer was prepared by using EPI as cross-linker and tiron (1,2-dihydroxybenzene-3,5-disulfonic acid disodium salt) as modifier in three steps (**Figure 21**) [185]. The sulfonate functionality was determined to be 0.174 mmol g^{-1} by elemental analysis. The modified CDP was found to achieve an enhanced adsorption capacities in comparison with unmodified EPI-CDP toward methylene blue and basic magenta but phenolphthalein. This could be ascribed to the fact that the sulfonate groups attract the cationic amine groups of methylene blue and basic magenta but repel anionic carboxyl groups of phenolphthalein during adsorption. Based on the similar mechanism, the adsorption capacities of sulfonate modified starch polymers toward aniline increased with the increasing amounts of sulfonate groups loaded on the polymers [186]. Kyzas G. et al. grafted sulfonate or carboxybenzyl groups on GLA-cross-linked chitosan and the produced adsorbents were applied for the removal of pharmaceutical contaminant, pramipexole dihydrochloride, from environmental wastewaters [35]. The adsorption experiments showed a higher q_m value (1.186 mmol g^{-1}) of sulfonate modified chitosan than that of carboxybenzyl modified chitosan (1.080 mmol g^{-1}) since the amino groups of pramipexole dihydrochloride could interact with sulfonate groups via stronger electrostatic force in comparison with carboxyl groups (see **Figure 22**).

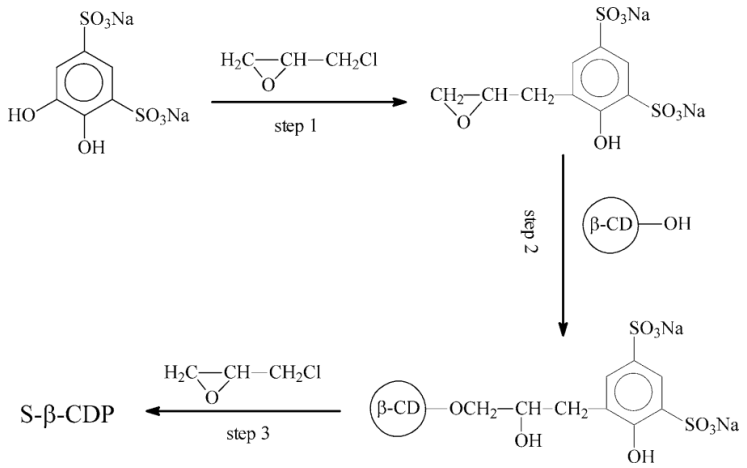

Figure 21. Reaction mechanism of the preparation of sulfonate modified β-CDP (Reproduced from ref.[185], with permission from Springer).

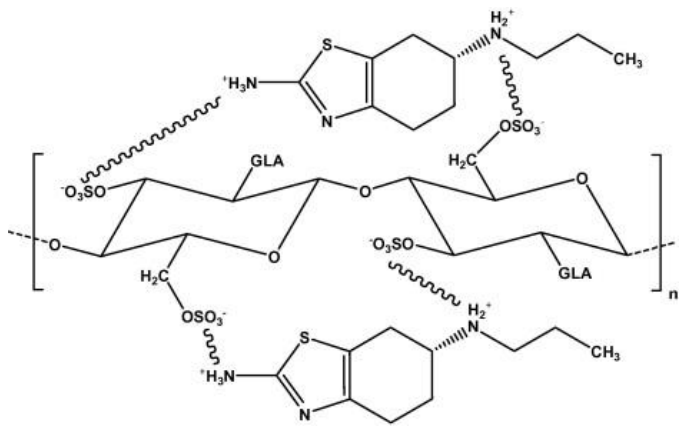

Figure 22. Adsorption mechanism of pramipexole dihydrochloride on sulfonate modified chitosan (Reproduced from ref.[35], with permission from Elsevier).

The thiol (-SH) groups are well known to form stable complexes with soft heavy metal ions of high polarizability such as mercury, silver, gold, and to a lesser extent, cadmium and zinc, while invalid in coordinating with the light metals such as sodium, calcium, and magnesium [187]. Merrifield J. D. et al. grafted thiol groups on the cross-linked chitosan beads as a

method to enhance its ability in removing mercury from aqueous solution [188]. The modified beads were prepared facilely by placing the GLA-CS in a 2 wt.% cysteine solution, where the amino groups of the cysteine attached to the aldehyde group of the residual free GLA via a Schiff base reaction. The equilibrium and kinetic uptake experiments showed that the sorption process was radial pore diffusion in the spherical beads and the modified chitosan adsorbent exhibited high sorption capacities (8.0 mmol g^{-1}) toward Hg(II). Atia A. A. synthesized 3-amino-1,2,4-triazole-5-thiol modified chitosan resin and successfully applied for the uptake of Hg(II) and UO_2(II) from aqueous solutions [189]. The Hg(II)- and UO_2(II)-loaded adsorbent could be regenerated using H_2SO_4 and HCl, respectively. Selective separation of Hg(II) from UO_2(II) was achieved at pH 2, due to the ability of Hg(II) to adsorb on chitosan resin through ion-exchange mechanism at acidic solution, while UO_2(II) could not:

$$2\ \mathrm{RSH} + \mathrm{Hg}^{2+} \rightarrow \mathrm{RSHgSR} + 2\mathrm{H}^{+}$$

$$\mathrm{RSH} + \mathrm{HgCl}^{+} \rightarrow \mathrm{RSHgCl} + \mathrm{H}^{+}$$

Thiourea is an organosulfur compound with the structure $S{=}C(NH_2)_2$ similar to urea, where a sulfur atom replace the oxygen atom. Guibal E. prepared thiourea and rubeanic acid (dithiooxamid, $NH_2(C{=}S)_2NH_2$) modified chitosan materials for efficient sorption of Pd(II) from dilute acidic solutions [190]. The modification gave the adsorbents a dual chelating (S atom and/or N atom coordination) and anion exchange structure. Ion exchange mechanism played more important role than coordination mechanism in acidic solutions. Rubeanic acid modified chitosan exhibited better sorption affinity to Pd(II) than thiourea modified chitosan due to the presence of more sulfur chelating moieties. Several thiourea-modified magnetic chitosan adsorbents and ion imprinted polymers have been prepared and applied for the adsorption of various metal ions [191-193]. The thiourea-modified adsorbents displayed higher efficiency in adsorbing Hg(II) and Ag(I) than Zn(II), Cu(II), and Ni(II), owing to the fact that 4d (Ag) and 5d (Hg) orbitals are spatially larger than 3d (Zn, Cu, Ni) orbitals and thus gave better orbital overlapping in bond formation with thiourea ligand. The used thiourea-modified magnetic chitosan adsorbents could be recovered by 0.1 M HCl, 0.1 M HNO_3, or 0.01-0.1 M EDTA solutions.

Xanthate, which usually refers to salts of xanthic acid with the formula R-OCS_2^- or esters with the structure of R-OC(=S)S-R', has been widely used as flotation reagents in the mining industry for the separation of transition metals [194]. Kannamba B. et al. chemically modified EPI cross-linked chitosan with xanthate through a treatment of the EPI-CS with 14% NaOH solution and CS_2 [195]. The modified chitosan was used as sorbent for the removal of Cu(II) from aqueous medium. The introduction of xanthate groups on the chitosan adsorbent was proved to enhance the interaction with Cu(II) in solution and thus increase the adsorption capacity of Cu(II). Later, a xanthate-modified magnetic cross-linked chitosan (XMCS) was synthesized and applied for the removal of Co(II) from aqueous solution [196]. The characteristics and mechanism of Co(II) adsorption were investigated. The FT-IR and XPS spectra provided evidence that Co(II) sorption was mainly through forming coordination bonds with the sulphur atoms (xanthate group) and nitrogen atoms (amino group) in XMCS. The xanthate modification occurs at –OH position, thus the amino groups still remain in the obtained adsorbent. The competitive adsorption of Pb(II), Cu(II) and Zn(II) onto xanthate-modified magnetic chitosan was investigated in single and ternary metal systems [197]. The adsorption capacity (in mg g^{-1}) was higher for Pb(II) than Cu(II) and Zn(II) for both single and ternary systems. Authors explained the differences in covalent index (based on electronegativity and ionic radius) might be the reason causing the selective adsorption of the studied metals. Notably, this work also suggested that the metals preferentially interacted with the functional groups in order S > N > O containing group.

Table 10. Sulfur-modified cross-linked chitosan and β-CD adsorbents.

Polysaccharide	Cross-linkers	Modifier	Target pollutants	Time (h)	pH	q_m (mmol g^{-1})	Ref
β-CD	EPI	Tiron	Methylene blue	6	-	0.013	[185]
			Basic magenta	4		0.007	
			Phenolphthalein	4		0.007	
Starch	EPI	TSSA 1[a]	Aniline	1	4.6	0.801	[186]

		TSSA 2[a]				1.038	
		TSSA 3[a]				1.161	
Chitosan	GLA	Sulfonate	Pramipexole dihydrochloride	24	10	1.186	[35]
Chitosan	Sodium cyanoborohydride	4-Formyl-1,3-benzene sodium disulfonate	Basic Blue 3	1	3.0	0.463	[198]
Chitosan	EPI	Heparin	Cu(II)	25	6.0	1.282	[199]
Chitosan	GLA	Thiol	Hg(II)	-	7	8.0	[188]
Chitosan	GLA	3-amino-1,2,4-triazole-5-thiol	Hg(II)	3	5.1	2.21	[189]
			UO_2(II)		3.9	1.60	
Chitosan	GLA	Thiourea	Pd(II)	72	2.2	2.608	[190]
		Rubeanic acid				3.308	
Chitosan-Fe_3O_4	GLA	Thiourea	Hg(II)	8	5.0	3.117	[191]
			Cu(II)			1.049	
			Ni(II)			0.261	
Chitosan-Fe_3O_4	GLA	Thiourea	Zn(II)	0.5	5.0	0.492	[192]
Chitosan-Fe_3O_4	GLA	Thiourea	Ag(I)	1	5	5.29	[193]
Chitosan	EPI	Xanthate	Cu(II)	24	5.0	0.685	[195]
Chitosan-Fe_3O_4	GLA	Xanthate	Co(II)	6	5.0	0.314	[196]
Chitosan-Fe_3O_4	GLA	Xanthate	Pb(II)	-	5.0	0.371	[197]
			Cu(II)			0.543	

	Zn(II)	0.318

[a] Sulfur contents of the obtained polymers were 13.09%, 15.58%, 18.82% for TSSA (trisulfonated sodium amine) 1, 2, and 3, respectively.

3.2.4 Modified by other functional groups

Modification of cross-linked chitosan and CDs by other functional groups tabulated in **Table 11**, such as crown ether, 8-Hydroxyquinoline and amino acids, has also attracted increasing attentions in the past decade. Tan S. et al. immobilized two crown ethers onto cross-linked chitosan, and used them successfully for adsorption and separation of heavy metals [200]. Batch experiments showed that the two cross-linked chitosan derivatives had not only high sorption capacities toward Pb(II) and Cu(II), but also with high selectivity toward Pb(II) and Cu(II) in the coexistence of Cr(III) and Ni Cr(II). 8-Hydroxyquinoline, another excellent chelating agent, has been grafted on chitosan beads as active sites for adsorption and retention of heavy metals [201, 202]. The adsorption capacities of cross-linked chitosan toward precious metals were significantly enhanced by glycine and L-lysine due to the simultaneous introduction of amino and carboxyl groups [203, 204]. Interestingly, Reactive Blue 2 dye, which contains three sulfonate groups, four amino groups, and one chlorotriazine group, was immobilized on chitosan microspheres through nucleophilic substitution reaction for enhanced adsorption of Cu(II) and Ni(II) from aqueous solution [205].

Table 11. Cross-linked chitosan and β-CD modified by other functional groups adsorbents.

Polysaccharide	Cross-linkers	Modifier	Target pollutants	Time (h)	pH	q_m (mmol g^{-1})	Ref
Chitosan	EPI	Crown ether 1	Pb(II)	12	5.6	0.141	[200]
			Cu(II)			0.376	
			Cr(III)			0.333	

			Ni(II)			0.012	
		Crown ether 2	Pb(II)			0.291	
			Cu(II)			0.493	
			Cr(III)			0.587	
			Ni(II)			0.070	
Chitosan	EPI	8-Hydroxyquinoline	Cu(II)	4	5.0	1.126	[202]
			Zn(II)			0.148	
			Ni(II)			0.223	
Chitosan	EDGE	Glycine	Au(III)	4	2.0	0.863	[203]
			Pt(IV)			0.628	
			Pd(II)			1.131	
Chitosan	EDGE	L-lysine	Pt(IV)	4	1.0	0.663	[204]
			Pd(II)		2.0	1.029	
			Au(III)		2.0	0.357	
Chitosan	-	Reactive Blue 2	Cu(II)	36	7.0	0.90	[205]
			Ni(II)		8.5	0.19	
Chitosan	GLA	BPMAMFP[b]	Cu(II)	2	5.5	1.72	[206]
Chitosan	GLA	BPMAMFP[b]	Cu(II)	3.5	6.0	1.717	[207]
			Cd(II)	2	2.0	0.344	
			Ni(II)	7	3.0	0.164	
β-CD	1,4-Butanediol diglycidyl ether	1-(2-pyridylazo)-2-naphthol	Co(II)	1	9.5	100[c]	[208]

[a] Crown ether 1: dibenzo-16-*c*-5 chloracetate crown ether; Crown ether 2: 3,5-di-*tert*-butyl dibenzo-14-*c*-4 dichloracetate crown ether.

[b] 2[-bis-(pyridylmethyl) aminomethyl]4-methyl-6-formyl-phenol

[c] Preconcentration factor

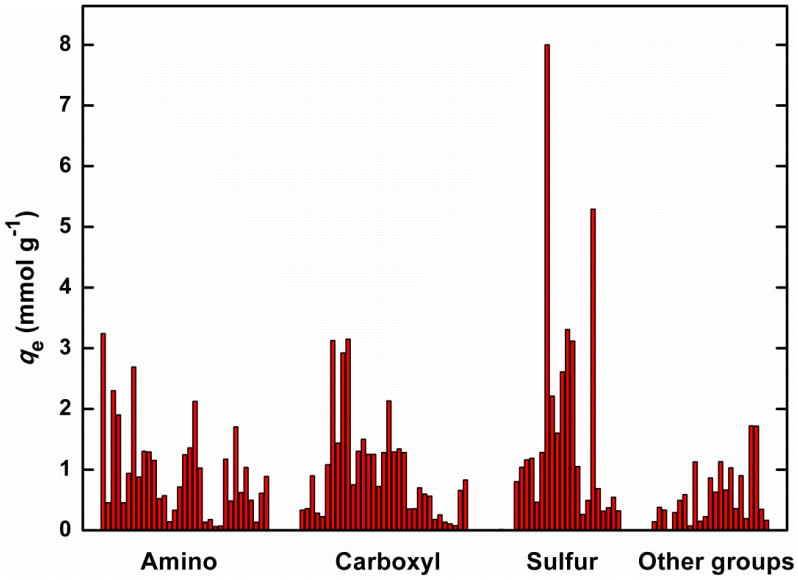

Figure 23. Maximum adsorption capacities for different pollutants for cross-linked chitosan and CDs modified with various functional groups. Data taken from **Table 8-11**.

In general, comparison of **Table 8-11** with **Table 1-7** reveals that usually higher adsorption capacities are obtained for the modified cross-linked chitosan and CD adsorbents than those unmodified, especially cross-linked by common cross-linker. The sorption capacities of the cross-linked adsorbents modified with different functional groups is illustrated in **Figure 23**, and followed the order sulfur groups > carboxyl groups > amino groups > other groups. The best sorption has been reported by Merrifield J. D. et al. for Hg(II) uptake (8.0 mmol g^{-1}) by thiol-modified chitosan beads [188], and by Fan L. et al. for Ag(I) removal (5.29 mmol g^{-1}) by Ag(I) imprinted magnetic thiourea-modified chitosan beads [193].

The section above discussed the adsorption properties of the modified chitosan and CD materials. However, it is difficult to say which type of modification is better, since each of them has its own advantages and disadvantages. For instance, the thiol-modified materials showed the excellent adsorption, however, thiol groups is known to be unsafe due to its

renal toxicity and other negative effects to environment [209]. Even the comparison of adsorption capacities is also difficult since the different laboratory conditions and sorption parameters applied by different researchers. There is still great room for improvement in this field of research: i) developing effective as well as environmentally friendly modification technologies; ii) applying the functional polysaccharides commercially instead of laboratory scale; iii) developing a multipurpose polysaccharide adsorbent for simultaneous removal of different types of pollutants from real industrial effluents.

4. APPLICATIONS OF CROSS-LINKED ADSORBENTS IN WATER TREATMENT

Functionalization of chitosan and CD adsorbents by cross-linking and surface modification is essential to alter the properties of the adsorbents toward the desirable direction. The cross-linking reinforces the mechanical behavior, modifies the hydrophobicity, and enhances the chemical stability of the polysaccharides in acidic media. The cross-linked adsorbents are usually further modified by functional groups to maximize the adsorption capability and to improve the selectivity. The cross-linked polysaccharide adsorbents are mainly applied in the simultaneous removal of multi pollutants from contaminated waters, selective adsorption and separation of target pollutants, and preconcentration of target adsorbates from diluted aqueous solutions.

4.1 Simultaneous removal of multi pollutants from wastewater

In principle, most of the prepared adsorbents were tested in synthetic wastewater containing only one kind of the target pollutant. However, more than one type of pollutants coexist in the effluent of various industrial branches [210]. For instance, the wastewaters from dyes manufacturing and textile finishing factories contain not only dyes but also substantial heavy metals, which are used as mordant in the dyeing process [211]. What is worse, the different physical and chemical properties of the multi contaminant classes as well as the interface interaction between the pollutants make the treatment more challenging [212]. Therefore, the simultaneous removal of the co-existed pollutants from wastewaters becomes urgent and crucial.

The plenty and diverse functional groups on chitosan and CD make the polysaccharide based materials potential for simultaneous removal of multi classes of contaminants. A chitosan, cross-linked by GLA and modified with N-(2-carboxybenzyl) groups, was successfully applied for effective adsorption of both cations (Cu(II), q_m 4.847 mmol g^{-1} and Ni(III), q_m 6.492 mmol g^{-1}) and anions (Cr(VI), q_m 3.365 mmol g^{-1} and As(V), q_m 2.777 mmol g^{-1}) [213]. In this study, however, the simultaneous removal experiments were not conducted. Recently, an EPI-cross-linked chitosan/activated carbon composite was employed to remove Cr(VI) and

aniline from aqueous solution simultaneously [214]. The results showed that both of these pollutants could be removed at natural pH simultaneously and efficiently (> 95%), and the presence of Cr(VI) enhanced the sorption of aniline, while the presence of aniline almost had no effect on the sorption of Cr(VI). More recently, Bikiaris group synthesized a succinyl-modified chitosan adsorbent and used it for the simultaneous removal of Zn(II) and cationic dye Remarcyl Red [36]. The antagonistic effect was observed in binary adsorption experiments since the two target adsorbates competed for the single functional group (carboxyl group) on the adsorbent. Yang et al. employed a Fe_3O_4@β-CD adsorbent to remove Co(II) and 1-naphthol simultaneously [215]. The simultaneous removal was achieved via the inclusion of 1-naphthol into the CD cavities of the adsorbent and the binding of Co(II) on the external surface sites. A CD-graphene oxide material was synthesized by a polymerization method and applied for simultaneous removal of U(VI) and humic acid from wastewater [216]. It is found that the presence of humic acid enhanced U(VI) adsorption and the authors described the surface adsorbed that the humic acid acted as a “bridge” between U(VI) and the CD based adsorbent.

Generally, most of the studies about simultaneous removal of multi pollutants from aqueous solutions discussed above were achieved via single functional groups. As the name suggests, however, all of the target pollutants bind to the sole adsorption site, resulting unavoidable competitive adsorption. Therefore, more advanced adsorbents containing dual- or multi-functional groups would be a viable alternative for the simultaneous treatment of the coexistent toxic pollutants.

4.2 Selective adsorption and separation of target pollutants

In some other purposes, such as reuse of the precious metals from wastewater, high specific selectivity is required for the advanced adsorbents. Moreover, various pollutants commonly coexist in the practical contaminated water resources. Thus, it is of great significance to separate and recover them in their individual purified forms for the potential reuse, and also prevent a secondary pollution. The chelating effect of chitosan and host-guest inclusion

property of CDs endow them promising application in selective adsorption and separation of target pollutants from wastewaters.

Physical and chemical modifications have been shown to improve the selectivity for metal ions [217]. Yan H. et al. reported that GLA-cross-linked chitosan hydrogel beads surface modified with carboxymethyl groups showed not only enhanced but also selective adsorption for Cu(II) from Pb(II) and Mg(II) from aqueous solutions, while the unmodified chitosan beads had no selectivity for Cu(II) [218]. The enhanced adsorption was attributed to the formation of bidentate chelate complexes between Cu(II) and carboxyl groups, while the selectivity was attributed to the higher binding affinity of carboxyl groups toward Cu(II) over Pb(II) and Mg(II). Repo E. et al. have also reported an EDTA-modified chitosan and silica hybrid adsorbent for possible separation of Pb(II) and Ni(II) from Cd(II) and Co(II) [38]. High adsorption capacity and selectivity could also be achieved by ion-imprinted polymers (IIP). Zhou L. and co-workers prepared ion-imprinted magnetic chitosan polymers by using U(VI) as a template and GLA as a cross-linker [219]. The obtained IIP magnetic chitosan adsorbents showed higher uptake for the U(VI) than those of non-imprinted magnetic chitosan. The IIP adsorbents also performed strong ability to selectively adsorb U(VI) from other cations (i.e., Th(IV), Fe(III), Zn(II), Ni(II), Co(II), and Cu(II)), which commonly coexist with U(VI) in natural sources.

CDs have been widely applied for the selective recognition and separation of target molecules such as amino acid [220], lysozyme [221], and cholesterol [222] in medicine and biological industries due to their inclusion ability toward hydrophobic guests. The great priority of selective incorporation ability of CDs has also been given to the development of selective separation technique in water treatment. Kitaoka M. and Hayashi K. synthesized an insoluble EPI cross-linked β-CD and used it for the effective and selective removal of bisphenol A from a solution containing amino acids [223]. Pan J. et al. synthesized molecularly imprinted β-CD/attapulgite polymers (MIP) by using 2,4-dichlorophenol as a template and ethyl glycol dimethacrylate (EGDMA) as cross-linker [224]. After the removal of the template molecules, the produced MIP displayed high selectivity for target 2,4-dichlorophenol over competitive phenolic compounds in wastewater. Another β-CD MIP was

prepared by “one-step method” (**Figure 24**) using TDI as cross-linker [109]. The obtained dye-CD-MIP showed high selectivity to Remazol Red 3BS (the template molecule) from a trichromatic dye solution in the presence of other two dyes (Remazol Blue RN and Remazol Yellow gelb). The selectivity of MIP was much greater than the non-imprinted one.

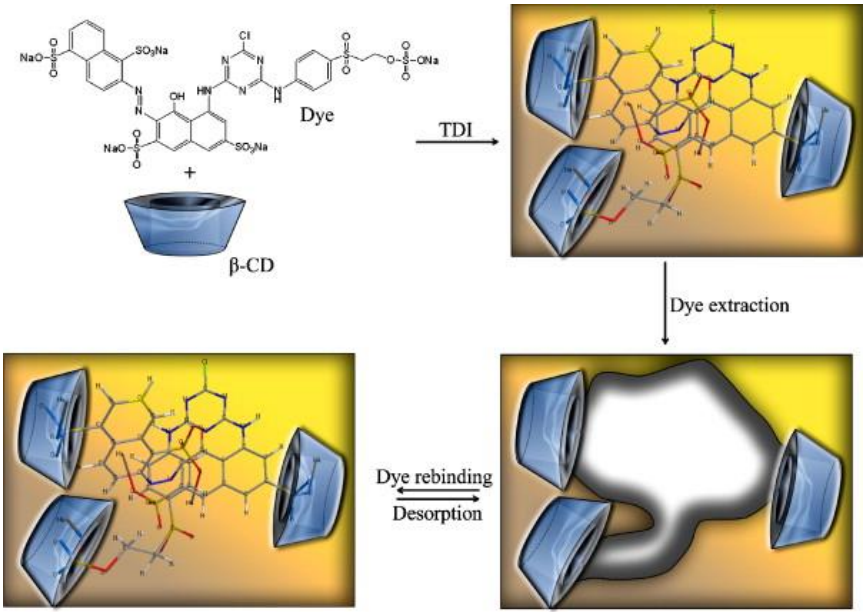

Figure 24. Synthesis route and mechanism of CD-MIP (Reproduced from ref.[109], with permission from Elsevier).

4.3 Preconcentration of trace adsorbates

In recent decades, the trace levels of pollutants have received raising attention worldwide due to their toxicity and widespread distribution. Moreover, the ever-increasing REEs demand requires the recovery of these valuable metals from extremely diluted streams such as industrial effluent and seawater. However, the direct determination of the trace level adsorbates has been very difficult since the levels of analytes are usually below the determination limit (DL) of the most of the instruments. Therefore, the preconcentration

procedures conducted prior to the analytical determination of trace amounts of compounds have become more and more important [225].

The use of chitosan as substrate for an ion exchange and a chelating resin of preconcentration has attracted great attention due to its advantages such as hydrophilic properties and easy modification of its amino groups. A GLA-cross-linked and 8-hydroxyquinoline-modifed chitosan chelating resin was successfully used in an automated on-line preconcentration system for the determination of trace level of Cd(II), Cu(II) [201], and Zn(II) [226] by flame atomic absorption spectrometry (FAAS). EDTA- and DTPA-functionalized chitosan polymers have also been applied for adsorptive enrichment and chromatographic separation of REEs [138]. Another chitosan resin cross-linked with EGDE and modified by 2-amino-5-hydroxy benzoic acid, was utilized in an on-line preconcentration system coupled with inductively coupled plasma-atomic emission spectrometry (ICP-AES) for the collection and determination of trace elements, such as Ag, Be, Cd, Co, Cu, Ni, Pb, U, V, and REEs in river water [227].

CDs have excellent capability in the preconcentration of organic pollutants from water resources by forming inclusion complexes [228]. GLA and EGDMA cross-linked β-CD microbeads were employed for the removal and preconcentration of phenolic species [229]. In this study, after the preconcentration, the DL of the phenolic species were improved at least 500-fold for the UV-Vis spectrophotometric determination. Yu J. et al. used EPI-cross-linked β-CDP as a solid-phase extraction adsorbent for twelve trace aromatic compounds in water samples, followed by gas chromatography-mass spectrometry (GC-MS) and UV for detection [230]. The 90-101% recoveries were achieved for aromatic compounds at 0.02-1.67 ppm levels. Moreover, the EPI-β-CDP has also been used to preconcentrate trace Co(II) coupled with ICP-MS for the determine of Co(II) [231]. This method was based on α-pyridylazo-β-naphthol (PAN) as the complexing agent for Co(II)-PAN, which was further adsorbed on EPI-β-CDP. The DL by this mothed reached as low as 5.84 ng L^{-1}, and the preconcentration factor was 10.

5. OBJECTIVES AND STRUCTURE OF THE WORK

The overall aim of the thesis was to investigate the potential of aminopolycarboxylic acids (APCAs) or their dianhydrides cross-linked chitosan and/or β-cyclodextrin adsorbents for water treatment applications (**Figure 25**). The research focus was on heavy metals, dyes, REEs, and organic micropollutants. The specific objectives of this study were:

- To prepare five different kinds of cross-linked chitosan and/or β-cyclodextrin adsorbents (1) EGTA-modified chitosan for metals removal (Paper I); (2) magnetic EDTAD-cross-linked chitosan adsorbents for metals removal (Paper II); (3) magnetic DTPAD-cross-linked chitosan adsorbents for metals removal (Paper II); (4) EDTA-cross-linked β-cyclodextrin for simultaneous removal of metals and cationic dyes, and for the adsorption and preconcentration of REEs (Paper III, IV); (5) EDTA-cross-linked chitosan-β-cyclodextrin for the removal of metals and organic micropollutants (Paper V). Moreover, magnetic GLA-cross-linked chitosan microspheres (Paper II) and EPI-cross-linked β-CDP (Paper III-V) were prepared as a control.

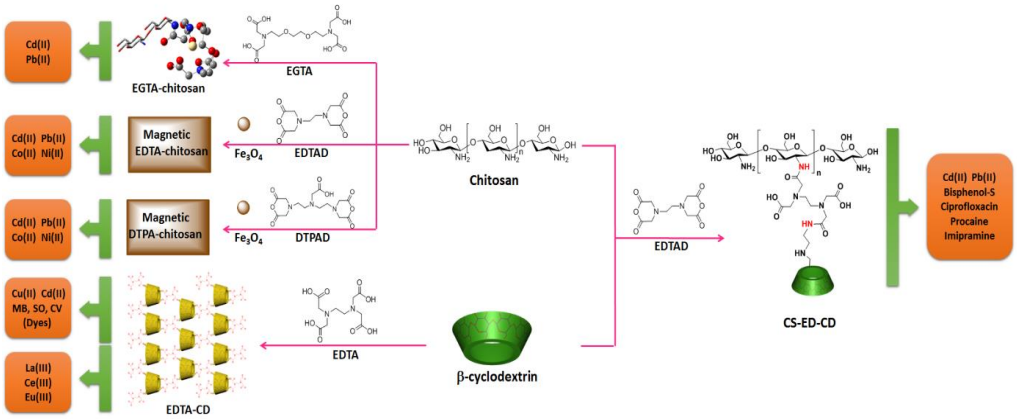

Figure 25. Schematic overview of the contents of this thesis.

- To investigate the effects of initial pH, contact time, and initial adsorbate concentration as well as the regeneration condition for the used adsorbents (Paper I-V). Importantly, the possible adsorption mechanism was explored and explicated (Paper I-V).
- To fit the experimental data obtained from kinetic and isotherm studies to various kinetic and isotherm models, which indicate various adsorption theories. The modeling of kinetics and isotherms for single-component system is presented in Paper I-V. Moreover, Paper I presents modeling isotherms for two-component system, while Paper IV presents modeling isotherms for three-component system.
- To test the cross-linked adsorbents in selective adsorption and separation of target metals (Paper I, II, and IV), in simultaneous removal of pollutants from binary- or multi-component system (Paper III), in preconcentration of trace level of REEs (Paper IV), and the application in practical industrial effluents (Paper II and III), seawater (Paper IV) as well as the application at environmentally relevant concentrations (Paper V).

6. Experimental section

6.1 Synthesis of the adsorbents

Five different cross-linked chitosan and/or β-CD adsorbents were synthesized: the synthesis of EGTA-modified chitosan is described in detail in Paper I, the magnetic EDTAD- and DTPAD-cross-linked chitosan in Papers II, the EDTA-cross-linked β-CD in Paper III and V, the EDTA cross-linked chitosan-β-CD in Papers V.

Briefly, the EGTA-modified chitosan (EGTA-chitosan) was prepared by reacting chitosan with EGTA in presence of a coupling agent, EDC in NaOH solution (Paper I). The magnetic EDTAD- and DTPAD-cross-linked chitosan (MEDCS and MDTCS) were fabricated via an emulsion cross-linking method in the presence of Fe_3O_4 magnetic nanoparticles (MNPs) using EDTAD and DTPAD as the cross-linkers, respectively (Paper II). The EDTA-cross-linked β-CD polymer (EDTA-CDP) was prepared through the esterification-polycondensation reaction of β-CD with EDTA as cross-linker and Na_2HPO_4 as a catalyst (Paper III and IV). Finally, the chitosan and β-CD hybrid material (CS-ED-CS) was prepared by one-pot synthesis method following a similar EDTAD-cross-linking as in the case of chitosan (Paper V).

6.2 Characterization of the adsorbents

The Fourier transform infrared (FTIR) spectroscopy of the type VERTEX 70 (Bruker, Germany) with a platinum ATR attachment was employed to qualitatively identify the functional groups of the prepared adsorbents (Paper I-V). Quantitative analyses of the amounts of the functional groups and the contents of each components in hybrid polymer were performed with a 2400 Series II CHNS/O Analyzer (PerkinElmer, U.S.A.) (Paper I, III, and V). The amount of carboxylic acid groups on the adsorbents was evaluated via Conductometric-potentiometric titration method using a Metrohm 809 Titrando autotitrator (Switzerland) (Paper V). The amount of active ß-CD cavities on CS-ED-CD was determined through Photometric Titration with UV-vis spectrometry (PerkinElmer Lambda 45, U.S.A.) by using phenolphthalein as indicator (Paper IV and V). The surface morphologies of the as-prepared polymers were investigated using a Jeol JSM-5800 (Japan) scanning electron microscope

(SEM) at an acceleration voltage of 5.0 kV (Paper II-V). Elemental Mapping was performed during the SEM examination (acceleration voltage 20.0 kV) by Thermo Scientific Ultra Dry SDD Energy-dispersive X-ray spectroscopy (EDS) (Paper III, IV and V). The EDS analyses were performed in Paper II and III. High-resolution transmission electron microscopy (HRTEM) was performed using a double-aberration corrected JEOL 2200FS (Japan) to examine the morphology and structure of the adsorbents (Paper II). The ζ-potentials of the adsorbents were measured by using a Zetasizer Nano ZEN3500 (Malver, U.K.) (Paper II, III and V). Thermogravimetric analysis (TGA) and derivative thermogravimetric (DTG) tests were conducted using a NETZSCH TG 209F1 (Germany) at a heating rate of 10 ^{o}C min^{-1} under a nitrogen atmosphere from 25 ^{o}C to 1000 ^{o}C (Paper II, III and V). The crystal lattice structure of the particles was defined by X-ray diffraction (XRD) PANalytical X-ray diffractometer (Netherland). The magnetic characteristics of the magnetic cross-linked chitosan adsorbents were examined using a vibrating sample magnetometer (VSM) Lake Shore 7407 (U.S.A.) (Paper II).

6.3 Adsorption and desorption experiments

Adsorption and desorption experiments are described in detail in Paper I-V. Briefly, the solutions containing known concentration of adsorbates were mixed with a known dose of adsorbent for a designated time, after which the adsorbent was separated from the solution. The adsorption capacities (q_e, mmol g^{-1}) was calculated as follows:

$$q_e = \frac{(C_i - C_e)}{M} V \qquad (1)$$

where C_i and C_e are the initial and the equilibrium concentrations (mmol L^{-1}) of adsorbates, while m and V are the weight of the adsorbent (g) and the volume of the solution (L), respectively.

The regeneration efficiency (%RE) of the adsorbent was calculated as follows:

$$\%RE = \frac{q_r}{q_0} \times 100\% \qquad (2)$$

where q_0 and q_r are the adsorption capacities of the adsorbents (mmol g^{-1}) before and after regeneration, respectively.

6.4 Analysis of solutions

The concentrations of target metals before and after adsorption were analyzed by an inductively coupled plasma optical atomic emission spectrometry (ICP-OES) Model Icap 6300 instrument (Thermo Electron Corporation, U.S.A.). The used wavelengths for various metals were: Cd(II): 226.502 nm (Paper I-III and V), Pb(II): 220.353 nm (Paper I, II and V), Co(II): 228.616 nm, Ni(II): 231.605 nm (Paper II), Cu(II): 324.754 nm (Paper III), La(III): 333.749 nm, Ce(III): 404.076 nm, and Eu(III): 381.967 nm (Paper IV). The concentrations of dyes and organic micropollutants were determined by UV-vis spectrometry (PerkinElmer Lambda 45, U.S.A.) at the maximum absorbance of methylene blue (MB) at 668 nm, safranin O (SO) at 516 nm, crystal violet (CV) at 583 nm, Bisphenol-S (BPS) at 258 nm, Ciprofloxacin (CIP) at 277 nm, Procaine at 290 nm, and Imipramine at 249 nm.

6.5 Simultaneous removal experiments

Binary systems of metal-dye were used in the simultaneous adsorption experiments (Paper III). Batch adsorption tests were performed by using initial concentration ranging from 10 to 200 mg L^{-1} for metal and from 30 to 200 mg L^{-1} for dye. As presented in **Table 12**, a full factorial design that the main factors of the adsorption process were the initial concentration of metal and dye, was conducted in this work. For the comparison purpose, the data of mono adsorption at the same operation conditions such as pH, time, and dosage as binary ones, were also involved in this factorial design experiments.

Table 12. Experimental design used for the simultaneous adsorption of metal and dye on adsorbent

	Levels	Factor A: initial concentration of metal, mg L^{-1}				
		0	10	50	100	200
Factor B:	0		$q_{e,[10,0]}$	$q_{e,[50,0]}$	$q_{e,[100,0]}$	$q_{e,[200,0]}$

initial concentration of dye, mg L^{-1}	30	$q_{e,[0,30]}$	$q_{e,[10,30]}$	$q_{e,[50,30]}$	$q_{e,[100,30]}$	$q_{e,[200,30]}$
	60	$q_{e,[0,60]}$	$q_{e,[10,60]}$	$q_{e,[50,60]}$	$q_{e,[100,60]}$	$q_{e,[200,60]}$
	100	$q_{e,[0,100]}$	$q_{e,[10,100]}$	$q_{e,[50,100]}$	$q_{e,[100,100]}$	$q_{e,[200,100]}$
	200	$q_{e,[0,200]}$	$q_{e,[10,200]}$	$q_{e,[50,200]}$	$q_{e,[100,200]}$	$q_{e,[200,200]}$

6.6 Preconcentration experiments

The tested matrices included pure water, tap water, and seawater (Paper IV). Two kinds of seawater, obtained from Gulf of Finland (salinity value 6‰) and Gulf of Mexico (salinity value 32‰), were used in the preconcentration experiments. Aliquots of 400 mL solution containing REEs were mixed with 400 mg of adsorbent (dosage: 1 g L^{-1}) and agitated in a rotary oscillator for 4 h. After separation, REEs were eluted using 4 mL of 1 M HNO_3. The concentrated samples (100-fold) were analyzed by ICP-OES.

6.7 Practical industrial effluent experiments

The real metal wastewater used in Paper II was collected from a nonferrous metal smelter plant in Hunan province, China. The practical effluent samples were allowed to settle for one day and the supernatants were used for adsorption. The metal concentrations before and after adsorption were analyzed by ICP-OES. A synthetic sewage used in Paper III was prepared according to OECD guideline [232]. Then this sewage was employed to prepare the model textile effluent containing 30 mg L^{-1} of Cu(II) and 300 mg L^{-1} of MB, which are close to a real textile sewage from Mumbai, India [233, 234]. The concentrations of Cu(II) and MB before and after adsorption were determined by ICP-OES and UV-vis spectrometry, respectively.

6.8 Environmentally (µg L^{-1}) relevant concentration adsorption experiments

100 mg of the adsorbent was mixed with 100 mL of the diluted mixture (100 µg L^{-1} Cd(II) and 50 µg L^{-1} CIP). After adsorption, the residual Cd(II) concentration was analyzed by ICP-OES, as well as the CIP concentrations was analyzed by ultra-high performance liquid chromatography (UHPLC) coupled with a Xevo TQ mass spectrometer (MS) (Waters, UK).

Deuterated ciprofloxacin ($^2H_8$) was used as an internal standard. Samples were injected and loaded onto an Acquity UPLC BEH (Waters) C18 Column (2.1 mm × 50 mm, particle size 1.7 μm).

6.9 Modeling of adsorption isotherms and kinetics

6.9.1 Adsorption isotherms

The adsorption isotherms are fundamental in describing the interactive behavior between the adsorption sites and adsorbates in the solution. Langmuir (Paper I-V), Freundlich (Paper I, II, and IV), BiLangmuir (Paper I and II), and Sips (Paper II, III-V) were used for the modeling the single adsorption. Extended BiLangmuir (Paper I) and extended Sips (Paper IV) were employed for the modeling the binary and multi-component adsorption, respectively. The modeling calculations were carried out by using OriginPro software version 9.1.

Langmuir model

The Langmuir model is widely applicable for homogeneous adsorption, based on the following assumptions: (i) homogeneous surface, where all adsorption sites are energetically equivalent; (ii) each of the adsorption site can only bind one adsorbate; (iii) monolayer coverage of adsorbates on the surface; (iv) there is not interaction between the adsorbates on neighbor adsorption sites. The general Langmuir equation is given as follows:

$$q_{\mathrm{e}} = \frac{q_m K_{\mathrm{L}} C_{\mathrm{e}}}{1 + K_{\mathrm{L}} C_{\mathrm{e}}} \qquad (3)$$

where q_e (mmol g^{-1}) and C_e (mmol L^{-1}) are the adsorption capacity and the equilibrium concentration of the adsorbate, respectively, while q_m (mmol g^{-1}) and K_L (L $mmol^{-1}$) present the maximum adsorption capacity and the adsorption energy constant, respectively.

Freundlich model

The Freundlich model is the simplest isotherm that takes the surface heterogeneity and multilayer adsorption into account. The Freundlich equation is given as follows:

$$q_e = K_F C_e^{1/n_F} \qquad (4)$$

where K_F ((mmol g^{-1})/ (L mmol^{-1})^{nF}) is a unit capacity coefficient and n_F is the Freundlich constant associated to the degree of heterogeneity. The greater the n_F value is, the more heterogeneous the adsorption is.

BiLangmuir model (Two-site Langmuir)

The BiLangmuir model assumes that the surface contains two different active sites with different affinities toward adsorbates that follow a Langmuir behavior. The BiLangmuir model incorporates two Langmuir equation as follows:

$$q_e = \frac{q_{m,1} K_1 C_e}{1+K_1 C_e} + \frac{q_{m,2} K_2 C_e}{1+K_2 C_e} \qquad (5)$$

where $q_{m,1}$ and $q_{m,2}$ (mmol g^{-1}) are the maximum adsorption capacities of the two different active sites, while K_1 and K_2 (L mmol^{-1}) are the adsorption energy constants corresponding to adsorption sites 1 and 2. Notably, both of the active sites are homogeneous and can bind only one adsorbate like Langmuir model.

Sips model (Langmuir-Freundlich)

The Sips model, which is a combination of the Langmuir and Freundlich models and takes heterogeneity into account, is usually applicable when both Langmuir and Freundlich models fail. The Sips model is given as follows:

$$q_e = \frac{q_m (K_S C_e)^{1/n_S}}{1+(K_S C_e)^{1/n_S}} \qquad (6)$$

where K_S (L mmol^{-1}) is the Langmuir energy parameter, while n_S presents the Freundlich heterogeneity factor. This Sips model behavior is the same as that of Freundlich model at low adsorbate concentrations, while at sufficiently high concentrations, it possess a finite saturation plateau as the Langmuir model. When n_S closes unity, the Sips isotherm returns to Langmuir and indicates homogeneous adsorption. On the other side, when n_S differs from unity significantly, it predicts heterogeneous adsorption.

Extended BiLangmuir model

The isotherm models introduced above are applicable for one-component adsorption systems. In most of cases, however, more than one component adsorbates coexist in the real systems. Thus, some of the one-component isotherm models have been extended to be applicable for multi-component adsorption systems. The equilibrium data of two-component systems were modeled by extended BiLangmuir model in Paper I as follows:

$$q_{\mathrm{e}1} = \frac{q_{m,1,1}K_{1,1}C_{\mathrm{e}1}}{1+K_{1,1}C_{\mathrm{e}1}+K_{2,1}C_{\mathrm{e}}2} + \frac{q_{m,1,2}K_{1,2}C_{\mathrm{e}1}}{1+K_{1,2}C_{\mathrm{e}1}+K_{2,2}C_{\mathrm{e}2}} \quad (7)$$

$$q_{\mathrm{e}2} = \frac{q_{m,2,1}K_{2,1}C_{\mathrm{e}2}}{1+K_{1,1}C_{\mathrm{e}1}+K_{2,1}C_{\mathrm{e}}2} + \frac{q_{m,2,2}K_{2,2}C_{\mathrm{e}2}}{1+K_{1,2}C_{\mathrm{e}1}+K_{2,2}C_{\mathrm{e}2}} \quad (8)$$

where $q_{\mathrm{e}1}$ and $q_{\mathrm{e}2}$ (mmol g^{-1}) are uptake amounts of component 1 and 2 at equilibrium, $q_{\mathrm{m},1,1}$ and $q_{\mathrm{m},1,2}$ (mmol g^{-1}) are the maximum adsorption capacities of the component 1 on the two different active sites, while $K_{1,1}$ and $K_{1,2}$ (L mmol^{-1}) are the adsorption energy constants corresponding to the adsorption of the component 1 on the two different active sites. Correspondingly, $q_{\mathrm{m},2,1}$, $q_{\mathrm{m},2,2}$, $K_{2,1}$, and $K_{2,2}$ (L mmol^{-1}) are the parameters related to the adsorption of component 2 on the two different active sites.

Extended Sips model

For multi-component isotherms, an extended Sips model which considers the interaction factors between individual components, was employed in Paper IV as follows:

$$q_{\mathrm{e}i} = \frac{q_{\mathrm{m}i}(K_{\mathrm{s}i}C_{\mathrm{e}i})^{n_{\mathrm{S}i}}}{1+\sum_{j=1}^{N}(K_{\mathrm{s}j}C_{\mathrm{e}j})^{n_{\mathrm{S}j}}} \quad (9)$$

which for a ternary system of La(III), Ce(III), and Eu(III) could be decomposed into three equations as follows:

$$q_{\mathrm{e}1} = \frac{q_{\mathrm{m}1}(K_{\mathrm{s}1}C_{\mathrm{e}1})^{n_{\mathrm{S}1}}}{1+(K_{\mathrm{s}1}C_{\mathrm{e}1})^{n_{\mathrm{S}1}}+(K_{\mathrm{s}2}C_{\mathrm{e}2})^{n_{\mathrm{S}2}}+(K_{\mathrm{s}3}C_{\mathrm{e}3})^{n_{\mathrm{S}3}}} \quad (10)$$

$$q_{\mathrm{e}2} = \frac{q_{\mathrm{m}2}(K_{\mathrm{s}2}C_{\mathrm{e}2})^{n_{\mathrm{S}2}}}{1+(K_{\mathrm{s}1}C_{\mathrm{e}1})^{n_{\mathrm{S}1}}+(K_{\mathrm{s}2}C_{\mathrm{e}2})^{n_{\mathrm{S}2}}+(K_{\mathrm{s}3}C_{\mathrm{e}3})^{n_{\mathrm{S}3}}} \quad (11)$$

$$q_{e3} = \frac{q_{m3}(K_{s3}C_{e3})^{n_{S3}}}{1+(K_{s1}C_{e1})^{n_{S1}}+(K_{s2}C_{e2})^{n_{S2}}+(K_{s3}C_{e3})^{n_{S3}}} \quad (12)$$

where q_{e1}, q_{e2}, and q_{e3} (mmol g^{-1}) are the amounts of component 1, 2, and 3 adsorbed at equilibrium, while q_{m1}, q_{m2}, and q_{m3} (mmol g^{-1}) are the maximum adsorption capacities of the three kinds of REEs, respectively. Correspondingly, K_{S1}, K_{S2}, and K_{S3} (L $mmol^{-1}$) are analogous to the Langmuir affinity constants and n_{S1}, n_{S2}, and n_{S3} present the heterogeneity constants, related to the adsorption of the three kinds of REEs.

6.9.2 Kinetic modeling

For the purpose of investigating the kinetic mechanism of the adsorption process as well as its potential rate-controlling step, four kinetic models, including pseudo-first-order, pseudo-second-order, Elovich, and the intraparticle diffusion models, were applied to analyze the experimental data (Paper 1-V).

The pseudo-first-order (PS1) model is the simplest and oldest empirical kinetic model [235]. PS1 model is associated with the kinetics of one-site adsorption governed by the rate of the surface action. The PS1 model is given as follows:

$$\frac{dq}{dt} = k_1(q_e - q) \quad (13)$$

By integrating this equation at the boundary conditions q = 0 at t = 0 and $q = q_t$ at $t = t$, it could be transformed into a linear form equation as follows:

$$\ln(q_e - q_t) = \ln(q_e) - k_1 t \quad (14)$$

where q_t and q_e (mmol g^{-1}) are the adsorption capacity at time t and at equilibrium, respectively, while k_1 (min^{-1}) is the PS1 rate constant.

The PS1 model was generalized to two-site adsorption to establish a pseudo-second-order (PS2) model as follows:

$$\frac{dq}{dt} = k_2(q_e - q)^2 \quad (15)$$

By integrating this equation at the boundary conditions q = 0 at t = 0 and $q = q_t$ at $t = t$, it could also be transformed into a linear form as follows:

$$\frac{t}{q_t} = \frac{1}{k_2 q_e^2} + \frac{1}{q_e} t \qquad (16)$$

where k_2 (g mmol^{-1}min^{-1}) is the PS2 rate constant and $k_2 q_e^2$ presents the initial adsorption rate.

The Elovich model was tested to fit the kinetic data in Paper II as follows:

$$q_t = \frac{1}{\beta}\ln(\alpha\beta) + \frac{1}{\beta}\ln(t) \qquad (17)$$

where the Elovich coefficients, α (mmol g^{-1} min^{-1}) is the initial adsorption rate, and β (g mmol^{-1}) is related to the extent of surface coverage and the activation energy for the chemisorption.

Furthermore, to investigate if film or pore diffusion was the controlling step in the adsorption, the intraparticle diffusion model was tested as follows:

$$q_t = k_{\mathrm{id}} t^{0.5} + C_{\mathrm{id}} \qquad (18)$$

where k_{id} (mmol g^{-1} min$^{-0.5}$) and C_{id} are the rate constant of intraparticle diffusion and the boundary layer diffusion effect, respectively.

7. RESULTS AND DISCUSSION

7.1 Characterization

The morphologies of the cross-linked chitosan and/or β-CD adsorbents were investigated by SEM (Paper I-V). **Figure 26** shows the differences of the morphologies between the studied chitosan and CD adsorbents. The EDTA-CDP and CS-ED-CD materials (**Figure 26**e-h) had rougher surface morphologies compared to cross-linked chitosan polymers (**Figure 26**a-d). The surface (**Figure 26**g) and cross-sectional (**Figure 26**h) morphologies of CS-ED-CD showed a continuous and porous structure, due to the ice crystal formation during the freeze dye procedure. The CS-ED-CD hydrogel was very light, which could stand on the stamens of a flower (inset of **Figure 26**h). TEM inspection was also employed to examine the distribution of the magnetic nanoparticles (MNPs) in the polymers in Paper II. The TEM images (**Figure 27**) shows that the MNPs were encapsulated evenly in the cross-linked chitosan adsorbents.

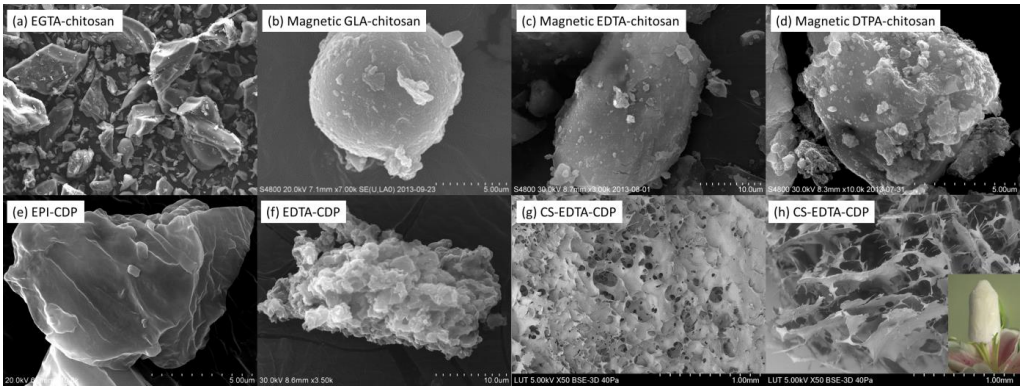

Figure 26. The SEM images of cross-linked chitosan and/or β-CD adsorbents.

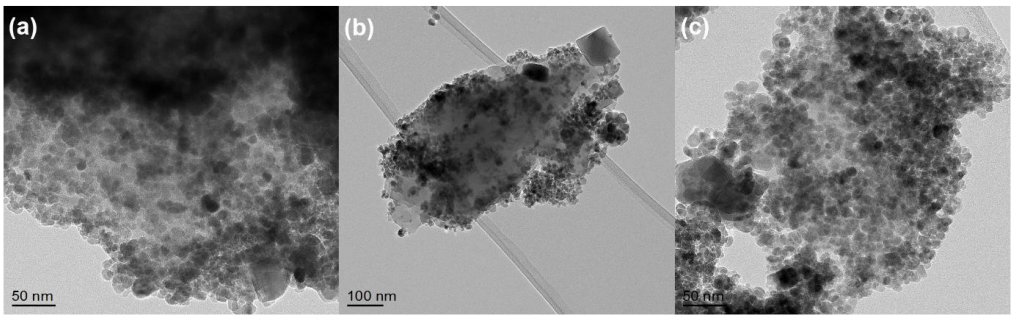

Figure 27. The TEM images of magnetic GLA-cross-linked chitosan (a), MEDCS (b), and MDTCS (c).

The functional groups of the prepared adsorbents were qualitatively defined by FT-IR spectroscopy (Paper I-V). **Table 13** summarizes the FT-IR characteristic bands of the studied cross-linked chitosan and/or β-CD adsorbents. The presence of the bands corresponding to the amide/ester bonds and carboxyl groups in the prepared adsorbents indicated the successful cross-linking of the polysaccharides with the PACs or PAC dianhydrides. The Fe-O band confirmed the embedding of MNPs in the magnetic chitosan adsorbents (Paper II). The presence of the characteristic bands of CD (R–1,4–bond skeleton vibration) also verified the successful introduction of CDs in the obtained polymers (Paper III-V).

Table 13. The FT-IR characteristic bands of cross-linked chitosan and/or β-CD adsorbents (Paper I-V).

Adsorbent	*v* band (cm^{-1})	IR vibration
EGTA-chitosan	1734	C=O vibration in -COOH
	1626	C=O vibration in amide
	1553	N-H vibration in amide
	1110	C-O vibration in ether
MEDCS	3160-3700	OH vibration in -COOH
	1740	C=O vibration in -COOH
	1640	C=O vibration in amide
	573	Fe-O vibration in Fe_3O_4

EDTA-CDP	1679	C=O vibration in -COOH
	1738	C=O vibration in ester
	1203	C-O vibration in ester
	938	R–1,4–bond skeleton vibration of ß-CD
CS-ED-CD	3260	-OH stretch vibration
	2914	C-H vibration in $–CH_2$
	2975	C-H vibration in $–CH_3$
	1722	C=O vibration in -COOH
	1616	C=O vibration in amide
	1149	C-O vibration in the oxygen bridge
	931	R–1,4–bond skeleton vibration of ß-CD

The amounts of the functional groups in the cross-linked adsorbents were quantitative determined by elemental analysis (CHNS/O) (Paper I, III, and V), EDS (Paper II), and titration (Paper III and V). The results were summarized in **Table 14**. MEDCS obtained the highest PAC amount, which could be attributed to the abundant amino groups on the chitosan. Analytical method might also effect the results, where the EDS only determines the elements on the surface while elemental analysis (CHNS/O) defines the elements of the whole material [236]. Notably, the EDTA amounts obtained from titrations were lower than those obtained from elemental analysis (Paper III and V). This could be attributed to the fact that a part of EDTA groups involved in cross-linking. This effect was not significant for the amount of CD cavities. Importantly, the amounts of PCA groups and CD cavities of the adsorbents were in good agreement with their uptake ability of metals and organic pollutants, respectively, which will be discussed in Section 7.2.3.

Table 14. The amounts of the functional groups in the prepared polysaccharide adsorbents.

Adsorbent	PCA amount (mmol g^{-1})	β-CD amount (mmol g^{-1})	Method
EGTA-chitosan	EGTA 1.40	-	Elemental analysis (CHNS/O)
MEDCS	EDTA 2.24	-	EDS

MDTCS	DTPA 1.62	-	EDS
EDTA-CDP	EDTA 2.21	0.31	Elemental analysis (CHNS/O)
	EDTA 1.46	0.29	Back titration and photometric titration
CS-ED-CD	EDTA 2.05	0.17	Elemental analysis (CHNS/O)
	EDTA 1.36	0.147	Conductometric-potentiometric titration and photometric titration

The isoelectric point (the point of zero charge, pH_{PZC}) was measured by ζ-potential analyses for magnetic GLA-/EDTA-/DTPA-chitosan (Paper II), EPI-CDP, EDTA-CDP (Paper III), and CS-ED-CD (Paper V). The isoelectric point was found to be 6.85 for magnetic GLA-chitosan and 4.42 for EPI-CDP; the isoelectric point was determined as 3.35 for MEDCS, 3.65 for MDTCS, 2.23 for EDTA-CDP, and 3.81 for CS-ED-CD. Obviously, the PCAs and PCA dianhydrides cross-linked polysaccharides had much lower isoelectric point values than those of GLA and EPI cross-linked. This could be attributed to the fact that carboxylate groups were introduced in the materials during PCAs and PAC dianhydrides cross-linking process. A positive surface charge at $pH < pH_{PZC}$ means a protonation of the surface groups, while a negative surface charge at $pH > pH_{PZC}$ means the release of protons into the solution. Therefore, the lower pH_{PZC} values would bring benefit to the adsorbents when the target pollutants were cationic metals and organic compounds.

The thermal stabilities of MEDCS, MDTCS (Paper II), EDTA-CDP (Paper III), and CS-ED-CD (Paper V) were measured by TGA. For all these samples, the weight loss mostly occurred at three stages 60-120, 160-270, and 270-1000 ^{o}C, corresponding to water evaporation, EDTA/DTPA decomposition, and polysaccharides decomposition, respectively. The crystal lattice structure of magnetic adsorbents were determined by XRD in Paper II. All the index peaks of magnetite phase (JCPDS 19-0629) could be clearly found in the prepared magnetic adsorbents in Paper II. The magnetic properties of these magnetic adsorbents were also measured by VSM in Paper II. The results showed that these adsorbents possessed enough

magnetism to be rapidly separated from their well-dispersed water solutions by an external magnet.

7.2 Adsorption studies

7.2.1 Effect of solution pH

It is well known that the adsorption efficiency depends remarkably on the solution pH because pH affects not only the protonation of the surface groups but also the ionization degree of the adsorbates. Thus it is important to optimize the solution pH, in order to maximize the adsorption efficiency of the prepared adsorbents.

The adsorption efficiency of all the target heavy metals, REEs, cationic dyes, and organic pollutants were shown to be effected by the solution pH (Paper I-V). Alkaline solutions were not conducted for metals to avoid the formation of metal hydroxides (Visual MINTEQ ver. 3.0). For most of the target adsorbates, the similar trend was observed: low adsorption efficacy at low pH, due to the competition between the protons and the target cationic adsorbates in the strongly acidic media; adsorption efficiency soared with the increasing pH and reached an equilibrium plateau. The maximum adsorption of metals was found at pH range from 2.5 to 6 for EGTA-chitosan (Paper I), from 2.5 to 5.5 for MEDCS and MDTCS (Paper II), from 3.0 to 6.5 for EDTA-CDP (Paper III), and from 3.0 to 6.0 for CS-ED-CD (Paper V). The adsorption equilibrium plateau of cationic dyes on EDTA-CDP occurred at the pH range of 3-10 (Paper III), while 4-10 for the cationic organic pollutants onto CS-ED-CD (Paper V). The optimum pH for REEs adsorption by EDTA-CDP was observed at the range of 4-7 (Paper IV).

The adsorption efficiency soared with the increasing pH mostly from 1 to 2.5 in the studies, due to the increasing negative surface charge (e.g. COO^-) of the adsorbents with the raising pH, making the adsorbents more attractive for cationic metals and cationic organic pollutants. The equilibrium plateau could be attributed to the loading saturation and the stability of the surface-bound complexation. Notably, all the PCAs and PCA dianhydrides cross-linked polysaccharides adsorbents performed significantly higher adsorption efficiency,

in comparison to the pristine, GLA and EPI cross-linked polysaccharides, indicating the PCA groups play important role in adsorption.

7.2.2 Adsorption kinetics

In order to determine the equilibration time for the maximum adsorption as well as the rate-determining step of the adsorption, the time effect and kinetics were studied for the adsorption of metals, REEs, dyes, and organic pollutants on all the as-prepared adsorbents (Paper I-V).

Figure 28 shows the effect of time on the adsorption of Cd(II) by the PCAs and PCA dianhydrides cross-linked polysaccharide adsorbents. For all the adsorbents, the adsorption was very rapid at initial adsorption stage and even could attain more than 60% of maximum sorption capacities within 5 min. For instance, the adsorption capacity of MEDCS at 5 min reached 1.28 mmol g^{-1}, which was even higher than the maximum adsorption capacity of some adsorbents with 24 h. This is because there are abundant active adsorption sites available on the surface of the adsorbents at the initial stage. After that the adsorption slowed down probably due to the reducing of the binding sites on the adsorbents as well as the decrease of adsorbates in the solution. Then the adsorption of Cd(II) gradually reached equilibrium at 180 min for EGTA-chitosan, 120 min for MEDCS, 240 min for MDTCS, 150 min for EDTA-CDP, and 60 min for CS-ED-CD. Similar adsorption kinetics were found for the dyes (Paper III), REEs (Paper IV), and organic pollutants (Paper V).

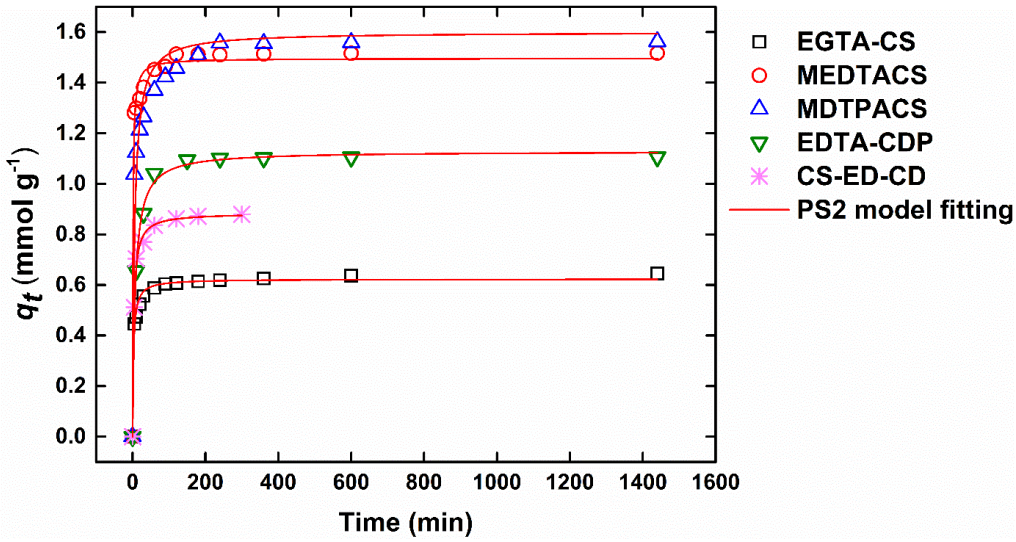

Figure 28. Effect of time on the adsorption of Cd(II) by the as-prepared cross-linked adsorbents. Results collected from Paper I-III and V. Adsorption conditions: dose 2 g L^{-1}, pH 4.0, C_i 1.5 mmol L^{-1} for EGTA-chitosan; dose 2 g L^{-1}, pH 3.5, C_i 3.4 mmol L^{-1} for MEDCS and MDTCS; dose 2 g L^{-1}, pH 6.02, C_i 4.45 mmol L^{-1} for EDTA-CDP; dose 1 g L^{-1}, pH 4.12, C_i 0.89 mmol L^{-1} for CS-ED-CD.

The kinetics of all the prepared adsorbents were studied by various models and the obtained PS2 and intraparticle diffusion parameters were given in **Table 15**. We applied linear fittings of the models in Paper I-V. The results showed that PS2 could estimate experimental q_m values relatively better and the obtained relatively higher correlation coefficient (R^2) values rather than PS1 model in Paper I, II, and IV. Moreover, besides PS1 and PS2 models, Elovich was also tested to describe the adsorption kinetics of MEDCS and MDTCS adsorbents in Paper II. It was found that the fittings of the models followed the order PS2 > Elovich > PS1. All these indicate that the adsorption process was controlled by the surface reaction [237]. At the same initial concentrations, the MEDCS showed higher rate constants (K_2 values) compared to MDTCS, indicating faster adsorption kinetics of magnetic EDTA-chitosan rather than magnetic DTPA-chitosan, which is in good agreement with the adsorption equilibrium time. This could be attributed to the higher functional groups on MEDCS (2.24 mmol g^{-1}) than MDTCS (1.62 mmol g^{-1}). In Paper III, the dyes had faster kinetics than those of heavy

metals and REEs on EDTA-CDP, implying that the host-guest inclusion interaction of CD cavities might be faster than EDTA complexing. In addition to surface reaction, some other process such as diffusion might also be the rate-controlling step. Intraparticle diffusion model was performed to examine this in Paper I, II and IV. Three slopes observed could be assigned to film diffusion, macropores diffusion, and diffusion in regions, with diffusion constant $K_{id,1}$ $K_{id,2}$, and $K_{id,3}$, respectively [132]. In general, the obtained $K_{id,1}$ values were much higher than those of $K_{id,2}$ and $K_{id,3}$, indicating that the film diffusion is the rate-controlling step during diffusion. Comparison of the diffusion rate constants of chitosan adsorbents and CD adsorbents in **Table 15** suggests that faster film diffusion occurred in chitosan rather than in CD materials. This could be attributed to the higher swelling ability of chitosan [28].

Table 15. PS2 and intraparticle diffusion model parameters of Cd(II), Pb(II), REEs, dyes, and organic pollutants by the cross-linked polysaccharide adsorbents in Paper I-V.

Adsorbate	C_i (mmol L^{-1})	$q_{e,exp}$ (mmol g^{-1})	PS2 model			Intraparticle diffusion model		
			$q_{e,cal}$ (mmol g^{-1})	K_2 (g $mmol^{-1}$ min^{-1})	R^2	$K_{id,1}$ (mmol g^{-1} $min^{-0.5}$)	$K_{id,2}$ (mmol g^{-1} $min^{-0.5}$)	$K_{id,3}$ (mmol g^{-1} $min^{-0.5}$)
EGTA-chitosan								
Cd(II)	1.5	0.644	0.638	0.318	0.999	0.199	0.027	0.003
Pb(II)	1.5	0.544	0.547	0.546	1.000	0.139	0.024	0.008
MEDCS								
Cd(II)	3.4	1.517	1.519	0.353	1.000	0.573	0.027	2.08×10^{-4}
Pb(II)	3.4	0.934	0.940	0.130	1.000	0.283	0.021	6.47×10^{-4}
MDTCS								
Cd(II)	3.4	1.562	1.569	0.108	1.000	0.464	0.037	2.76×10^{-4}

Pb(II)	3.4	0.878	0.887	0.078	1.000	0.224	0.021	4.11×10^{-4}
EDTA-CDP								
Cd(II)	4.46	1.106	1.110	0.209	1.000			
MB	0.94	0.261	0.262	0.679	1.000			
SO	0.86	0.161	0.162	0.827	1.000			
CV	0.74	0.254	0.255	0.882	1.000			
La(III)	1.33	0.310	0.311	0.367	0.999	0.059	0.005	7.41×10^{-4}
Ce(III)	1.33	0.337	0.339	0.218	0.999	0.050	0.009	1.06×10^{-3}
Eu(III)	1.33	0.353	0.356	0.268	0.999	0.108	0.020	7.08×10^{-4}
CS-ED-CD								
Pb(II)	0.242	0.239	0.241	1.877	1.000			
Cd(II)	0.446	0.440	0.445	0.606	1.000			
BPS	0.097	0.092	0.093	1.641	0.999			
CIP	0.090	0.079	0.082	1.300	1.000			
Procaine	0.086	0.080	0.082	1.596	0.999			
Imipramine	0.100	0.091	0.093	0.817	0.997			

7.2.3 Isotherm studies

6.2.3.1 Adsorption in single component solutions

Adsorption isotherms were studied by varying the initial adsorbate concentrations and keeping the other experimental conditions. The maximum adsorption capacity ($q_{m,exp}$) could be determined for the studied adsorbents by this way and the results are shown in **Table 16**. Moreover, to understand the adsorption mechanisms four isotherm models, e.g. Langmuir,

Freundlich, BiLangmuir and Sips, were applied for the single component systems in Paper I-V. Nonlinear fittings were applied for all the models in this thesis.

Table 16. Experimentally determined $q_{m,exp}$ of the targeted adsorbates by various studied adsorbents and the applied isotherms for modeling.

Adsorbent	Adsorbate	$q_{m,exp}$ (mmol g^{-1})	Applied isotherms
EGTA-chitosan	Cd(II)	0.737	Langmuir, Freundlich and BiLangmuir
	Pb(II)	0.502	
MEDCS	Cd(II)	1.499	Langmuir, Freundlich, BiLangmuir and Sips
	Pb(II)	1.030	
	Co(II)	1.236	
	Ni(II)	1.381	
MDTCS	Cd(II)	1.561	Langmuir, Freundlich, BiLangmuir and Sips
	Pb(II)	0.878	
	Co(II)	1.120	
	Ni(II)	1.087	
EDTA-CDP	Cu(II)	1.241	Langmuir and Sips
	Cd(II)	1.106	
	MB	0.262	
	SO	0.169	
	CV	0.280	
	La(III)	0.343	Langmuir, Freundlich and Sips
	Ce(III)	0.353	
	Eu(III)	0.365	
CS-ED-CD	Pb(II)	0.803	Langmuir and Sips
	Cd(II)	1.258	
	BPS	0.177	
	CIP	0.142	
	Procaine	0.203	
	Imipramine	0.149	

The fittings of the models were evaluated by the approximation of the nonlinear fitting curve, comparing the predicted q_m values with the experimental data, as well as the coefficient parameters. In Paper I, the BiLangmuir model gave the better fitting to the experimental isotherm data in comparison with Langmuir and Freundlich. As discussed in section 6.9.1 the BiLangmuir model assumes two kinds of active sites with different affinities. In Paper I, the low affinity sites were assigned to the residual amino groups of chitosan and high affinity sites to EGTA-groups. The high affinity site value was further compared with the amount of EGTA groups on the adsorbent. In Paper II, the isotherm fittings followed the order Sips $\approx$ BiLangmuir > Langmuir > Freundlich (**Figure 29**). In this study, however, the amino groups of chitosan were reacted with dianhydrides more thoroughly, resulting in higher EDTA or DTPA loading and less residual amino groups on the adsorbents. Based on this, the low and high affinity sites obtained from BiLangmuir in Paper II were assigned to the species distribution of EDTA or DTPA at the experimental pH (See Paper II). Moreover, the predicted maximum adsorption capacities of Sips (q_m) were slightly closer to the experimental data ($q_{m,exp}$), in comparison with BiLangmuir ($q_m = q_{m,1} + q_{m,2}$). The n_S values unequal to unity verified the heterogeneous adsorption sites. The higher K_S value of MEDCS than that of MDTCS could be due to the higher affinity of EDTA toward Cd(II) [235].

For the cross-linked CDP adsorbents, including EDTA-CDP and CS-ED-CD, the Langmuir model could fit better the metal adsorption data (**Table 17**), while the Sips model gave the better fitting for organic pollutants (**Table 18**) (Paper III and V). This suggested a homogeneous adsorption for metals and a heterogeneous adsorption for organic pollutants on the surface of the CDP adsorbents. The homogeneous adsorption sites for metals could be assigned to the EDTA-chelating groups and the heterogeneous sites for the cationic organic pollutants could be assigned to both EDTA groups and CD cavities. The adsorption affinity constants (K_L/K_S) of organic pollutants was found to be relatively higher than metals, revealing that the CDP adsorbents possess stronger affinity toward organic pollutants in comparison with metals. Similarly, in Paper IV, we observed that fitting results for REEs by EDTA-CDP followed

the isotherm order Langmuir > Sips > Freundlich, based on nonlinear curve approximation, q_m prediction, and R^2 value. This indicates a homogeneous adsorption surface (assigned to EDTA-group) for REEs on EDTA-CDP and discards the host-guest inclusion complexation of CD with REEs. EDTA-CDP performed lower uptake of REEs (0.34-0.37 mmol g^{-1}) than those of Cd(II) and Cu(II) (1.10-1.24 mmol g^{-1}), due to the lower stability constants of lanthanide(II)-EDTA complexes in comparison with metal(II)-EDTA complexes [132, 238]. The $q_{m,exp}$ of REEs followed the order La(III) < Ce(III) < Eu(III), good agreement with their corresponding stability constants of EDTA complexes (La(III)$EDTA^-$ 15.5 < Ce(III)$EDTA^-$ 15.9 < Eu(III)$EDTA^-$ 17.3) [238, 239].

Table 17. Fitting results of different isotherms for Cd(II) adsorption by cross-linked polysaccharide adsorbents.

Model	Isotherm parameter	EGTA-chitosan	MEDCS	MDTCS	EDTA-CDP	CS-ED-CD
	$q_{m,exp}$ (mmol g^{-1})	0.737	1.499	1.561	1.106	1.258
Langmuir	q_m (mmol g^{-1})	0.689	1.435	1.499	1.103	1.269
	K_L (L $mmol^{-1}$)	161.949	61.946	66.835	10.882	20.219
	R^2	0.968	0.979	0.965	0.970	0.996
Freundlich	K_F (L $mmol^{-1}$)	0.725	1.443	1.534		
	n_F	5.579	1.309	4.543		
	R^2	0.917	0.928	0.949		
Sips	q_m (mmol g^{-1})		1.580	1.642	1.211	1.247
	K_S (L $mmol^{-1}$)		36.863	32.469	7.039	23.487
	n_S		1.499	1.786	1.253	1.285
	R^2		0.997	0.999	0.969	0.976
BiLangmuir	$q_{m,1}$ (mmol g^{-1})	0.354	0.765	0.441		
	$q_{m,2}$ (mmol g^{-1})	0.391	0.777	1.140		
	K_1 (L $mmol^{-1}$)	14.518	8.231	953.730		

	K_2 (L mmol^{-1})	507.755	188.072	18.987
	R^2	0.997	0.998	0.987

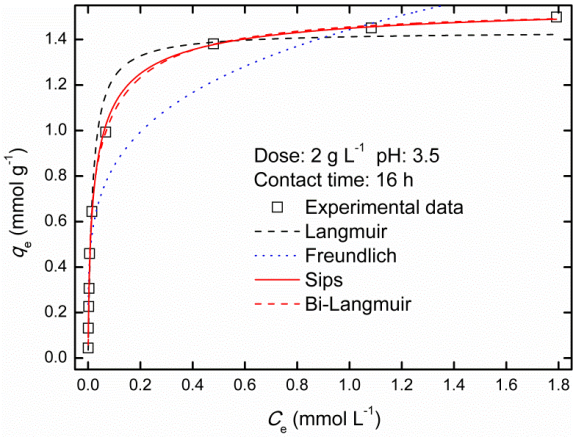

Figure 29. Adsorption equilibrium data of Cd(II) on MEDCS and fitting results of different isotherms from Paper II.

Table 18. Isotherm parameters of Langmuir and Sips models for organic pollutants by CDP adsorbents.

Sorbent	Pollutant	$q_{m,exp}$ (mmol g^{-1})	Langmuir model			Sips model			
			q_m (mmol g^{-1})	k_L (L mmol^{-1})	R^2	q_m (mmol g^{-1})	K_S (L mmol^{-1})	n_S	R^2
EDTA-CDP	MB	0.262	0.276	27.960	0.975	0.275	28.228	0.991	0.979
CS-ED-CD	BPS	0.177	0.196	108.847	0.934	0.177	162.623	2.241	0.997

6.2.3.2 Adsorption in binary and multi component solutions

The experimental data of two-component systems was obtained by using solutions containing different molar ratios (1:2, 1:1, and 2:1) of Cd(II) and Pb(II) (Paper I). It was observed that EGTA-chitosan possessed higher selectivity toward Cd(II) rather than Pb(II) at all the studied molar ratios, due to the higher stability constant of Cd(II)EGTA complex (see section 3.5.3 of Paper I). The obtained data were modeled by using the extended form of BiLangmuir isotherm. In this model, both the competitive ions form a mixed monolayer on the two kinds of active sites. The modeling results were presented in Figure 10 and Table 7 in Paper I. The sum of each metal uptake by both active sites 1 and 2 was calculated to be very close to the experimental $q_{m,exp}$ values. In general, the complex ligands possess certain stability constant (K) with each metal. In the modeling, however, different K values were obtained from the same binary systems with different initial molar ratios. This might be attributed to the competition, displacement, or interaction effects in two-component systems [240]. The excellent curve approximation, reliable q_m prediction, and high coefficient parameters gave evidence of the applicability of the extended BiLangmuir model for two-component systems. Interestingly, a synergistic phenomenon was clearly observed for the EGTA-chitosan in binary systems. For instance, q_m value of Cd(II) in two-component system was higher than that in single component system. This could be attributed to the positive synergy of chelation and electrostatic interaction between the co-exist ions [241].

In Paper IV we also studied the modeling of REEs adsorption in ternary systems by using Extended Sips model. The fitting results were presented in Figure 5 and Table 4 in Paper IV. The experimental data was well fitted by the Extended Sips model, reflecting in the good curve fitting and the close predicated q_m values for each REE. When compared to single-component adsorption, the obtained isotherm parameters of each REEs in ternary system such as predicted q_m values, affinity constant K_S, and heterogeneous factor n_S, were affected by the presence of other REEs. All the q_m values of each REEs were found to be less in ternary systems than in single systems, suggesting the competition and inhibition effects occurred. This inhibition effect could be interpreted by Pearson law [242]: La(III), Ce(III), and Eu(III) are classified as hard metal species and notable ionic competition occurs between the

metals from the same class. In single component systems, the adsorption capacities followed the order Eu(III) > Ce(III) > La(III), but the amount differences were slight (Table 2 in Paper IV). In the ternary systems, these differences were significantly widened and the advantage of Eu(III) became evident Eu(III) >> Ce(III) > La(III) (Table 4 in Paper IV). This could be attributed to the dual effects of stability constants and water structure constants [243] (see section 3.2.4 in Paper IV).

7.3 Application testing of the cross-linked polysaccharide adsorbents

7.3.1 Simultaneous removal of heavy metal and dyes from wastewater

Besides the binary metal adsorption experiments by EGTA-chitosan, the simultaneous adsorption of metal and dyes was also investigated in this thesis. In Paper III, EDTA-CDP was applied to remove simultaneously Cu(II) and cationic dyes such as MB, SO, and CV (Figure 3 and S8 in Paper III). Results showed that the adsorption capacities of Cu(II) were significantly enhanced by the presence of dyes ($q_{m,Cu(II)}$ in single system: 1.11 mmol g^{-1}, while $q_{m,Cu(II)}$ 1.36, 1.50, and 1.47 mmol g^{-1} in the presence of 200 mg L^{-1} of MB, SO, CV, respectively). This synergy effect on Cu(II) adsorption could be attributed to that the presence of dyes on the surface of the adsorbent via CDs inclusion complexation might provide extra adsorption sites for Cu(II), such as nitrogen-containing groups. However, in turn, the presence of Cu(II) did not enhance the adsorption of dyes in the binary systems. This could be explained by the EDTA-metal chelating mechanism that divalent metals were surrounded in EDTA octahedral structures, which were not able to supply extra active sites for dyes. The adsorption capacities of dyes were not affected by the presence of Cu(II), because each of them has their own adsorption site, i.e., CD cavities were expected to capture dyes while EDTA groups for metals. Overall, the dual functional EDTA-CDP showed potential for efficient and simultaneous removal of metal and dye pollutants.

7.3.2 Selective adsorption test

In the Paper II, the selectivity of metal ions on MEDCS and DTCS were also studied. The selective adsorption tests were carried out in the solutions containing same molar amount of

Cd(II), Pb(II), Co(II), and Ni(II). Results showed that the adsorption of the metals under competition conditions followed the order Ni(II) > Pb(II) >> Cd(II) > Co(II) for magnetic EDTA-chitosan and Pb(II) > Ni(II) >> Co(II) > Cd(II) for magnetic DTPA-chitosan (Figure S6 in Paper II). The selective tests in multi-metal systems suggested that the both MEDCS and MDTCS could be applied for the selective adsorption and separation of Pb(II) and Ni(II) from Cd(II) and Co(II) in aqueous solutions.

7.3.3 Practical industrial effluent experiments

The final target of adsorbents is their use in practical effluents. In Paper II, we tested MEDCS and MDTCS for the removal of metals in a real industrial effluents from a nonferrous metal smelter. The initial physical and chemical characteristics were examined and presented in section 3.5 of Paper II. The results showed that over 90% of Cu, Pb, Zn, Fe, and Ni removal from the real smelter effluent could be achieved by both the adsorbents (Table 2 in Paper II). The removal of As and Cr was not efficient probably because the species distribution of these two metals at the tested pH value (3.5) were mainly negative $H_2AsO_3^-$, $H_2AsO_4^-$, and $Cr_2O_7^{2-}$ [238], probably repulsed by COO^- on the surface of the adsorbents. Moreover, the adsorption capacities were also found to be negatively affected by the presence of other cations and anions such as Na^+, Ca^{2+}, SO_4^{2-}, PO_4^{3-}, and other organic pollutants in real wastewater. Overall, both the MEDCS and MDTCS were verified to be effective adsorbents for the practical industrial effluents containing Cu, Pb, Zn, Fe, and Ni.

7.3.4 Environmentally (μg L^{-1}) relevant concentration adsorption experiments

In Paper V, the CS-ED-CD was tested in simultaneous adsorption of Cd(II) and CIP at environmentally relevant concentration of 50-100 μg L^{-1}, the concentration which the micropolluants mostly exist in aqueous environment. The results showed that 92% of Cd(II) and 83% of CIP could be effectively and simultaneously removed after 6 h at a dosage of 1 g L^{-1} (Figure 11 Paper V). The results suggested that CS-ED-CD is a promising adsorbent for application in the removal of pollutants at environmentally relevant concentrations.

7.3.5 Preconcentration of trace adsorbates

Preconcentration is a very significant application for an advanced adsorbent. In particular, the determination of REEs from practical matrix solutions such as seawater requires preconcentration prior to analysis by instruments to increase the accuracy of the approach [244]. The results of the preconcentration of REEs in pure water, tap water, and seawater by EDTA-CDP were presented in Table 5 of Paper IV. It was found the preconcentration and recovery of REEs from all the studied matrix solutions were accurate and effective (84-105%). Moreover, the concentrations after 100-fold preconcentration exceeded the determination limits greatly, which is enough to guarantee the accuracy of the analysis method by ICP-OES.

7.4 Adsorption mechanism

Paper I, III, IV and V present the probable mechanisms of target adsorbates for EGTA-chitosan, EDTA-CDP and CS-ED-CD.

In the case of EGTA-chitosan (Paper I), EGTA-groups were consider as the dominant adsorption sites for Cd(II) and Pb(II) ions as follows:

$$\mathrm{R{-}H}_i\mathrm{EGTA}^{i-3} + \mathrm{M}^{2+} \rightleftharpoons (\mathrm{RHEGTA})\mathrm{M} + (i-1)\mathrm{H}^+ \qquad (19)$$

where R is chitosan, M represents divalent metal Cd(II) and Pb(II), and *i* is the number of hydrogen in the immobilized EGTA ranging from 0 to 1, since the major species of EGTA at the studied pH (4.0) are H_2EGTA^{2-} and $HEGTA^{3-}$ [238]. Moreover, the FT-IR spectra of EGTA-chitosan before and after metal adsorption verified the complex reaction between EGTA groups and divalent metals (Figure 6 in Paper I). The point charge calculation by density functional theory (DFT) further revealed that the adsorption mechanism of octahedral chelate structures (Figure 7 in Paper I).

Similarly, in Paper IV, the mechanism of REEs adsorption onto EDTA-CDP from an aqueous solution could be expressed as follows:

$$\mathrm{R{-}H}_i\mathrm{EDTA}^{i-3} + \mathrm{Ln}^{3+} \rightleftharpoons (\mathrm{REDTA})\mathrm{Ln} + i\mathrm{H}^+ \qquad (20)$$

Furthermore, as shown in Figure 6 of Paper IV, FT-IR confirmed the reaction between REE ion and EDTA groups (the peak of C=O shifted and the peaks of –OH and –NH2 weakened in the FT-IR spectra). Elemental mapping showed that the REEs were evenly loaded on the surface of EDTA-CDP (Figure 7, Paper IV).

The elemental mapping results in Figure S9 of Paper III clearly showed the well-distribution of the adsorption sites on EDTA-CDP for both metals and dyes. A probable simultaneous adsorption mechanism was proposed on the basis of the elemental mapping, thermodynamics, and FT-IR results (Figure 4 in Paper III): the EDTA moieties act as both cross-linkers and adsorption sites for metals via chelating; the CD cavities are responsible for the capture of the dyes through host-guest inclusion interaction. Moreover, the CD cavities were discarded to host metal ions but the EDTA moieties were found to be involved in adsorption of cation dyes via electrostatic interaction.

A similar mechanism of simultaneous adsorption of metals and organic pollutants onto CS-ED-CD was proposed in Paper V (Figure 9). The cross-linkage, EDTA, linked not only between intra- or inter-chitosan chains but also between chitosan and amino-modified CD cavities. Moreover, the FT-IR results provided evidence of the interaction between metals and EDTA moieties, resulting chelates. The CD cavities captured the organic pollutants. The isotherm studies confirmed this simultaneous adsorption mechanism.

7.5 Regeneration study

For the practical application, stability and reuse ability are important features of an advance adsorbents. In Paper I, Cd(II) and Pb(II) were desorbed from EGTA-chitosan by using 2 M HNO_3. The regeneration was conducted 10 times without a significant loss of adsorption efficiency. Similarly, the spent MEDCS and MDTCS adsorbents were regenerated by 2 M HNO_3 in Paper II. The results showed that the regeneration efficiencies of the magnetic adsorbents could remain 90% after sixth cycles. Moreover, the magnetic adsorbents were found stable in acidic media, where no significant leaching of iron was observed.

Cu(II)-loaded EDTA-CDP was successfully regenerated by using 1 M HNO_3 for 5 cycles. In the case of dye-loaded EDTA-CDP, three elution solutions including ethanol, 1% HCl in ethanol (v/v), and 5% HCl in ethanol (v/v) were applied. The results showed that the 5% HCl in ethanol (v/v) had the best regeneration efficiency, which retained above 90% after the fifth cycle (Figure 5 in Paper III). Moreover, the simultaneous adsorbed adsorbent could be regenerated by 5% HCl in ethanol and 1 M HNO_3 successively (**Figure 30**). The regenerated EDTA-CDP was reused for the simultaneous adsorption of Cu(II) and MB in a model textile effluent. The regeneration efficiencies were found to be higher than 85% (Figure S12 in Paper III). In Paper IV, the REE-loaded EDTA-CDP could be regenerated by 1 M HNO_3 for 5 cycles with the regeneration efficiencies ranging from 88.6% to 91.3%. The results of the regeneration study in Paper V indicate that Cd(II)-loaded CS-ED-CD could be used repeatedly using 1 M HNO_3 as regenerant, while BPS-loaded CS-ED-CD could be successfully regenerated by 5% HCl in ethanol. The results of the regeneration studies for all the studied cross-linked polysaccharide adsorbents are summarized in **Table 19**.

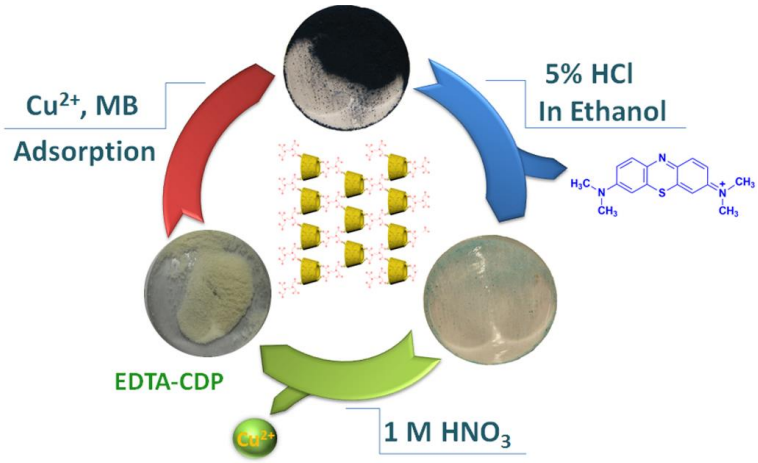

Figure 30. The schematic of the regeneration of the simultaneous adsorbed EDTA-CDP.

Table 19. The results of regeneration studies.

Adsorbent	Adsorbate	Adsorption mechanism	Regeneration solution	No. of cycle	Regeneration efficiency (%)

EGTA-chitosan	Cd(II)	Chelation	2 M HNO_3	10	99.18	Paper I
	Pb(II)	Chelation	2 M HNO_3	10	99.91	
MEDCS	Cd(II)	Chelation	2 M HNO_3	10	85.65	Paper II
MDTCS	Cd(II)	Chelation	2 M HNO_3	10	81.43	
EDTA-CDP	Cu(II)	Chelation	1 M HNO_3	5	88.71	Paper III
	MB	Host-guest inclusion	Ethanol	5	63.24	
	MB	Host-guest inclusion	1% HCl/Ethanol	5	81.57	
	MB	Host-guest inclusion	5% HCl/Ethanol	5	91.12	
EDTA-CDP	La(III)	Chelation	1 M HNO_3	5	88.59	Paper IV
	Ce(III)	Chelation	1 M HNO_3	5	93.73	
	Eu(III)	Chelation	1 M HNO_3	5	91.30	
CS-ED-CD	Cd(II)	Chelation	1 M HNO_3	5	90.48	Paper V
	BPS	Host-guest inclusion	Ethanol	5	64.77	
	BPS	Host-guest inclusion	5% HCl/Ethanol	5	86.24	

7.6 Cost estimation of synthesized adsorbents

As shown in Table 20 and 21, a cost analysis based on the yields and raw material costs of all the studied adsorbents revealed that the prices of magnetic EDTA or DTPA cross-linked chitosan are quite comparable to the commercial GLA cross-linked chitosan. The EGTA-chitosan costs higher due to the high price of original EGTA, but this situation will get better along with the price drop of EGTA, which has been more and more used. The cost of EDTA-CD is relatively high due to the low yield of water-insoluble polymer during the polycondensation reaction where most of the by-products are water-soluble CD oligomers. Importantly, in the CS-ED-CD system, the yield of adsorbent was much improved due to the fact that even the oligomers can be immobilized on the cross-linked chitosan chain. The cost

of CS-ED-CD is close to the commercial EPI-CD. Considered on the overwhelming metal adsorption ability and the excellent regeneration ability to the commercial adsorbents, it can be safely concluded that all the synthesized adsorbents are promising materials in practical application.

Table 20. The wholesale cost of reagents.

Reagent	Cost ($/kg)[a]
Granular activated carbons	22
Chitosan	14
β-cyclodextrin	2
EDTA	2.2
DTPA	2.5
EGTA	55
Acetic anhydride	6.2
EPI	10
GLA 50% solution	2.1
EDAC	18

[a] Prices obtained from wholesale suppliers (metric ton scale).

Table 21. Functional cost analysis of the studied adsorbents in this thesis.

Adsorbents	Chitosan (g)	β-CD/ Amino-β-CD (g)	Cross-linker (g)	Product (g)	Yield (%)	Raw materials ($/kg)[a]	Pilot-scale ($/kg)[b]
GLA-CS	0.7	-	0.5	0.79	65.83	13.73	41.20
EGTA-CS	1.0	-	1.6	1.59	61.15	64.15	192.45
EDTA-CS	1.0	-	6.0	1.66	23.71	16.40	49.46
DTPA-CS	1.0	-	6.0	1.43	20.71	20.28	60.84
EPI-CD	-	4.0	3.0	4.73	67.57	8.03	24.09
EDTA-CD	-	4.0	6.0	0.72	7.20	29.44	88.33

CS-ED-CD	1.0	0.5	6.0	2.15	31.33	13.12	39.35

[a] Calculated based on the raw materials required to produce 1 kg of adsorbent in quantitative yield, according to Alsbaiee's method.[1]

[b] The costs of the raw materials were scaled by 300% as a rough estimate of the cost associated with an optimized process in a pilot scale manufacturing plant, according to Alsbaiee's method.[1]

8. CONCLUSIONS AND FURTHER RESEARCH

The adsorption of Cd(II), Pb(II), Co(II), Ni(II), Cu(II), La(III), Ce(III), Eu(III), MB, SO, CV, BPS, CIP, procaine, and imipramine from aqueous solutions by five different cross-linked chitosan and/or β-CD adsorbents was investigated in this thesis. The model adsorbents that were employed to study the adsorptive behavior of polysaccharide-based adsorbents were EGTA-chitosan for metals removal, magnetic EDTAD/DTPAD cross-linked chitosan materials for metals removal, EDTA-cross-linked β-CD polymer for simultaneous removal of metals and cationic dyes, and for recovery of REEs, EDTA-cross-linked chitosan and β-CD hydrogel for metals and organic micropollutants removal.

The adsorbents were characterized by SEM, FTIR, elemental analyses, and titrations to verifying the surface morphology and functional groups. The SEM results showed different surface morphologies due to different base materials and also different cross-linking methods. The results of qualitative and quantitative analyses of functional groups indicated that there were enough active sites on the adsorbents for the studied adsorbates.

The clear benefit in the use of PCAs or PCA dianhydrides as cross-linkers is the easy one-pot synthesis method. The other important advantage is the dual functionalities that PCAs act the roles not only as linkages but also as active sites for metals. The experimental conditions, such as pH and contact time, were optimized by batch adsorption studies. Most of the studied adsorbents were effective at extreme pH conditions, due to the presence of PCA-groups in the adsorbents. The adsorption of most of the adsorbents were fast and even could attain great than 60% of maximum uptake within 5 min, and achieve the equilibrium

within 60-240 min. The kinetic studies revealed that the surface reaction and the film diffusion are the rate-controlling steps. The adsorbents showed remarkable potential for the removal of divalent metals (q_m 0.5-1.5 mmol g^{-1}), REEs (q_m ~0.35 mmol g^{-1}), dyes (q_m 0.17-0.28 mmol g^{-1}), and organic micropollutants (q_m 0.14-0.20 mmol g^{-1}) from aqueous solutions. The isotherms depended not only on the adsorbents but also on the adsorbates. For instance, the EDTA-CDP performed heterogeneous surface for cationic dyes, while homogeneous surface for divalent metals and REEs. In general, the five adsorbents showed heterogeneous adsorption for most of the studied adsorbates, due to the availability of multi-functional groups on the cross-linked adsorbents.

In application testing, EDTA-CDP was found as effective dual-functional adsorbent for simultaneous removal of divalent metals and cationic dyes from aqueous solutions. Especially a synergy effect on Cu(II) adsorption was observed in presence of dyes. In addition, preconcentration studies suggested that EDTA-CDP could be applied to preconcentrate trace-level of REEs from seawaters. In multi-metal systems, both magnetic EDTA-chitosan and magnetic DTPA-chitosan showed selective adsorption and separation of Pb(II) and Ni(II) from Cd(II) and Co(II) in aqueous solutions. Importantly, these two magnetic adsorbents were successfully applied for the treatment of heavy metals in a real industrial effluent from a nonferrous metal smelter. CS-ED-CD was proved as an effective adsorbent for application in the removal of pollutants at environmentally relevant concentrations. More significantly, all these adsorbents showed reliable reusability by using different regenerants. The chelation and host-guest inclusion were proposed as the dominant adsorption mechanisms, based on FT-IR, DFT calculation, elemental mapping, and thermodynamic studies.

By keeping eye on the future studies, the cross-linked chitosan and/or CD adsorbents represent good alternatives to replace the commercial adsorbents. From a future perspective, these novel adsorbents should be further studied in column tests, prior to full-scale industrial applications.

Moreover, besides the PCAs and PCA dianhydrides in this thesis, other novel economic and green cross-linkers should also be explored for the synthesis of polysaccharide-based adsorbents. Hyper-branched polymers contains abundant functional groups, such as polyethylenimine and poly(amidoamine), are possible to be used as novel cross-linkers. In addition, these novel cross-linker could also be applied for cross-linking of other polysaccharides such as cellulose and starch.

Due to the swelling behavior of polysaccharides, the separation of the adsorbents from wastewater is a major challenge by sediment, centrifugation, and filtration. Thus the addition of magnetic technology would be a promising alternative. Besides the preconcentration of REEs, similar procedures could be further studied, such as the recovery of nutrients and critical materials. The adsorbents could be tested in more challenging applications such as the treatment of difficult-to-treat acid mine drainage (AMD) wastewater and the separation of REE(III) from Fe(III).

REFERENCES

[1] A. Alsbaiee, B.J. Smith, L. Xiao, Y. Ling, D.E. Helbling, W.R. Dichtel, Rapid removal of organic micropollutants from water by a porous beta-cyclodextrin polymer, Nature 529 (2016) 190-194.

[2] R.P. Schwarzenbach, B.I. Escher, K. Fenner, T.B. Hofstetter, C.A. Johnson, U. von Gunten, B. Wehrli, The challenge of micropollutants in aquatic systems, Science 313 (2006) 1072-1077.

[3] E. Repo, T.A. Kurniawan, J.K. Warchol, M.E.T. Sillanpää, Removal of Co(II) and Ni(II) ions from contaminated water using silica gel functionalized with EDTA and/or DTPA as chelating agents, J. Hazard. Mater. 171 (2009) 1071-1080.

[4] R. Vinu, G. Madras, Kinetics of sonophotocatalytic degradation of anionic dyes with Nano-TiO2, Environ. Sci. Technol. 43 (2009) 473-479.

[5] K. Malachova, Z. Rybkova, H. Sezimova, J. Cerven, C. Novotny, Biodegradation and detoxification potential of rotating biological contactor (RBC) with Irpex lacteus for remediation of dye-containing wastewater, Water Res. 47 (2013) 7143-7148.

[6] F. Martinez, M.J. Lopez-Munoz, J. Aguado, J.A. Melero, J. Arsuaga, A. Sotto, R. Molina, Y. Segura, M.I. Pariente, A. Revilla, L. Cerro, G. Carenas, Coupling membrane separation and photocatalytic oxidation processes for the degradation of pharmaceutical pollutants, Water Res. 47 (2013) 5647-5658.

[7] T. Thiebault, R. Guegan, M. Boussafir, Adsorption mechanisms of emerging micro-pollutants with a clay mineral: Case of tramadol and doxepine pharmaceutical products, J. Colloid. Interface Sci. 453 (2015) 1-8.

[8] Z. Thong, G. Han, Y. Cui, J. Gao, T.S. Chung, S.Y. Chan, S. Wei, Novel nanofiltration membranes consisting of a sulfonated pentablock copolymer rejection layer for heavy metal removal, Environ. Sci. Technol. 48 (2014) 13880-13887.

[9] Q. Ge, P. Wang, C. Wan, T.S. Chung, Polyelectrolyte-promoted forward osmosis-membrane distillation (FO-MD) hybrid process for dye wastewater treatment, Environ. Sci. Technol. 46 (2012) 6236-6243.

[10] A. Salima, B. Benaouda, B. Noureddine, L. Duclaux, Application of Ulva lactuca and Systoceira stricta algae-based activated carbons to hazardous cationic dyes removal from industrial effluents, Water Res. 47 (2013) 3375-3388.

[11] Y. Sun, Z.Y. Wu, X. Wang, C. Ding, W. Cheng, S.H. Yu, X. Wang, Macroscopic and Microscopic Investigation of U(VI) and Eu(III) Adsorption on Carbonaceous Nanofibers, Environ. Sci. Technol. 50 (2016) 4459-4467.

[12] I.A. Shabtai, Y.G. Mishael, Efficient Filtration of Effluent Organic Matter by Polycation-Clay Composite Sorbents: Effect of Polycation Configuration on Pharmaceutical Removal, Environ. Sci. Technol. 50 (2016) 8246-8254.

[13] C. Cai, H. Zhang, X. Zhong, L. Hou, Electrochemical enhanced heterogeneous activation of peroxydisulfate by Fe-Co/SBA-15 catalyst for the degradation of Orange II in water, Water Res. 66 (2014) 473-485.

[14] H. Wang, Z.J. Ren, Bioelectrochemical metal recovery from wastewater: a review, Water Res. 66 (2014) 219-232.

[15] M. Li, F. Zhao, M. Sillanpää, Y. Meng, D. Yin, Electrochemical degradation of 2-diethylamino-6-methyl-4-hydroxypyrimidine using three-dimensional electrodes reactor with ceramic particle electrodes, Sep. Purif. Technol. 156, Part 2 (2015) 588-595.

[16] F. Mendez-Arriaga, R.A. Torres-Palma, C. Petrier, S. Esplugas, J. Gimenez, C. Pulgarin, Mineralization enhancement of a recalcitrant pharmaceutical pollutant in water by advanced oxidation hybrid processes, Water Res. 43 (2009) 3984-3991.

[17] X. Xiao, X. Zeng, A.T. Lemley, Species-dependent degradation of ciprofloxacin in a membrane anodic Fenton system, J. Agric. Food Chem. 58 (2010) 10169-10175.

[18] S. Sekar, M. Surianarayanan, V. Ranganathan, D.R. MacFarlane, A.B. Mandal, Choline-based ionic liquids-enhanced biodegradation of azo dyes, Environ. Sci. Technol. 46 (2012) 4902-4908.

[19] Z. Kurt, K. Shin, J.C. Spain, Biodegradation of Chlorobenzene and Nitrobenzene at Interfaces between Sediment and Water, Environ. Sci. Tech. 46 (2012) 11829-11835.

[20] L. Zhou, C. Gao, W. Xu, Magnetic dendritic materials for highly efficient adsorption of dyes and drugs, ACS Appl. Mater. Interfaces 2 (2010) 1483-1491.

[21] G.S. Miguel, S.D. Lambert, N.J. Graham, The regeneration of field-spent granular-activated carbons, Water Res. 35 (2001) 2740-2748.

[22] Q. Shi, L. Yan, T. Chan, C. Jing, Arsenic Adsorption on Lanthanum-Impregnated Activated Alumina: Spectroscopic and DFT Study, ACS Appl. Mater. Interfaces 7 (2015) 26735-26741.

[23] V. Rakic, L. Damjanovic, V. Rac, D. Stosic, V. Dondur, A. Auroux, The adsorption of nicotine from aqueous solutions on different zeolite structures, Water Res. 44 (2010) 2047-2057.

[24] L. Li, F. Liu, X. Jing, P. Ling, A. Li, Displacement mechanism of binary competitive adsorption for aqueous divalent metal ions onto a novel IDA-chelating resin: isotherm and kinetic modeling, Water Res. 45 (2011) 1177-1188.

[25] T.A. Kurniawan, G.Y. Chan, W.H. Lo, S. Babel, Comparisons of low-cost adsorbents for treating wastewaters laden with heavy metals, Sci. Total Environ. 366 (2006) 409-426.

[26] J. Luo, Y. Gao, K. Tan, W. Wei, X. Liu, Preparation of a Magnetic Molecularly Imprinted Graphene Composite Highly Adsorbent for 4-Nitrophenol in Aqueous Medium, ACS Sustainable Chem. Eng. 4 (2016) 3316-3326.

[27] M. Vakili, M. Rafatullah, B. Salamatinia, A.Z. Abdullah, M.H. Ibrahim, K.B. Tan, Z. Gholami, P. Amouzgar, Application of chitosan and its derivatives as adsorbents for dye removal from water and wastewater: A review, Carbohydr. Polym. 113 (2014) 115-130.

[28] G. Crini, Recent developments in polysaccharide-based materials used as adsorbents in wastewater treatment, Prog. Polym. Sci. 30 (2005) 38-70.

[29] N. Morin-Crini, G. Crini, Environmental applications of water-insoluble β-cyclodextrin–epichlorohydrin polymers, Prog. Polym. Sci. 38 (2013) 344-368.

[30] G. Crini, P.-M. Badot, Application of chitosan, a natural aminopolysaccharide, for dye removal from aqueous solutions by adsorption processes using batch studies: A review of recent literature, Prog. Polym. Sci. 33 (2008) 399-447.

[31] W.S. Wan Ngah, L.C. Teong, M.A.K.M. Hanafiah, Adsorption of dyes and heavy metal ions by chitosan composites: A review, Carbohydr. Polym. 83 (2011) 1446-1456.

[32] P. Miretzky, A.F. Cirelli, Hg(II) removal from water by chitosan and chitosan derivatives: a review, J. Hazard. Mater. 167 (2009) 10-23.

[33] F.-C. Wu, R.-L. Tseng, R.-S. Juang, A review and experimental verification of using chitosan and its derivatives as adsorbents for selected heavy metals, J. Environ. Manage. 91 (2010) 798-806.

[34] M. Hossein Beyki, F. Shemirani, M. Shirkhodaie, Aqueous Co(II) adsorption using 8-hydroxyquinoline anchored γ-Fe2O3@chitosan with Co(II) as imprinted ions, Int. J. Biol. Macromolec. 87 (2016) 375-384.

[35] G.Z. Kyzas, M. Kostoglou, N.K. Lazaridis, D.A. Lambropoulou, D.N. Bikiaris, Environmental friendly technology for the removal of pharmaceutical contaminants from wastewaters using modified chitosan adsorbents, Chem. Eng. J. 222 (2013) 248-258.

[36] G.Z. Kyzas, P.I. Siafaka, E.G. Pavlidou, K.J. Chrissafis, D.N. Bikiaris, Synthesis and adsorption application of succinyl-grafted chitosan for the simultaneous removal of zinc and cationic dye from binary hazardous mixtures, Chem. Eng. J. 259 (2015) 438-448.

[37] E. Repo, J.K. Warchoł, A. Bhatnagar, A. Mudhoo, M. Sillanpää, Aminopolycarboxylic acid functionalized adsorbents for heavy metals removal from water, Water Res. 47 (2013) 4812-4832.

[38] E. Repo, J.K. Warchoł, A. Bhatnagar, M. Sillanpää, Heavy metals adsorption by novel EDTA-modified chitosan–silica hybrid materials, J. Colloid Interface Sci. 358 (2011) 261-267.

[39] L. Wang, A. Wang, Adsorption characteristics of Congo Red onto the chitosan/montmorillonite nanocomposite, J. Hazard. Mater. 147 (2007) 979-985.

[40] L. Fan, C. Luo, X. Li, F. Lu, H. Qiu, M. Sun, Fabrication of novel magnetic chitosan grafted with graphene oxide to enhance adsorption properties for methyl blue, J. Hazard. Mater. 215-216 (2012) 272-279.

[41] M. Adeli, Y. Yamini, M. Faraji, Removal of copper, nickel and zinc by sodium dodecyl sulphate coated magnetite nanoparticles from water and wastewater samples, Arabian J. Chem.

[42] J. Zhang, P.X. Ma, Cyclodextrin-based supramolecular systems for drug delivery: recent progress and future perspective, Adv. Drug Deliv. Rev. 65 (2013) 1215-1233.

[43] H. Liu, X. Cai, Y. Wang, J. Chen, Adsorption mechanism-based screening of cyclodextrin polymers for adsorption and separation of pesticides from water, Water Res. 45 (2011) 3499-3511.

[44] M.L. Brusseau, X. Wang, W.-Z. Wang, Simultaneous Elution of Heavy Metals and Organic Compounds from Soil by Cyclodextrin, Environ. Sci. Technol. 31 (1997) 1087-1092.

[45] R. Sawicki, L. Mercier, Evaluation of mesoporous cyclodextrin-silica nanocomposites for the removal of pesticides from aqueous media, Environ. Sci. Technol. 40 (2006) 1978-1983.

[46] G. Crini, M. Morcellet, Synthesis and applications of adsorbents containing cyclodextrins, J. Sep. Sci. 25 (2002) 789-813.

[47] N. Lin, A. Dufresne, Supramolecular hydrogels from in situ host-guest inclusion between chemically modified cellulose nanocrystals and cyclodextrin, Biomacromolecules 14 (2013) 871-880.

[48] E.M.M. Del Valle, Cyclodextrins and their uses: a review, Process Biochem. 39 (2004) 1033-1046.

[49] A. Concheiro, C. Alvarez-Lorenzo, Chemically cross-linked and grafted cyclodextrin hydrogels: from nanostructures to drug-eluting medical devices, Adv. Drug Deliv. Rev. 65 (2013) 1188-1203.

[50] C.Y. Quan, J.X. Chen, H.Y. Wang, C. Li, C. Chang, X.Z. Zhang, R.X. Zhuo, Core-shell nanosized assemblies mediated by the alpha-beta cyclodextrin dimer with a tumor-triggered targeting property, ACS nano 4 (2010) 4211-4219.

[51] N. Lin, A. Dufresne, Supramolecular Hydrogels from In Situ Host–Guest Inclusion between Chemically Modified Cellulose Nanocrystals and Cyclodextrin, Biomacromolecules 14 (2013) 871-880.

[52] O.Y. Yu, J.W. Chung, S.Y. Kwak, Reduced migration from flexible poly(vinyl chloride) of a plasticizer containing beta-cyclodextrin derivative, Environ. Sci. Technol. 42 (2008) 7522-7527.

[53] N. Qiu, L. Cai, W. Wang, G. Wang, X. Cheng, Q. Xu, J. Wen, J. Liu, Y. Wei, L. Chen, Barbigerone-in-hydroxypropyl-β-cyclodextrin-liposomal nanoparticle: preparation, characterization and anti-cancer activities, J. Inclusion Phenom.Macrocyclic Chem. 82 (2015) 505-514.

[54] D.M. Alzate-Sánchez, B.J. Smith, A. Alsbaiee, J.P. Hinestroza, W.R. Dichtel, Cotton Fabric Functionalized with a β-Cyclodextrin Polymer Captures Organic Pollutants from Contaminated Air and Water, Chem. Mater. 28 (2016) 8340-8346.

[55] B. Gidwani, A. Vyas, Synthesis, characterization and application of epichlorohydrin-beta-cyclodextrin polymer, Colloids Surf. B Biointerfaces 114 (2014) 130-137.

[56] Z.-J. Yang, H. Zeng, X.-T. Zhou, H.-B. Ji, Enhanced catalytic activity and recyclability for oxidation of cinnamaldehyde catalysed by β-cyclodextrin cross-linked with chitosan, Supramol. Chem. 25 (2013) 233-245.

[57] J. Morales-Sanfrutos, F.J. Lopez-Jaramillo, M.A. Elremaily, F. Hernandez-Mateo, F. Santoyo-Gonzalez, Divinyl sulfone cross-linked cyclodextrin-based polymeric materials: synthesis and applications as sorbents and encapsulating agents, Molecules 20 (2015) 3565-3581.

[58] S. Nagireddi, V. Katiyar, R. Uppaluri, Pd(II) adsorption characteristics of glutaraldehyde cross-linked chitosan copolymer resin, Int. J. Biol. Macromol. 94 (2016) 72-84.

[59] C. Xiao, R. You, Y. Fan, Y. Zhang, Tunable functional hydrogels formed from a versatile water-soluble chitosan, Int. J. Biol. Macromol. 85 (2016) 386-390.

[60] A.H. Chen, S.C. Liu, C.Y. Chen, C.Y. Chen, Comparative adsorption of Cu(II), Zn(II), and Pb(II) ions in aqueous solution on the crosslinked chitosan with epichlorohydrin, J. Hazard. Mater. 154 (2008) 184-191.

[61] D.Y. Pratt, L.D. Wilson, J.A. Kozinski, A.M. Mohart, Preparation and sorption studies of β-cyclodextrin/epichlorohydrin copolymers, J. Appl. Polym. Sci. 116 (2010) 2982-2989.

[62] K. Azlan, W.N. Wan Saime, L. Lai Ken, Chitosan and chemically modified chitosan beads for acid dyes sorption, J. Environ. Sci. 21 (2009) 296-302.

[63] H. Kono, T. Nakamura, H. Hashimoto, Y. Shimizu, Characterization, molecular dynamics, and encapsulation ability of beta-cyclodextrin polymers crosslinked by polyethylene glycol, Carbohydr. Polym. 128 (2015) 11-23.

[64] T.S. Anirudhan, S. Rijith, Glutaraldehyde cross-linked epoxyaminated chitosan as an adsorbent for the removal and recovery of copper(II) from aqueous media, Colloids Surf., A 351 (2009) 52-59.

[65] K. Singh, P.G. Ingole, H.C. Bajaj, H. Gupta, Preparation, characterization and application of β-cyclodextrin-glutaraldehyde crosslinked membrane for the enantiomeric separation of amino acids, Desalin. 298 (2012) 13-21.

[66] E.Y. Ozmen, M. Yilmaz, Use of beta-cyclodextrin and starch based polymers for sorption of Congo red from aqueous solutions, J. Hazard. Mater. 148 (2007) 303-310.

[67] S. Stranges, M. Alagia, P. Decleva, M. Stener, G. Fronzoni, D. Toffoli, M. Speranza, D. Catone, S. Turchini, T. Prosperi, N. Zema, G. Contini, Y. Keheyan, The valence electronic structure and conformational flexibility of epichlorohydrin, Phys. Chem. Chem. Phys. 13 (2011) 12517-12528.

[68] E.Y. Ozmen, M. Sezgin, A. Yilmaz, M. Yilmaz, Synthesis of beta-cyclodextrin and starch based polymers for sorption of azo dyes from aqueous solutions, Bioresour. Technol. 99 (2008) 526-531.

[69] I. Vélaz, J. Isasi, M. Sánchez, M. Uzqueda, G. Ponchel, Structural characteristics of some soluble and insoluble β-cyclodextrin polymers, J. Inclusion Phenom.Macrocyclic Chem. 57 (2007) 65-68.

[70] Q. Chen, Y. Wen, Y. Cang, L. Li, X. Guo, R. Zhang, Selective removal of phenol by spherical particles of α-, β-and γ-cyclodextrin polymers: kinetics and isothermal equilibrium, Front. Chem. Sci. Eng. 7 (2013) 162-169.

[71] G. Crini, H.N. Peindy, Adsorption of C.I. Basic Blue 9 on cyclodextrin-based material containing carboxylic groups, Dyes Pigm. 70 (2006) 204-211.

[72] M.T. Sikder, M.S. Islam, T. Kikuchi, J. Suzuki, T. Saito, M. Kurasaki, Removal of copper ions from water using epichlorohydrin cross-linked β-cyclodextrin polymer: characterization, isotherms and kinetics, Water Environ. Res. 86 (2014) 296-304.

[73] C.G. Li, F. Wang, W.G. Peng, Y.H. He, Preparation of chitosan and epichlorohydrin cross-linked adsorbents and adsorption property of dyes, in: Appl. Mech. Mater., Trans Tech Publ, 2013, pp. 584-587.

[74] T.-Y. Kim, S.-S. Park, S.-Y. Cho, Adsorption characteristics of Reactive Black 5 onto chitosan beads cross-linked with epichlorohydrin, J. Ind. Eng. Chem. 18 (2012) 1458-1464.

[75] R. Laus, V.T. de Favere, Competitive adsorption of Cu(II) and Cd(II) ions by chitosan crosslinked with epichlorohydrin-triphosphate, Bioresour. Technol. 102 (2011) 8769-8776.

[76] G. Wang, J. Liu, X. Wang, Z. Xie, N. Deng, Adsorption of uranium (VI) from aqueous solution onto cross-linked chitosan, J. Hazard. Mater. 168 (2009) 1053-1058.

[77] X. Zhang, Y. Wang, Y. Yi, Synthesis and characterization of grafting β - cyclodextrin with chitosan, J. Appl. Polym. Sci. 94 (2004) 860-864.

[78] J.-M. Li, X.-G. Meng, C.-W. Hu, J. Du, Adsorption of phenol, p-chlorophenol and p-nitrophenol onto functional chitosan, Bioresour. Technol. 100 (2009) 1168-1173.

[79] R.S. Vieira, M.M. Beppu, Interaction of natural and crosslinked chitosan membranes with Hg(II) ions, Colloids Surf., A 279 (2006) 196-207.

[80] P. Baroni, R.S. Vieira, E. Meneghetti, M.G. da Silva, M.M. Beppu, Evaluation of batch adsorption of chromium ions on natural and crosslinked chitosan membranes, J. Hazard. Mater. 152 (2008) 1155-1163.

[81] Y. Liu, Y. Liu, X. Cao, R. Hua, Y. Wang, C. Pang, M. Hua, X. Li, Biosorption studies of uranium (VI) on cross-linked chitosan: isotherm, kinetic and thermodynamic aspects, J. Radioanal. Nucl. Chem. 290 (2011) 231-239.

[82] N. Grisdanurak, S. Akewaranugulsiri, C.M. Futalan, W.C. Tsai, C.C. Kan, C.W. Hsu, M.W. Wan, The study of copper adsorption from aqueous solution using crosslinked chitosan immobilized on bentonite, J. Appl. Polym. Sci. 125 (2012).

[83] H. Ge, S. Huang, Microwave preparation and adsorption properties of EDTA - modified cross - linked chitosan, J. Appl. Polym. Sci. 115 (2010) 514-519.

[84] I.X. Garcia-Zubiri, G. Gonzalez-Gaitano, J.R. Isasi, Isosteric heats of sorption of 1-naphthol and phenol from aqueous solutions by beta-cyclodextrin polymers, J. Colloid Interface Sci. 307 (2007) 64-70.

[85] L.-C. Zhou, X.-G. Meng, J.-W. Fu, Y.-C. Yang, P. Yang, C. Mi, Highly efficient adsorption of chlorophenols onto chemically modified chitosan, Appl. Surf. Sci. 292 (2014) 735-741.

[86] E. Zeiger, B. Gollapudi, P. Spencer, Genetic toxicity and carcinogenicity studies of glutaraldehyde—a review, Mutat. Res.-Rev. Mutat. 589 (2005) 136-151.

[87] O.A.C. Monteiro Jr, C. Airoldi, Some studies of crosslinking chitosan–glutaraldehyde interaction in a homogeneous system, Int. J. Biol. Macromol. 26 (1999) 119-128.

[88] L. Poon, L.D. Wilson, J.V. Headley, Chitosan-glutaraldehyde copolymers and their sorption properties, Carbohydr. Polym. 109 (2014) 92-101.

[89] S. Dumitriu, Polysaccharides in medicinal applications, CRC Press, 1996.

[90] S.-I. Park, I.S. Kwak, S.W. Won, Y.-S. Yun, Glutaraldehyde-crosslinked chitosan beads for sorptive separation of Au(III) and Pd(II): Opening a way to design reduction-coupled selectivity-tunable sorbents for separation of precious metals, J. Hazard. Mater. 248–249 (2013) 211-218.

[91] A.R. Cestari, E.F.S. Vieira, A.M.G. Tavares, R.E. Bruns, The removal of the indigo carmine dye from aqueous solutions using cross-linked chitosan—Evaluation of adsorption thermodynamics using a full factorial design, J. Hazard. Mater. 153 (2008) 566-574.

[92] D.Y. Pratt, L.D. Wilson, J.A. Kozinski, Preparation and sorption studies of glutaraldehyde cross-linked chitosan copolymers, J. Colloid Interface Sci. 395 (2013) 205-211.

[93] J. Berger, M. Reist, J.M. Mayer, O. Felt, N.A. Peppas, R. Gurny, Structure and interactions in covalently and ionically crosslinked chitosan hydrogels for biomedical applications, Eur. J. Pharm. Biopharm. 57 (2004) 19-34.

[94] Y. Ren, H.A. Abbood, F. He, H. Peng, K. Huang, Magnetic EDTA-modified chitosan/SiO_2/Fe_3O_4 adsorbent: Preparation, characterization, and application in heavy metal adsorption, Chem. Eng. J. 226 (2013) 300-311.

[95] L.D. Wilson, D.Y. Pratt, J.A. Kozinski, Preparation and sorption studies of beta-cyclodextrin-chitosan-glutaraldehyde terpolymers, J. Colloid Interface Sci. 393 (2013) 271-277.

[96] B. Blanco-Fernandez, M. Lopez-Viota, A. Concheiro, C. Alvarez-Lorenzo, Synergistic performance of cyclodextrin–agar hydrogels for ciprofloxacin delivery and antimicrobial effect, Carbohydr. Polym. 85 (2011) 765-774.

[97] N. Li, R. Bai, A Novel Amine-Shielded Surface Cross-Linking of Chitosan Hydrogel Beads for Enhanced Metal Adsorption Performance, Ind. Eng. Chem. Res. 44 (2005) 6692-6700.

[98] H. Kono, K. Onishi, T. Nakamura, Characterization and bisphenol A adsorption capacity of beta-cyclodextrin-carboxymethylcellulose-based hydrogels, Carbohydr. Polym. 98 (2013) 784-792.

[99] A. Ramesh, H. Hasegawa, W. Sugimoto, T. Maki, K. Ueda, Adsorption of gold(III), platinum(IV) and palladium(II) onto glycine modified crosslinked chitosan resin, Bioresour. Technol. 99 (2008) 3801-3809.

[100] Y.-H. Mao, Y. Guan, Q.-K. Zheng, X.-N. Feng, X.-X. Wang, Adsorption thermodynamic and kinetic of disperse dye on cotton fiber modified with tolylene diisocyanate derivative, Cellul. 18 (2011) 271-279.

[101] A. Romo, F.J. Peñas, J.R. Isasi, I.X. García-Zubiri, G. González-Gaitano, Extraction of phenols from aqueous solutions by β-cyclodextrin polymers. Comparison of sorptive capacities with other sorbents, React. Funct. Polym. 68 (2008) 406-413.

[102] E.Y. Ozmen, M. Sezgin, A. Yilmaz, M. Yilmaz, Synthesis of β-cyclodextrin and starch based polymers for sorption of azo dyes from aqueous solutions, Bioresour. Technol. 99 (2008) 526-531.

[103] T. Hishiya, M. Shibata, M. Kakazu, H. Asanuma, M. Komiyama, Molecularly Imprinted Cyclodextrins as Selective Receptors for Steroids, Macromol. 32 (1999) 2265-2269.

[104] F. Zha, S. Li, Y. Chang, Preparation and adsorption property of chitosan beads bearing β-cyclodextrin cross-linked by 1,6-hexamethylene diisocyanate, Carbohydr. Polym. 72 (2008) 456-461.

[105] M. Prabaharan, J.F. Mano, Chitosan derivatives bearing cyclodextrin cavitiesas novel adsorbent matrices, Carbohydr. Polym. 63 (2006) 153-166.

[106] S.-H. Chiu, T.-W. Chung, R. Giridhar, W.-T. Wu, Immobilization of β-cyclodextrin in chitosan beads for separation of cholesterol from egg yolk, Food Res. Int. 37 (2004) 217-223.

[107] W.J. Hehre, A.J. Shusterman, Organic chemistry, Prentice Hall, 2001.

[108] S. Kumar, V. Deepak, M. Kumari, P.K. Dutta, Antibacterial activity of diisocyanate-modified chitosan for biomedical applications, Int. J. Biol. Macromol. 84 (2016) 349-353.

[109] G.Z. Kyzas, N.K. Lazaridis, D.N. Bikiaris, Optimization of chitosan and β-cyclodextrin molecularly imprinted polymer synthesis for dye adsorption, Carbohydr. Polym. 91 (2013) 198-208.

[110] C.Q. Yang, X. Wang, Infrared spectroscopy studies of the cyclic anhydride as the intermediate for the ester crosslinking of cotton cellulose by polycarboxylic acids. II. Comparison of different polycarboxylic acids, J. Polym. Sci., Part A: Polym. Chem. 34 (1996) 1573-1580.

[111] C.Q. Yang, X. Wang, I.-S. Kang, Ester crosslinking of cotton fabric by polymeric carboxylic acids and citric acid, Text. Res. J. 67 (1997) 334-342.

[112] N. Reddy, Y. Li, Y. Yang, Alkali - catalyzed low temperature wet crosslinking of plant proteins using carboxylic acids, Biotechnol. Progr. 25 (2009) 139-146.

[113] T. Ghosh Dastidar, A.N. Netravali, 'Green' crosslinking of native starches with malonic acid and their properties, Carbohydr. Polym. 90 (2012) 1620-1628.

[114] L. Goetz, A. Mathew, K. Oksman, P. Gatenholm, A.J. Ragauskas, A novel nanocomposite film prepared from crosslinked cellulosic whiskers, Carbohydr. Polym. 75 (2009) 85-89.

[115] N. Reddy, Y. Yang, Citric acid cross-linking of starch films, Food Chem. 118 (2010) 702-711.

[116] B. Martel, M. Weltrowski, D. Ruffin, M. Morcellet, Polycarboxylic acids as crosslinking agents for grafting cyclodextrins onto cotton and wool fabrics: study of the process parameters, J. Appl. Polym. Sci. 83 (2002) 1449-1456.

[117] B. Martel, M. Morcellet, D. Ruffin, L. Ducoroy, M. Weltrowski, Finishing of polyester fabrics with cyclodextrins and polycarboxylic acids as crosslinking agents, J. Inclusion Phenom.Macrocyclic Chem. 44 (2002) 443-446.

[118] D. Alonso, M. Gimeno, R. Olayo, H. Vázquez-Torres, J.D. Sepúlveda-Sánchez, K. Shirai, Cross-linking chitosan into UV-irradiated cellulose fibers for the preparation of antimicrobial-finished textiles, Carbohydr. Polym. 77 (2009) 536-543.

[119] H.M. Fahmy, M.M.G. Fouda, Crosslinking of alginic acid/chitosan matrices using polycarboxylic acids and their utilization for sodium diclofenac release, Carbohydr. Polym. 73 (2008) 606-611.

[120] C.Q. Yang, Infrared spectroscopy studies of the cyclic anhydride as the intermediate for the ester crosslinking of cotton cellulose by polycarboxylic acids. I. Identification of the cyclic anhydride intermediate, J. Polym. Sci., Part A: Polym. Chem. 31 (1993) 1187-1193.

[121] L. Shen, H. Xu, L. Kong, Y. Yang, Non-Toxic Crosslinking of Starch Using Polycarboxylic Acids: Kinetic Study and Quantitative Correlation of Mechanical Properties and Crosslinking Degrees, J. Polym. Environ. 23 (2015) 588-594.

[122] D. Zhao, L. Zhao, C. Zhu, Z. Tian, X. Shen, Synthesis and properties of water-insoluble β-cyclodextrin polymer crosslinked by citric acid with PEG-400 as modifier, Carbohydr. Polym. 78 (2009) 125-130.

[123] D. Zhao, L. Zhao, C.-S. Zhu, X. Shen, X. Zhang, B. Sha, Comparative study of polymer containing β-cyclodextrin and –COOH for adsorption toward aniline, 1-naphthylamine and methylene blue, J. Hazard. Mater. 171 (2009) 241-246.

[124] L. Ducoroy, B. Martel, B. Bacquet, M. Morcellet, Ion exchange textiles from the finishing of PET fabrics with cyclodextrins and citric acid for the sorption of metallic cations in water, J. Inclusion Phenom.Macrocyclic Chem. 57 (2007) 271-277.

[125] S.H. Hsieh, E.S. Lin, H.C. Wei, Effect of chitosan addition to BTCA/CA processed cotton fabrics for adsorbing metallic ions from waste water, J. Appl. Polym. Sci. 101 (2006) 3264-3269.

[126] L. Ducoroy, M. Bacquet, B. Martel, M. Morcellet, Removal of heavy metals from aqueous media by cation exchange nonwoven PET coated with β-cyclodextrin-polycarboxylic moieties, React. Funct. Polym. 68 (2008) 594-600.

[127] D. Zhao, L. Zhao, C.-S. Zhu, W.-Q. Huang, J.-L. Hu, Water-insoluble β-cyclodextrin polymer crosslinked by citric acid: synthesis and adsorption properties toward phenol and methylene blue, J. Inclusion Phenom.Macrocyclic Chem. 63 (2009) 195-201.

[128] I.S. Lima, C. Airoldi, Interaction of copper with chitosan and succinic anhydride derivative—a factorial design evaluation of the chemisorption process, Colloids Surf., A 229 (2003) 129-136.

[129] T. Girek, C.A. Kozlowski, J.J. Koziol, W. Walkowiak, I. Korus, Polymerisation of β-cyclodextrin with succinic anhydride. Synthesis, characterisation, and ion flotation of transition metals, Carbohydr. Polym. 59 (2005) 211-215.

[130] H. Ge, H. Chen, S. Huang, Microwave preparation and properties of O‐crosslinked maleic acyl chitosan adsorbent for Pb2+ and Cu2+, J. Appl. Polym. Sci. 125 (2012) 2716-2723.

[131] H. Karaer, İ. Uzun, Adsorption of basic dyestuffs from aqueous solution by modified chitosan, Desalin. Water Treat. 51 (2013) 2294-2305.

[132] E. Repo, J.K. Warchol, T.A. Kurniawan, M.E.T. Sillanpää, Adsorption of Co(II) and Ni(II) by EDTA- and/or DTPA-modified chitosan: Kinetic and equilibrium modeling, Chem. Eng. J. 161 (2010) 73-82.

[133] Z. Sun, Y. Liu, Y. Huang, X. Tan, G. Zeng, X. Hu, Z. Yang, Fast adsorption of Cd^{2+} and Pb^{2+} by EGTA dianhydride (EGTAD) modified ramie fiber, J. Colloid Interface Sci. 434 (2014) 152-158.

[134] H. Kono, M. Zakimi, Preparation, water absorbency, and enzyme degradability of novel chitin‐and cellulose/chitin‐based superabsorbent hydrogels, J. Appl. Polym. Sci. 128 (2013) 572-581.

[135] H. Kono, I. Oeda, T. Nakamura, The preparation, swelling characteristics, and albumin adsorption and release behaviors of a novel chitosan-based polyampholyte hydrogel, React. Funct. Polym. 73 (2013) 97-107.

[136] H. Kono, T. Nakamura, Polymerization of β-cyclodextrin with 1,2,3,4-butanetetracarboxylic dianhydride: Synthesis, structural characterization, and bisphenol A adsorption capacity, React. Funct. Polym. 73 (2013) 1096-1102.

[137] F.V. Pereira, L.V. Gurgel, L.F. Gil, Removal of Zn2+ from aqueous single metal solutions and electroplating wastewater with wood sawdust and sugarcane bagasse modified with EDTA dianhydride (EDTAD), J. Hazard. Mater. 176 (2010) 856-863.

[138] J. Roosen, K. Binnemans, Adsorption and chromatographic separation of rare earths with EDTA- and DTPA-functionalized chitosan biopolymers, J. Mater. Chem. A 2 (2014) 1530-1540.

[139] J. Roosen, S. Van Roosendael, C.R. Borra, T. Van Gerven, S. Mullens, K. Binnemans, Recovery of scandium from leachates of Greek bauxite residue by adsorption on functionalized chitosan-silica hybrid materials, Green Chemistry 18 (2016) 2005-2013.

[140] F.T. de Almeida, B.C. Ferreira, A.L. Moreira, R.P. de Freitas, L.F. Gil, L.V. Gurgel, Application of a new bifunctionalized chitosan derivative with zwitterionic characteristics for the adsorption of Cu(2+), Co(2+), Ni(2+), and oxyanions of Cr(6+) from aqueous solutions: Kinetic and equilibrium aspects, J. Colloid Interface Sci. 466 (2016) 297-309.

[141] L.B. Maktouf, I. Ghorbel, A. Afli, S. Abid, A. Gandini, Polyimides based on furanic diamines and aromatic dianhydrides: synthesis, characterization and properties, Polym. Bull. 67 (2011) 1111-1122.

[142] I. Kavianinia, P.G. Plieger, N.G. Kandile, D.R.K. Harding, New hydrogels based on symmetrical aromatic anhydrides: Synthesis, characterization and metal ion adsorption evaluation, Carbohydr. Polym. 87 (2012) 881-893.

[143] N.M. Julkapli, H.M. Akil, Z. Ahmad, Thermal properties of 4, 4-oxydiphathalic anhydride chitosan filled chitosan bio-composites, J. Therm. Anal. Calorim. 107 (2012) 365-376.

[144] F. Li, X. Sun, H. Zhang, B. Li, F. Gan, Pyromellitic dianhydride - modified β - cyclodextrin microspheres for Pb (II) and Cd (II) adsorption, J. Appl. Polym. Sci. 105 (2007) 3418-3425.

[145] Z. Tan, H. Peng, H. Liu, L. Wang, J. Chen, X. Lu, Facile preparation of EDTA - functionalized chitosan magnetic adsorbent for removal of Pb (II), J. Appl. Polym. Sci. 132 (2015).

[146] L. Wan, Y. Wang, S. Qian, Study on the adsorption properties of novel crown ether crosslinked chitosan for metal ions, J. Appl. Polym. Sci. 84 (2002) 29-34.

[147] S. Ding, X. Zhang, X. Feng, Y. Wang, S. Ma, Q. Peng, W. Zhang, Synthesis of N,N′ -diallyl dibenzo 18-crown-6 crown ether crosslinked chitosan and their adsorption properties for metal ions, React. Funct. Polym. 66 (2006) 357-363.

[148] X. Zhang, S. Ding, Y. Wang, X. Feng, Q. Peng, S. Ma, Synthesis and adsorption properties of metal ions of novel azacrown ether crosslinked chitosan, J. Appl. Polym. Sci. 100 (2006) 2705-2709.

[149] A.A. Radwan, F.K. Alanazi, I.A. Alsarra, Microwave irradiation-assisted synthesis of a novel crown ether crosslinked chitosan as a chelating agent for heavy metal ions (M(+n)), Molecules 15 (2010) 6257-6268.

[150] M. Monier, D.M. Ayad, Y. Wei, A.A. Sarhan, Preparation and characterization of magnetic chelating resin based on chitosan for adsorption of Cu(II), Co(II), and Ni(II) ions, React. Funct. Polym. 70 (2010) 257-266.

[151] M. Monier, D. Ayad, D. Abdel-Latif, Adsorption of Cu (II), Cd (II) and Ni (II) ions by cross-linked magnetic chitosan-2-aminopyridine glyoxal Schiff's base, Colloids Surf., B 94 (2012) 250-258.

[152] M. Monier, D.M. Ayad, Y. Wei, A.A. Sarhan, Adsorption of Cu(II), Co(II), and Ni(II) ions by modified magnetic chitosan chelating resin, J. Hazard. Mater. 177 (2010) 962-970.

[153] K.R. Krishnapriya, M. Kandaswamy, Synthesis and characterization of a crosslinked chitosan derivative with a complexing agent and its adsorption studies toward metal(II) ions, Carbohydr. Res. 344 (2009) 1632-1638.

[154] H. Li, B. Meng, S.-H. Chai, H. Liu, S. Dai, Hyper-crosslinked β-cyclodextrin porous polymer: an adsorption-facilitated molecular catalyst support for transformation of water-soluble aromatic molecules, Chem. Sci. 7 (2016) 905-909.

[155] M. Monier, D.M. Ayad, D.A. Abdel-Latif, Adsorption of Cu(II), Cd(II) and Ni(II) ions by cross-linked magnetic chitosan-2-aminopyridine glyoxal Schiff's base, Colloids Surf., B 94 (2012) 250-258.

[156] H.L. Vasconcelos, T.P. Camargo, N.S. Gonçalves, A. Neves, M.C.M. Laranjeira, V.T. Fávere, Chitosan crosslinked with a metal complexing agent: Synthesis, characterization and copper(II) ions adsorption, React. Funct. Polym. 68 (2008) 572-579.

[157] F. Delval, G. Crini, N. Morin, J. Vebrel, S. Bertini, G. Torri, The sorption of several types of dye on crosslinked polysaccharides derivatives, Dyes Pigm. 53 (2002) 79-92.

[158] F. Delval, G. Crini, S. Bertini, C. Filiatre, G. Torri, Preparation, characterization and sorption properties of crosslinked starch-based exchangers, Carbohydr. Polym. 60 (2005) 67-75.

[159] F. Delval, G. Crini, J. Vebrel, Removal of organic pollutants from aqueous solutions by adsorbents prepared from an agroalimentary by-product, Bioresour. Technol. 97 (2006) 2173-2181.

[160] X.-Y. Huang, J.-P. Bin, H.-T. Bu, G.-B. Jiang, M.-H. Zeng, Removal of anionic dye eosin Y from aqueous solution using ethylenediamine modified chitosan, Carbohydr. Polym. 84 (2011) 1350-1356.

[161] X.Y. Huang, X.Y. Mao, H.T. Bu, X.Y. Yu, G.B. Jiang, M.H. Zeng, Chemical modification of chitosan by tetraethylenepentamine and adsorption study for anionic dye removal, Carbohydr. Res. 346 (2011) 1232-1240.

[162] X.J. Hu, J.S. Wang, Y.G. Liu, X. Li, G.M. Zeng, Z.L. Bao, X.X. Zeng, A.W. Chen, F. Long, Adsorption of chromium (VI) by ethylenediamine-modified cross-linked magnetic chitosan resin: isotherms, kinetics and thermodynamics, J. Hazard. Mater. 185 (2011) 306-314.

[163] L. Zhou, Z. Liu, J. Liu, Q. Huang, Adsorption of Hg(II) from aqueous solution by ethylenediamine-modified magnetic crosslinking chitosan microspheres, Desalin. 258 (2010) 41-47.

[164] L. Zhou, J. Xu, X. Liang, Z. Liu, Adsorption of platinum(IV) and palladium(II) from aqueous solution by magnetic cross-linking chitosan nanoparticles modified with ethylenediamine, J Hazard Mater 182 (2010) 518-524.

[165] H. Ohashi, Y. Hiraoka, T. Yamaguchi, An Autonomous Phase Transition−Complexation/Decomplexation Polymer System with a Molecular Recognition Property, Macromol. 39 (2006) 2614-2620.

[166] H. Ohashi, T. Abe, T. Tamaki, T. Yamaguchi, Influence of Spacer Length between Actuator and Sensor on Their Mutual Communications in Poly(N-Isopropylacrylamide-co-β-Cyclodextrin), an Autonomous Coordinative Shrinking/Swelling Polymer, Macromol. 45 (2012) 9742-9750.

[167] H. Wang, Y.-g. Liu, G.-m. Zeng, X.-j. Hu, X. Hu, T.-t. Li, H.-y. Li, Y.-q. Wang, L.-h. Jiang, Grafting of β-cyclodextrin to magnetic graphene oxide via ethylenediamine and application for Cr(VI) removal, Carbohydr. Polym. 113 (2014) 166-173.

[168] Y. Pang, G. Zeng, L. Tang, Y. Zhang, Y. Liu, X. Lei, Z. Li, J. Zhang, G. Xie, PEI-grafted magnetic porous powder for highly effective adsorption of heavy metal ions, Desalin. 281 (2011) 278-284.

[169] S. Chatterjee, T. Chatterjee, S.H. Woo, Influence of the polyethyleneimine grafting on the adsorption capacity of chitosan beads for Reactive Black 5 from aqueous solutions, Chem. Eng. J. 166 (2011) 168-175.

[170] G.Z. Kyzas, M. Kostoglou, A.A. Vassiliou, N.K. Lazaridis, Treatment of real effluents from dyeing reactor: Experimental and modeling approach by adsorption onto chitosan, Chem. Eng. J. 168 (2011) 577-585.

[171] N. Li, X. Wei, Z. Mei, X. Xiong, S. Chen, M. Ye, S. Ding, Synthesis and characterization of a novel polyamidoamine-cyclodextrin crosslinked copolymer, Carbohydr. Res. 346 (2011) 1721-1727.

[172] N. Li, Z. Mei, X. Wei, Study on sorption of chlorophenols from aqueous solutions by an insoluble copolymer containing β-cyclodextrin and polyamidoamine units, Chem. Eng. J. 192 (2012) 138-145.

[173] Y. Yi, Y. Wang, F. Ye, Synthesis and properties of diethylene triamine derivative of chitosan, Colloids Surf., A 277 (2006) 69-74.

[174] A. Masykur, S.J. Santosa, D.S. dan Jumina, Cross-linking of succinate-grafted chitosan and its effect on the capability to adsorb Pb (II) ion, in: IOP Conference Series: Materials Science and Engineering, IOP Publishing, 2016, pp. 012014.

[175] B. Özkahraman, A. Bal, I. Acar, G. Güçlü, Adsorption of brilliant green from aqueous solutions onto crosslinked chitosan graft copolymers, Clean–Soil, Air, Water 39 (2011) 1001-1006.

[176] Y. Xing, X. Sun, B. Li, Poly (methacrylic acid) - modified chitosan for enhancement adsorption of water - soluble cationic dyes, Polym. Eng. Sci. 49 (2009) 272-280.

[177] Y. Xing, X.-M. Sun, B.-H. Li, Pyromellitic dianhydride-modified chitosan microspheres for enhancement of cationic dyes adsorption, Environ. Eng. Sci. 26 (2009) 551-558.

[178] Y. Shimizu, S. Izumi, Y. Saito, H. Yamaoka, Ethylenediamine tetraacetic acid modification of crosslinked chitosan designed for a novel metal - ion adsorbent, J. Appl. Polym. Sci. 92 (2004) 2758-2764.

[179] H. Yang, Y. Li, S.S.H. Ho, X. Tian, Y. Xia, Y. Shen, M. Zhao, G. Pan, Preparation and characterization of EDTAD-modified magnetic-Fe_3O_4 chitosan composite: application of comparative adsorption of dye wastewater with magnetic chitosan, Water Sci. Technol. 68 (2013) 209-216.

[180] Y. Xia, X. Dai, S. Huang, X. Tian, H. Yang, Y. Li, Y. Liu, M. Zhao, Fast and highly efficient removal of methylene blue by a novel EDTAD-modified magnetic chitosan material, Desalin. Water Treat. 51 (2013) 7586-7595.

[181] Y.-C. Liao, M.-J. Syu, Novel immobilized metal ion affinity adsorbent based on cross-linked β-cyclodextrin matrix for repeated adsorption of α-amylase, Biochem. Eng. J. 23 (2005) 17-24.

[182] G. Crini, H.N. Peindy, F. Gimbert, C. Robert, Removal of C.I. Basic Green 4 (Malachite Green) from aqueous solutions by adsorption using cyclodextrin-based adsorbent: Kinetic and equilibrium studies, Sep. Purif. Technol. 53 (2007) 97-110.

[183] G. Crini, Kinetic and equilibrium studies on the removal of cationic dyes from aqueous solution by adsorption onto a cyclodextrin polymer, Dyes Pigm. 77 (2008) 415-426.

[184] S. Yong, N. Bolan, E. Lombi, W. Skinner, E. Guibal, Sulfur-containing chitin and chitosan derivatives as trace metal adsorbents: a review, Crit rev env sci tech 43 (2013) 1741-1794.

[185] D. Zhao, L. Zhao, C.-S. Zhu, J. Wang, X.-H. Lv, A novel β-cyclodextrin polymer modified by sulfonate groups, J. Inclusion Phenom.Macrocyclic Chem. 73 (2012) 93-98.

[186] L. Guo, G. Li, J. Liu, P. Yin, Q. Li, Adsorption of Aniline on Cross-Linked Starch Sulfate from Aqueous Solution, Ind. Eng. Chem. Res. 48 (2009) 10657-10663.

[187] S.M. Ritchie, K.E. Kissick, L.G. Bachas, S.K. Sikdar, C. Parikh, D. Bhattacharyya, Polycysteine and other polyamino acid functionalized microfiltration membranes for heavy metal capture, Environ. Sci. Technol. 35 (2001) 3252-3258.

[188] J.D. Merrifield, W.G. Davids, J.D. MacRae, A. Amirbahman, Uptake of mercury by thiol-grafted chitosan gel beads, Water Res. 38 (2004) 3132-3138.

[189] A.A. Atia, Studies on the interaction of mercury(II) and uranyl(II) with modified chitosan resins, Hydrometallurgy 80 (2005) 13-22.

[190] E. Guibal, N. Von Offenberg Sweeney, T. Vincent, J.M. Tobin, Sulfur derivatives of chitosan for palladium sorption, React. Funct. Polym. 50 (2002) 149-163.

[191] L. Zhou, Y. Wang, Z. Liu, Q. Huang, Characteristics of equilibrium, kinetics studies for adsorption of Hg(II), Cu(II), and Ni(II) ions by thiourea-modified magnetic chitosan microspheres, J. Hazard. Mater. 161 (2009) 995-1002.

[192] L. Fan, C. Luo, Z. Lv, F. Lu, H. Qiu, Preparation of magnetic modified chitosan and adsorption of Zn^{2+} from aqueous solutions, Colloids Surf., B 88 (2011) 574-581.

[193] L. Fan, C. Luo, Z. Lv, F. Lu, H. Qiu, Removal of Ag^{+} from water environment using a novel magnetic thiourea-chitosan imprinted Ag^{+}, J. Hazard. Mater. 194 (2011) 193-201.

[194] Y. Xu, J.P. Lay, F. Korte, Fate and effects of xanthates in laboratory freshwater systems, Bull. Environ. Contam. Toxicol. 41 (1988) 683-689.

[195] B. Kannamba, K.L. Reddy, B.V. AppaRao, Removal of Cu(II) from aqueous solutions using chemically modified chitosan, J. Hazard. Mater. 175 (2010) 939-948.

[196] Y. Chen, J. Wang, The characteristics and mechanism of Co(II) removal from aqueous solution by a novel xanthate-modified magnetic chitosan, Nucl. Eng. Des. 242 (2012) 452-457.

[197] Y. Zhu, J. Hu, J. Wang, Competitive adsorption of Pb(II), Cu(II) and Zn(II) onto xanthate-modified magnetic chitosan, J. Hazard. Mater. 221–222 (2012) 155-161.

[198] G. Crini, F. Gimbert, C. Robert, B. Martel, O. Adam, N. Morin-Crini, F. De Giorgi, P.-M. Badot, The removal of Basic Blue 3 from aqueous solutions by chitosan-based adsorbent: Batch studies, J. Hazard. Mater. 153 (2008) 96-106.

[199] T.C. Coelho, R. Laus, A.S. Mangrich, V.T. de Fávere, M.C.M. Laranjeira, Effect of heparin coating on epichlorohydrin cross-linked chitosan microspheres on the adsorption of copper (II) ions, React. Funct. Polym. 67 (2007) 468-475.

[200] S. Tan, Y. Wang, C. Peng, Y. Tang, Synthesis and adsorption properties for metal ions of crosslinked chitosan acetate crown ethers, J. Appl. Polym. Sci. 71 (1999) 2069-2074.

[201] A.O. Martins, E.L. da Silva, E. Carasek, N.S. Gonçalves, M.C.M. Laranjeira, V.T. de Fávere, Chelating resin from functionalization of chitosan with complexing agent 8-hydroxyquinoline: application for metal ions on line preconcentration system, Anal. Chim. Acta 521 (2004) 157-162.

[202] F.C. Barros, F.W. Sousa, R.M. Cavalcante, T.V. Carvalho, F.S. Dias, D.C. Queiroz, L.C. Vasconcellos, R.F. Nascimento, Removal of Copper, Nickel and Zinc Ions from Aqueous Solution by Chitosan - 8 - Hydroxyquinoline Beads, Clean – Soil, Air, Water 36 (2008) 292-298.

[203] A. Ramesh, H. Hasegawa, W. Sugimoto, T. Maki, K. Ueda, Adsorption of gold(III), platinum(IV) and palladium(II) onto glycine modified crosslinked chitosan resin, Bioresour. Technol. 99 (2008) 3801-3809.

[204] K. Fujiwara, A. Ramesh, T. Maki, H. Hasegawa, K. Ueda, Adsorption of platinum (IV), palladium (II) and gold (III) from aqueous solutions onto l-lysine modified crosslinked chitosan resin, J. Hazard. Mater. 146 (2007) 39-50.

[205] H.L. Vasconcelos, V.T. Fávere, N.S. Gonçalves, M.C.M. Laranjeira, Chitosan modified with Reactive Blue 2 dye on adsorption equilibrium of Cu(II) and Ni(II) ions, React. Funct. Polym. 67 (2007) 1052-1060.

[206] K.C. Justi, M.C.M. Laranjeira, A. Neves, A.S. Mangrich, V.T. Fávere, Chitosan functionalized with 2[-bis-(pyridylmethyl) aminomethyl]4-methyl-6-formyl-phenol: equilibrium and kinetics of copper (II) adsorption, Polym. 45 (2004) 6285-6290.

[207] K.C. Justi, V.T. Fávere, M.C.M. Laranjeira, A. Neves, R.A. Peralta, Kinetics and equilibrium adsorption of Cu(II), Cd(II), and Ni(II) ions by chitosan functionalized with 2[-bis-(pyridylmethyl)aminomethyl]-4-methyl-6-formylphenol, J. Colloid Interface Sci. 291 (2005) 369-374.

[208] S. Jaggi, U. Gupta, Chelate Modified β-CDP as a Green and Economical Sorbent for Separation and Preconcentration of Co (II), Iran. J. Anal. Chem. 1 (2014) 97-105.

[209] U. Bierbach, T.W. Hambley, N. Farrell, Modification of Platinum(II) Antitumor Complexes with Sulfur Ligands. 1. Synthesis, Structure, and Spectroscopic Properties of Cationic Complexes of the Types [PtCl(diamine)(L)]NO3 and [{PtCl(diamine)}2(L-L)](NO3)2 (L = Monofunctional Thiourea Derivative; L-L = Bifunctional Thiourea Derivative), Inorg. Chem. 37 (1998) 708-716.

[210] H. Kyung, J. Lee, W. Choi, Simultaneous and synergistic conversion of dyes and heavy metal ions in aqueous TiO_2 suspensions under visible-light illumination, Environ. Sci. Technol. 39 (2005) 2376-2382.

[211] C. Ling, F.-Q. Liu, C. Long, T.-P. Chen, Q.-Y. Wu, A.-M. Li, Synergic removal and sequential recovery of acid black 1 and copper (II) with hyper-crosslinked resin and inside mechanisms, Chem. Eng. J. 236 (2014) 323-331.

[212] M.E. Skold, G.D. Thyne, J.W. Drexler, D.L. Macalady, J.E. McCray, Enhanced solubilization of a metal-organic contaminant mixture (Pb, Sr, Zn, and perchloroethylene) by cyclodextrin, Environ. Sci. Technol. 42 (2008) 8930-8934.

[213] G.Z. Kyzas, M. Kostoglou, N.K. Lazaridis, D.N. Bikiaris, N-(2-Carboxybenzyl) grafted chitosan as adsorptive agent for simultaneous removal of positively and negatively charged toxic metal ions, J. Hazard. Mater. 244–245 (2013) 29-38.

[214] R. Huang, B. Yang, Q. Liu, Y. Liu, Simultaneous adsorption of aniline and Cr (VI) ion by activated carbon/chitosan composite, J. Appl. Polym. Sci. 131 (2014).

[215] X. Zhang, Y. Wang, S. Yang, Simultaneous removal of Co(II) and 1-naphthol by core-shell structured Fe_3O_4@cyclodextrin magnetic nanoparticles, Carbohydr. Polym. 114 (2014) 521-529.

[216] W. Song, D. Shao, S. Lu, X. Wang, Simultaneous removal of uranium and humic acid by cyclodextrin modified graphene oxide nanosheets, Sci. China Chem. 57 (2014) 1291-1299.

[217] A. Heidari, H. Younesi, Z. Mehraban, H. Heikkinen, Selective adsorption of Pb(II), Cd(II), and Ni(II) ions from aqueous solution using chitosan–MAA nanoparticles, Int. J. Biol. Macromol. 61 (2013) 251-263.

[218] H. Yan, J. Dai, Z. Yang, H. Yang, R. Cheng, Enhanced and selective adsorption of copper(II) ions on surface carboxymethylated chitosan hydrogel beads, Chem. Eng. J. 174 (2011) 586-594.

[219] L. Zhou, C. Shang, Z. Liu, G. Huang, A.A. Adesina, Selective adsorption of uranium(VI) from aqueous solutions using the ion-imprinted magnetic chitosan resins, J. Colloid Interface Sci. 366 (2012) 165-172.

[220] T. Osawa, K. Shirasaka, T. Matsui, S. Yoshihara, T. Akiyama, T. Hishiya, H. Asanuma, M. Komiyama, Importance of the Position of Vinyl Group on β-Cyclodextrin for the Effective Imprinting of Amino Acid Derivatives and Oligopeptides in Water, Macromol. 39 (2006) 2460-2466.

[221] W. Zhang, L. Qin, X.W. He, W.Y. Li, Y.K. Zhang, Novel surface modified molecularly imprinted polymer using acryloyl-beta-cyclodextrin and acrylamide as monomers for selective recognition of lysozyme in aqueous solution, J. Chromatogr. A 1216 (2009) 4560-4567.

[222] H. Li, M.H. El-Dakdouki, D.C. Zhu, G.S. Abela, X. Huang, Synthesis of beta-cyclodextrin conjugated superparamagnetic iron oxide nanoparticles for selective binding and detection of cholesterol crystals, Chem. Commun. 48 (2012) 3385-3387.

[223] M. Kitaoka, K. Hayashi, Adsorption of bisphenol A by cross-linked β-cyclodextrin polymer, J. Inclusion Phenom.Macrocyclic Chem. 44 (2002) 429-431.

[224] J. Pan, X. Zou, X. Wang, W. Guan, Y. Yan, J. Han, Selective recognition of 2,4-dichlorophenol from aqueous solution by uniformly sized molecularly imprinted microspheres with β-cyclodextrin/attapulgite composites as support, Chem, Eng, J. 162 (2010) 910-918.

[225] P. Liang, Y. Liu, L. Guo, J. Zeng, H. Lu, Multiwalled carbon nanotubes as solid-phase extraction adsorbent for the preconcentration of trace metal ions and their determination by inductively coupled plasma atomic emission spectrometry, J. Anal. At. Spectrom. 19 (2004) 1489-1492.

[226] J.S. Carletto, K.C.D.P. Roux, H.F. Maltez, E. Martendal, E. Carasek, Use of 8-hydroxyquinoline-chitosan chelating resin in an automated on-line preconcentration system for determination of zinc(II) by F AAS, J. Hazard. Mater. 157 (2008) 88-93.

[227] A. Sabarudin, N. Lenghor, M. Oshima, L. Hakim, T. Takayanagi, Y.-H. Gao, S. Motomizu, Sequential-injection on-line preconcentration using chitosan resin functionalized with 2-amino-5-hydroxy benzoic acid for the determination of trace elements in environmental water samples by inductively coupled plasma-atomic emission spectrometry, Talanta 72 (2007) 1609-1617.

[228] D. Shao, G. Sheng, C. Chen, X. Wang, M. Nagatsu, Removal of polychlorinated biphenyls from aqueous solutions using β-cyclodextrin grafted multiwalled carbon nanotubes, Chemosphere 79 (2010) 679-685.

[229] I. Abay, A. Denizli, E. Biskin, B. Salih, Removal and pre-concentration of phenolic species onto beta-cyclodextrin modified poly(hydroxyethylmethacrylate-ethyleneglycoldimethacrylate) microbeads, Chemosphere 61 (2005) 1263-1272.

[230] C.Y. Jimmy, Z.-T. Jiang, H.-Y. Liu, J. Yu, L. Zhang, β-Cyclodextrin epichlorohydrin copolymer as a solid-phase extraction adsorbent for aromatic compounds in water samples, Anal. Chim. Acta 477 (2003) 93-101.

[231] X. Zhu, M. Wu, Y. Gu, β-Cyclodextrin-cross-linked polymer as solid phase extraction material coupled with inductively coupled plasma mass spectrometry for the analysis of trace Co(II), Talanta 78 (2009) 565-569.

[232] P.-B.T. Guideline, OECD guideline for the testing of chemicals, in, The Hershberger assay, 2001.

[233] R.S. Lokhande, P.U. Singare, D.S. Pimple, Toxicity study of heavy metals pollutants in waste water effluent samples collected from Taloja Industrial Estate of Mumbai, India, Res. Environ. 1 (2011) 13-19.

[234] I. Nilsson, A. Möller, B. Mattiasson, M.S.T. Rubindamayugi, U. Welander, Decolorization of synthetic and real textile wastewater by the use of white-rot fungi, Enzyme Microb. Tech. 38 (2006) 94-100.

[235] E. Repo, EDTA- and DTPA-functionalized silica gel and chitosan adsorbents for the removal of heavy metals from aqueous solutions, in: Green Chemistry, Lappeenranta University of Technology, Mikkeli, Finland, 2011.

[236] Z. Sofer, O. Jankovsky, P. Simek, K. Klimova, A. Mackova, M. Pumera, Uranium- and thorium-doped graphene for efficient oxygen and hydrogen peroxide reduction, ACS nano 8 (2014) 7106-7114.

[237] S.-M. Alatalo, F. Pileidis, E. Mäkilä, M. Sevilla, E. Repo, J. Salonen, M. Sillanpää, M.-M. Titirici, Versatile Cellulose-Based Carbon Aerogel for the Removal of Both Cationic and Anionic Metal Contaminants from Water, ACS Appl. Mater. Interfaces 7 (2015) 25875-25883.

[238] L.D. Pettit, K. Powell, IUPAC stability constants database, in, York, UK, 2006.

[239] S. Durand, J.-P. Dognon, P. Guilbaud, C. Rabbe, G. Wipff, Lanthanide and alkaline-earth complexes of EDTA in water: a molecular dynamics study of structures and binding selectivities, J. Chem. Soc., Perkin Trans. 2 (2000) 705-714.

[240] S.K. Papageorgiou, F.K. Katsaros, E.P. Kouvelos, N.K. Kanellopoulos, Prediction of binary adsorption isotherms of Cu^{2+}, Cd^{2+} and Pb^{2+} on calcium alginate beads from single adsorption data, J. Hazard. Mater. 162 (2009) 1347-1354.

[241] R. Vieira, E. Guibal, E. Silva, M. Beppu, Adsorption and desorption of binary mixtures of copper and mercury ions on natural and crosslinked chitosan membranes, Adsorption 13 (2007) 603-611.

[242] R.G. Pearson, Hard and Soft Acids and Bases, J. Am. Chem. Soc. 85 (1963) 3533-3539.

[243] K. Vijayaraghavan, M. Sathishkumar, R. Balasubramanian, Interaction of rare earth elements with a brown marine alga in multi-component solutions, Desalination 265 (2011) 54-59.

[244] P. Liang, Y. Liu, L. Guo, Determination of trace rare earth elements by inductively coupled plasma atomic emission spectrometry after preconcentration with multiwalled carbon nanotubes, Spectrochim. Acta B 60 (2005) 125-129.

Paper I

Adsorption of Cd (II) and Pb (II) by a novel EGTA-modified chitosan material:

Kinetics and isotherms

Zhao, F., Repo, E., Yin, D., Sillanpää, M.

Journal of colloid and interface science 409 (2013) 174–182

Paper II

Green synthesis of magnetic EDTA-and/or DTPA-cross-linked chitosan adsorbents for highly efficient removal of metals

Zhao, F., Repo, E., Sillanpää, M., Meng, Y., Yin, D., Tang W.

Industrial & Engineering Chemistry Research 54 (2015) 1271-1281

Paper III

EDTA-Cross-Linked β-Cyclodextrin: An Environmentally Friendly Bifunctional Adsorbent for Simultaneous Adsorption of Metals and Cationic Dyes

Zhao, F., Repo, E., Yin, D., Meng, Y., Jafari, S., Sillanpää, M.

Environmental science & technology 49 (2015) 10570-10580

Paper IV

An EDTA-β-cyclodextrin material for the adsorption of rare earth elements and its application in preconcentration of rare earth elements in seawater

Zhao, F., Repo, E., Meng, Y., Wang, X., Yin, D., Sillanpää, M.

Journal of Colloid and Interface Science 465 (2016) 215–224

Paper V

One-pot synthesis of trifunctional chitosan-EDTA-β-cyclodextrin polymer for simultaneous removal of metals and organic micropollutants

Zhao, F., Repo, E., Yin, D., Chen, L., Kalliola, S., Tang, J., Iakovleva, E., Tam, M., Sillanpää, M.

Scientific Reports 7 (2017) 15811

ACTA UNIVERSITATIS LAPPEENRANTAENSIS

739. MATTHEWS, SAMI. Novel process development in post-forming of an extruded wood plastic composite sheet. 2017. Diss.

740. KÄHKÖNEN, TOMMI. Understanding and managing enterprise systems integration. 2017. Diss.

741. YLI-HUUMO, JESSE. The role of technical dept in software development. 2017. Diss.

742. LAYUS, PAVEL. Usability of the submerged arc welding (SAW) process for thick high strength steel plates for Arctic shipbuilding applications. 2017. Diss.

743. KHAN, RAKHSHANDA. The contribution of socially driven businesses and innovations to social sustainability. 2017. Diss.

744. BIBOV, ALEKSANDER. Low-memory filtering for large-scale data assimilation. 2017. Diss.

745. ROTICH, NICOLUS KIBET. Development and application of coupled discrete and continuum models in solid particles classification. 2017. Diss.

746. GAST, JOHANNA. The coopetition-innovation nexus: Investigating the role of coopetition for innovation in SMEs. 2017. Diss.

747. KAPOOR, RAHUL. Competition and disputes in the patent life cycle. 2017. Diss.

748. ALI-MARTTILA, MAAREN. Towards successful maintenance service networks – capturing different value creation strategies. 2017. Diss.

749. KASHANI, HAMED TASALLOTI. On dissimilar welding: a new approach for enhanced decision-making. 2017. Diss.

750. MVOLA BELINGA, ERIC MARTIAL. Effects of adaptive GMAW processes: performance and dissimilar weld quality. 2017. Diss.

751. KARTTUNEN, JUSSI. Current harmonic compensation in dual three-phase permanent magnet synchronous machines. 2017. Diss.

752. SHI, SHANSHUANG. Development of the EAST articulated maintenance arm and an algorithm study of deflection prediction and error compensation. 2017. Diss.

753. CHEN, JIE. Institutions, social entrepreneurship, and internationalization. 2017. Diss.

754. HUOTARI, PONTUS. Strategic interaction in platform-based markets: An agent-based simulation approach. 2017. Diss.

755. QU, BIN. Water chemistry and greenhouse gases emissions in the rivers of the "Third Pole" / Water Tower of Asia". 2017. Diss.

756. KARHU, PÄIVI. Cognitive ambidexterity: Examination of the cognitive dimension in decision-making dualities. 2017. Diss.

757. AGAFONOVA, OXANA. A numerical study of forest influences on the atmospheric boundary layer and wind turbines. 2017. Diss.

758. AZAM, RAHAMATHUNNISA MUHAMMAD. The study of chromium nitride coating by asymmetric bipolar pulsed DC reactive magnetron sputtering. 2017. Diss.

759. AHI, MOHAMADALI. Foreign market entry mode decision-making: Insights from real options reasoning. 2017. Diss.

760. AL HAMDI, ABDULLAH. Synthesis and comparison of the photocatalytic activities of antimony, iodide and rare earth metals on SnO2 for the photodegradation of phenol and its intermediates under UV, solar and visible light irradiations. 2017. Diss.

761. KAUTTO, JESSE. Evaluation of two pulping-based biorefinery concepts. 2017. Diss.

762. AFZALIFAR, ALI. Modelling nucleating flows of steam. 2017. Diss.

763. VANNINEN, HEINI. Micromultinationals - antecedents, processes and outcomes of the multinationalization of small- and medium-sized firms. 2017. Diss.

764. DEVIATKIN, IVAN. The role of waste pretreatment on the environmental sustainability of waste management. 2017. Diss.

765. TOGHYANI, AMIR. Effect of temperature on the shaping process of an extruded wood-plastic composite (WPC) profile in a novel post-production process. 2017. Diss.

766. LAAKKONEN, JUSSI. An approach for distinct information privacy risk assessment. 2017. Diss.

767. KASURINEN, HELI. Identifying the opportunities to develop holistically sustainable bioenergy business. 2017. Diss.

768. KESKISAARI, ANNA. The impact of recycled raw materials on the properties of wood-plastic composites. 2017. Diss.

769. JUKKA, MINNA. Perceptions of international buyer-supplier relational exchange. 2017. Diss.

770. BAYGILDINA, ELVIRA. Thermal load analysis and monitoring of doubly-fed wind power converters in low wind speed conditions. 2017. Diss.

771. STADE, SAM. Examination of the compaction of ultrafiltration membranes with ultrasonic time-domain reflectometry. 2017. Diss.

772. KOZLOVA, MARIIA. Analyzing the effects of a renewable energy support mechanism on investments under uncertainty: case of Russia. 2017. Diss.

773. KURAMA, ONESFOLE. Similarity based classification methods with different aggregation operators. 2017. Diss.

774. LYYTIKÄINEN, KATJA. Removal of xylan from birch kraft pulps and the effect of its removal on fiber properties, colloidal interactions and retention in papermaking. 2017. Diss.

775. GAFUROV, SALIMZHAN. Theoretical and experimental analysis of dynamic loading of a two-stage aircraft engine fuel pump and methods for its decreasing. 2017. Diss.

776. KULESHOV, DMITRII. Modelling the operation of short-term electricity market in Russia. 2017. Diss.

777. SAARI, JUSSI. Improving the effectiveness and profitability of thermal conversion of biomass. 2017. Diss.